

The role of hepatic cholesterol transporter ABCA1 for HDL metabolism in vivo

An adenovirus-mediated RNA interference approach in mice

(Mus musculus, Linnaeus 1758)

Dissertation

zur Erlangung des Doktorgrades
des Fachbereichs Biologie
der Universität Hamburg

vorgelegt von

Sergey Ragozin

aus Orenburg, Russland

Hamburg 2004

Моей маме с нежностью и любовью

Felix, qui potuit rerum cognoscere causas

Table of contents

1. Introduction	1
1.1. Lipoprotein metabolism	1
Lipoproteins	1
Exogenous metabolic pathway	3
Endogenous metabolic pathway	4
Reverse cholesterol transport	5
1.2. The role of ABCA1 transporter for HDL metabolism	7
Family of transmembrane transporters	7
ABCA1 – major transporter for cholesterol and phospholipids	9
Tanger Disease	12
Animal models for studying ABCA1 in HDL metabolism	12
1.3. Post-transcriptional gene silencing – RNA interference	14
Phenomenon and mechanism of RNA interference in vertebrates	15
Stable expression of the small interfering RNAs for functional gene knock-down	17
1.4. Adenoviral vectors and gene delivery	18
Structure and function of human adenovirus serotype 5	19
Recombinant adenovirus for <i>in vitro</i> and <i>in vivo</i> biological studies	20
1.5. The aim of the study	22
2. Methodological considerations	23
2.1. Materials	23
Diluents, solutions and buffers	23
Chemistry, proteins and enzymes	23
Kits	23

Primers	23
Antibodies	24
Plasmids, adenoviruses, bacterial strains, cells and animals	24
Cell culture materials	25
2.2. Methods	25
Bioinformatics	25
Directional cloning into plasmid vectors	25
Bacterial transformation	26
Glycerol stock of transformed bacteria	27
Preparation of plasmid DNA	27
Agarose gel electrophoresis	29
DNA purification	30
Spectrometric determination of DNA concentration	30
DNA sequencing	30
Total RNA extraction	31
Generating of cDNA by reverse transcription	31
Quantification of cDNA	32
Protein extraction	34
Determination of protein concentration by SDS-Lowry	35
SDS-PAGE	35
Western blot	36
Indirect immunofluorescence	37
Adenoviral culture	38
Adenoviral titration	41
Cell culture	42

Transfection of mammalian cells	43
Adenoviral infection of mammalian cells	43
Animal husbandry	44
Adenoviral administration	44
Blood puncture	44
Organs withdrawal	45
Histology	45
Plasma lipoproteins separation and lipids determination	46
Flow cytometry	47
Safety and waste disposal	48
Software and statistic	48
3. Results	49
3.1. ABCA1 knockdown mediated by RNA interference in vitro	49
Transient overexpression of murine ABCA1 in cell culture	49
Cloning of small interfering RNA-expressing vector for murine ABCA1 targeting	52
Characterisation of anti-ABCA1 RNA interference <i>in vitro</i>	55
Construction and characterisation of adenoviral vector for anti-ABCA1 small interfering RNA delivery	59
3.2. Liver specific ABCA1 knockdown in mice	64
Biodistribution of recombinant EGFP-adenovirus <i>in vivo</i>	64
Expression of some proteins involved in lipid metabolism in mice liver	67
Hepatocytes membrane proteins influenced by anti-ABCA1 RNA interference	69
Plasma lipoproteins in mice	71

4. Discussion	80
4.1. RNA interference	80
4.2. Adenovirus vector for small interfering RNA delivery	81
4.3. Hepatic ABCA1 transporter and HDL metabolism	82
5. Summary	87
6. Supplements	88
7. Appendix	92
7.1. Plasmid maps	92
7.2. Figures and tables	99
7.3. Abbreviations	101
7.4. Literature	103
7.5. Acknowledgments	118

1. Introduction

1.1. Lipoprotein metabolism

Lipids are a heterogeneous group of biomolecules. One property which unites them is having no or low water solubility. As one of the major components of human body, lipids play various roles in homeostasis. Fatty acids in triglycerides are energy sources, while phospholipids, glycolipids and cholesterol are membrane components. Moreover, steroids and eicosanoids are also signaling molecules and lipophilic vitamins are co-factors and co-enzymes for different reactions.

Mankind consumes tons of lipids annually. In the western world poor eating habits are becoming a significant epidemiological problem. Increased consumption of dietary fat when combined with heritable disorders of lipid metabolism results in most cardiovascular diseases and is, therefore, a leading factor in human mortality.

Lipoproteins

Lipids are too hydrophobic to be transported on their own in the circulation. Free fatty acids (FFA) are transported bound to albumin. Other molecules (triglycerides, cholesterol, phospholipids), if taken with a food or synthesised *de novo*, are incorporated into lipoprotein particles for transportation in the blood.

Diverse lipoprotein particles could be physically separated by their density or electrophoretic mobility and classified according to their different genesis and composition (tab. 1). The biggest triglyceride-rich lipoprotein particles are chylomicrons (CM). These are secreted by the intestinal cells into the lymphatic system and serve to transport dietary fat to the liver and other tissues. Lipids, taken up or synthesized by the liver are redistributed to other organs by very low density lipoproteins (VLDL) and low density lipoproteins (LDL). LDL is a result of the progressive intravascular catabolism of VLDL and contains relatively more cholesterol and fewer triglycerides. CM and VLDL are also called triglyceride rich lipoproteins (TRL). Finally, the excess of cholesterol, which needs to be collected from peripheral tissues and directed to the liver for bile excretion, is carried by high density lipoproteins (HDL).

Triglycerides and cholesterol esters are found in the core of the lipoprotein particles, surrounded by an amphipatic monolayer of phospholipids (PL) and unesterified cholesterol. The surface of the particles is also formed by structurally related apolipoproteins (apo). Apolipoproteins can also be ligand for lipoprotein receptors and therefore determine the destiny of the respective lipoprotein (tab. 2). Due to the particular distribution of lipoprotein receptors in different tissues, each organ varies in its ability to bind and internalise lipoprotein particles. For instance apoB100, which exclusively binds LDL receptor (LDLR) and apoE, which is a ligand for LDLR and LDLR-related protein (LRP) as well as all other LRP family members. In circulation, lipoproteins are modified by enzymes and transfer proteins. Lipoprotein lipase catalyses the hydrolysis of fatty acids from triglyceride; lecithin:cholesterol acyl transferase (LCAT) forms cholesterol esters in HDL by transferring a fatty acid (usually linoleic acid) from phosphatidylcholin to cholesterol; the cholesteryl esters from previous reaction are transferred to other lipoproteins by cholesteryl ester transfer protein (CETP). Some apolipoproteins are specific cofactors for these enzymes, e.g. LCAT is activated by apoAI, apoCII is an essential co-factor for LPL.

Table 1 Lipoprotein particles (Schlenck 1999)

Lipoproteins	Apoproteins	Diameter, nm	Density, g/mL	Dry weight, ~%			
				prot,	TG,	CH,	PL
Chylomicrons	B48, AI, AII, AIV	80-1200	<0.95	1-2	83	8	7
VLDL	B100, C, E	30-80	0.95-1.006	10	50	22	18
IDL	B100, E	25-35	1.006-1.019	18	31	29	22
LDL	B100	18-25	1.019-1.063	22	9	45	21
HDL	AI, AII	5-12	1.063-1.25	35	8	30	29

Table 2 Apolipoproteins (Mahley 1984, Sakurabayashi 2001)

Apolipoproteins	MW, kDa	Source	Human serum values, mg/L,	Function
AI	29	Liver, intestine	1.42±0.2	LCAT activation, HDL and CM structure HDL structure LCAT activation, HDL structure
AII	17		0.3±0.05	
AIV	43			
B48	241	Intestine*	0.87±0.18**	Chylomicrons structure LDL structure, LDL internalisation
B100	513	Liver		
CI	6,6	Liver	0.029±0.013 0.075±0.020	LPL Cofactor
CII	8,9			
CIII	8,8			
E	34	Liver	0.036±0.009	Internalisation of chylomicrons, HDL

*In humans apoB48 comes from chylomicron remnants only. In rodents apoB48 is also produced in the liver through editing of apoB100 mRNA.

**Both variants of apoB taken together.

Lipid metabolic pathways are described in the sections to follow. It is perhaps important not to take these points separated from each other as lipoprotein particles of all kind are closely related and exchange not only lipids but also apolipoproteins.

Exogenous metabolic pathway

In the small intestine, dietary fat is emulgated by bile salts and hydrolysed by pancreatic lipases. FFA, cholesterol, monoglycerides and glycerol are taken up by enterocytes. Lipids are re-esterified in cytoplasm and directed to the Golgi apparatus (Senior 1964). Intestinal cells synthesize apolipoproteins (primarily apoB48, apoAI and apoAIV) and assemble exogenous lipids into chylomicrons. As soon as CM enter the blood stream endothelial LPL becomes responsible for the intravascular hydrolysis of CM, producing FFA and chylomicron remnants (CR). For LPL catalytic activity apoCII is required as a cofactor. Abundantly expressed in muscle and adipose tissue, LPL plays a role in the supply of FFA to these tissues. Felts *et al.* were the first to postulate that after hydrolysis LPL remains attached to the remnant lipoprotein (Felts 1975, Goldberg 1986). CR have been shown to be rapidly taken up into the liver (Sherrill 1980). Uptake is mediated by the LDLR and LRP with apoE, LPL, and hepatic lipase as ligand proteins (Willnow 1994, Beisiegel 1989, Beisiegel 1991, Beisiegel 1994). The effect of LPL is mediated by its C-terminal domain and also involves interaction with cell surface heparan sulphat proteoglycans (HSPG) (Beisiegel 1997, Merkel 2002).

Furthermore, as demonstrated by Hussain *et al.*, CR are not solely catabolised in the liver, but can also be taken up into the bone marrow and the heart (Hussain 1989). It has been shown *in vitro* that CR uptake can be mediated by VLDL receptor and that LPL is an important ligand for this receptor (Niemeier 1996). The VLDL receptor might therefore represent the counterpart to LRP in peripheral tissues, facilitating the uptake of CR in addition to the uptake of VLDL and IDL.

The intracellular destinies of lipid/apoB and receptor/apoE fractions of the remnants are different. ApoB and lipids enter the lysosome, where these components are degraded by cathepsin and lysosomal acid lipase (Goldstein 1985). Surface components of TRL particles like apoE can be re-secreted via a recycling pathway (Heeren 1999). The apoE recycling is accompanied by cholesterol efflux to HDL. Re-

secreted apoE is found in association with HDL. Remarkably, HDL does not only act as an extracellular acceptor for recycled apoE, but also stimulates the recycling itself. As was shown by Dr. Beisiegel's group, apoE recycling implicates the intracellular trafficking of apoAI (derived from internalised HDL) to pre-existing and TRL-derived apoE/cholesterol-containing endosomes in the cytoplasm periphery (Heeren 2003). Thus, the exogenous pathway is connected to HDL metabolism by an intravascular and intracellular pathway.

Endogenous metabolic pathway

The liver plays a key role in the delivery of lipids to peripheral tissues. Triglycerides and cholesterol esters are directed to the Golgi apparatus of hepatocytes similar as for chylomicrons secretion (Gibbons 2004). A major structural component of VLDL particles produced by the liver is apoB100, one of the largest monomeric proteins with an extremely complicated secondary structure. Unlike the synthesis of the majority of hepatic secretory proteins, that of apoB100 is nearly constitutive. Its secretion is regulated mainly by co- and post-transcriptional degradation. This protein has large hydrophobic beta-sheet regions; therefore lipid association must occur simultaneously with transcription and translocation to prevent self-aggregation and cellular toxicity. The microsomal triglyceride transfer protein (MTP) catalyses this step of lipidation (Gordon 2000). When lipids are limited, the first step, translocation of synthesizing polypeptide, is impeded resulting in exposure of apoB to ubiquitin-proteasome degradation pathway – ER associated degradation (Fisher 2002). If nascent particles (pre-VLDL) are produced they might be secreted directly as large LDL (relatively TG-rich pool of LDL). However, the second step of pre-VLDL lipidation happens when lipid droplets come from Golgi, forming *bona fide* VLDL (Olofsson 2000). Hepatocytes secrete these particles into the circulation. Furthermore, apoB100 already incorporated into particles could be arrested in post-ER presecretory proteolysis (PERPP), resulting in a decrease of the secretion of most apoB lipoproteins (Fisher 2001). Fatty acids play a remarkable role in the fate of apoB100 by modulating its degradation in PERPP path. Saturated fatty acids are capable of inhibiting apoB proteolysis in the smaller particles (pre-Golgi), leading to an increase of secretion of the

large LDL. In contrast, n-3 polyunsaturated fatty acids stimulate PERPP of VLDL, decreasing their release (Pan 2004, Krauss 2004).

VLDL already contains apoE after secretion, while apoCII is transferred to the particle from HDL pool in circulation. Similar to chylomicrons, apoCII activated LPL rapidly hydrolyses VLDL's triglycerides. When fatty acids are progressively removed to the peripheral tissues, VLDL decreases in size, consequently becoming cholesterol-enriched IDL and further LDL. VLDL and its apoE-containing remnants are taken up by hepatocytes and peripheral tissues via a receptor specific mechanism. This employs binding to HSGP, while internalisation is mediated by the LDLR, LRP and VLDL receptor (Niemeir 1996). HDL may exchange cholesteryl esters for triglycerides of VLDL with the help of CETP and become enriched with phospholipids via PL transfer protein (PLTP) activity. ApoCII and apoE leave IDL back to HDL. Hepatic lipase is involved in IDL conversion to LDL (Rubinstein 1985). Remarkably, LDL finally contains only one molecule of apoB100 protein per particle. About 70% of LDL is internalised by the liver, the rest is taken up by extrahepatic tissues via interaction with ubiquitarily expressed LDL receptor.

Fatty acids are implicated in LDL metabolism by altering LDL receptor activity; the saturated lipids suppress receptor activity while the polyunsaturated fatty acids increase receptor-dependent LDL transport (Woollett 1992). Additionally, macrophages can bind modified (oxidized) LDL independently from the LDL receptor path, by expressing scavenger receptor (Illingworth 1993). In plenty of pathological circumstances LDL is becoming a major source of cholesterol for plasma hypercholesterinemia and in doing so it contributes greatly to the risk of arteriosclerosis development. Thus, LDL has deserved much attention during last few decades.

Reverse cholesterol transport

Peripheral (non-hepatic) cells obtain their cholesterol from a combination of local synthesis and the uptake of sterols from LDL and VLDL. The so-called "reverse cholesterol transport" (RCT) is the opposite movement of cholesterol from peripheral cells through the plasma compartment to the liver. This cholesterol is partly recycled by the liver in newly synthesized plasma lipoproteins like VLDL and partly appears in the bile as free cholesterol and bile acids. (Fielding 1995).

The RCT is mediated by HDL. Apolipoprotein AI is the major structural component of HDL (two to four apoAI molecules per particle) (Marcel 2003). It is expressed mostly by hepatocytes and enterocytes. Additionally apoAII, -AIV, -CII and -E are found on the particles. Apolipoproteins of HDL are exchangeable in contrast to apoB (Mahley 1984).

ATP-binding cassette transporter A1 (ABCA1, see below) translocates phospholipids and free cholesterol from cells to apoAI. This results in small discoidal particles, named prebeta-HDL (nascent HDL) (Chroni 2003, Denis 2004). Discoidal prebeta-HDL takes up cholesterol from peripheral cells, and changes to spherical particles, named HDL3 and later HDL2, as it becomes enriched in esterified cholesterol synthesized by LCAT (Glomset 1968). Two lipid transfer proteins contribute to further remodelling of HDL. PLTP supplies HDL with lecithin while CETP redistributes cholesteryl ester to TRL and LDL (Tollefson 1988, Tall 1993). HDL triglycerides are catabolised by the extracellular hepatic triglyceride lipase (Fielding 1991).

Scavenger receptor class B type 1 (SR-BI) is an authentic HDL receptor and mediates the selective uptake of HDL-derived cholesterol ester by the liver and triggers it to the bile degradation pathway (Acton 1996, Silver 2001). SR-BI is strongly expressed in liver parenchyma cells but also in adrenal glands and ovaries and moderately in macrophages, endothelial cells and vascular smooth muscle cells (Rhainds 2004). There is evidence suggesting that SR-BI is an endocytotic receptor in some circumstances, clearing HDL2 particles from circulation (Rhainds 2004). Although apoE containing HDL could be cleared by the liver via HSPG binding and LDL receptor and LRP uptake, it does not appear to represent a major pathway for the catabolism of the particles with simultaneous degradation of both apoAI and lipids. HDL is instead retroendocytosed by the liver and stimulates the redistribution of lipids and apoE recycling (Schmitz 1985, Heeren 2003).

1.2. The role of ABCA1 transporter in HDL metabolism

The transport of specific molecules across lipid membranes is an essential function of all living organisms and a large number of specific transporters have evolved to carry out this function. The largest transporter gene family is the ATP-binding cassette (ABC) transporter superfamily. These proteins translocate a wide variety of substrates including sugars, amino acids, metal ions, peptides, and proteins, and a large number of hydrophobic compounds and metabolites across extra- and intracellular membranes. ABC genes are essential for many processes in the cell, and mutations in these genes cause or contribute to several human genetic disorders, including cystic fibrosis, neurological disease, retinal degeneration, cholesterol and bile transport defects, anaemia and drug resistance. Characterisation of eukaryotic genomes has allowed the complete identification of all the ABC genes in *Saccharomyces cerevisiae*, *Drosophila melanogaster* and *Caenorhabditis elegans* genomes.

Many ABC genes play a role in the maintenance of the lipid bilayer and in the transport of fatty acids and sterols within the body (tab. 3, Dean 2001).

Family of transmembrane transporters

The ABC proteins bind ATP and use the energy to drive the transport of various molecules across the plasma membrane as well as intracellular membranes of the endoplasmic reticulum, peroxisome, and mitochondria (Dean 1995). ABC transporters contain a pair of ATP-binding domains, also known as nucleotide binding folds (NBF), and two sets of transmembrane (TM) domains, typically containing six membrane-spanning alpha-helices. The NBF contain three conserved domains: Walker A and B domains, found in all ATP-binding proteins and a signature (S) motif, located just upstream of the Walker B site (Hyde 1990). The S domain is specific to ABC transporters and distinguishes them from other ATP-binding proteins. The prototype ABC protein contains two NBF and two TM domains, with the NBF located in the cytoplasm. The molecules pump substrates in a single direction, typically out of the cytoplasm. For hydrophobic compounds, this movement is often from the inner leaf of the bilayer to the outer layer or to an acceptor molecule. ABC genes are organised as either full transporters containing two TM and two NBF or as half transporters containing one of each domain (Hyde 1990).

Table 3. List of some human ABC genes, chromosomal location, and function (Dean 2001)

Symbol	Location	Expression	Function
ABCA1	9q31.1	Ubiquitous	Cholesterol efflux onto HDL
ABCA2	9q34	Brain	Drug resistance
ABCA4	1p22.1–p21	Rod photoreceptors	N-retinylidene-PE efflux
ABCB1	7p21	Adrenal, kidney, brain	Multidrug resistance
ABCB2	6p21	All cells	Peptide transport
ABCB3	6p21	All cells	Peptide transport
ABCB4	7q21.1	Liver	PC transport
ABCB6	2q36	Mitochondria	Iron transport
ABCB7	Xq12–q13	Mitochondria	Fe/S cluster transport
ABCB11	2q24	Liver	Bile salt transport
ABCC1	16p13.1	Lung, testes, PBMC	Drug resistance
ABCC2	10q24	Liver	Organic anion efflux
ABCC3	17q21.3	Lung, intestine, liver	Drug resistance
ABCC4	13q32	Prostate	Nucleoside transport
ABCC5	3q27	Ubiquitous	Nucleoside transport
ABCC8	11p15.1	Pancreas	Sulfonylurea receptor
ABCD1	Xq28	Peroxisomes	VLCFA transport regulation
ABCG2	4q22	Placenta, intestine	Toxin efflux, drug resistance
ABCG5	2p21	Liver, intestine	Sterol transport
ABCG8	2p21	Liver, intestine	Sterol transport

PBMC, peripheral blood mononuclear cells; VLCFA, very long chain fatty acids.

The half transporters assemble as either homodimers or heterodimers to create a functional transporter. The ABC genes are widely dispersed in the genome (tab. 3) and show a high degree of amino acid sequence identity among eukaryotes. Phylogenetic analysis has allowed the gene superfamily to be divided into seven subfamilies and six of these subfamilies are found in both mammalian and the *S. cerevisiae* genome.

ABCA1 – major transporter for cholesterol and phospholipids

Structure and function of ABCA1 transporter. The cDNA of ABCA1 (NCBI Acc. Nr. AJ252277) contains an open reading frame encoding a 2261 amino acid polypeptide with a calculated molecular mass of 254 kDa. The human ABCA1 gene has been mapped to chromosome 9q31 and is composed of 50 exons spanning approximately 150 kb (Santamarina-Fojo 2000). ABCA1 is a full transporter. As a founding member of ABCA subfamily it consists of 14 hydrophobic domains (HD) and two ATP binding cassettes. Two TM domains are built up by HD1, 37 and HD 9-14 respectively. HD2 is exposed to the outer space of the cell; HD8 is a regulatory domain and located directly under the plasma membrane (fig. 1).

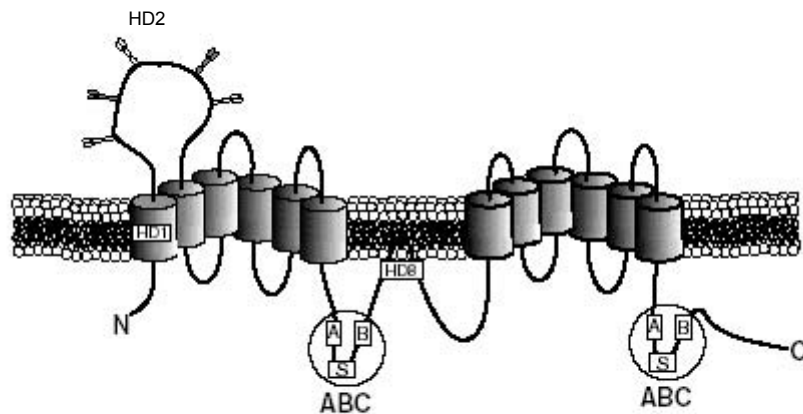


Figure 1. Model of the topological organisation of the human ABCA1 (Schmitz 2001)

ATP-binding cassette (ABC) consists of Walker A and B motifs and family specific signature (S) region; The location of consensus sequences for N-linked glycosylation is shown in the putative loop; The highly hydrophobic segment HD8 intersecting the regulatory domain dips into the inner leaflet of the membrane.

Transporter molecules are expressed ubiquitously by peripheral tissues and by the liver. Confocal fluorescent microscopy helped to localise ABCA1 transporter not only on the cell surface but also on the intracellular vesicles that include a novel subset of early endosomes, as well as late endosomes and lysosomes (Neufeld 2001). ABCA1 is expressed by hepatocytes solely on the basolateral surface and associated vesicles (Neufeld 2002).

Apolipoprotein AI, the structural component of HDL, is an essential lipid acceptor for ABCA1 dependent phospholipids and cholesterol co-transport. The first step in HDL formation involves a specific interaction of lipid-poor apoAI and ABCA1. There is evidence that apoAI binds to ABCA1 directly; however, it has also been suggested that apoAI may bind to a lipid domain created by ABCA1 activity (Wang 2000, Chambenoit 2001). Regardless of the interaction, the end result is a nascent HDL particle containing apoAI, phospholipids, and cholesterol. It remains unclear whether apoAI obtains phospholipids and cholesterol together or in a two-step process involving apoAI receiving phospholipids before obtaining cholesterol (Oram 2002, Wang 2001).

Two possibilities exist for the source of cholesterol utilised by ABCA1: plasma membrane or intracellular. Evidence exists that ABCA1 may also use plasma membrane cholesterol from isolated lipid rafts or caveolae (Drobnik 2002, Arakawa 2000). Alternatively, ABCA1 can mediate cellular lipidation of apoAI via endocytic pathway. ABCA1 resides on the plasma membrane as well as in endocytic vesicles and can shuttle between late endocytic compartments and the cell surface (Neufeld 2001). Takahashi provided evidence that cellular cholesterol efflux involves endocytosis and resecretion of apoAI (Takahashi 1999). Smith *et al.* have shown that apoAI co-localises with ABCA1-containing endosomes (Smith 2002). More recently, a study looking specifically at ABCA1-mediated cholesterol efflux showed that an endosomal-lysosomal pool is a preferred source (Neufeld 2004).

Additionally, SR-BI may consistently limit the extent of cholesterol, but not PL, efflux by ABCA1 in macrophages by capturing esterified cholesterol (synthesized by LCAT) (Chen 2000). Thus, a fraction of FC efflux by ABCA1 is recaptured by SR-BI selective lipid uptake and returns to the plasma membrane as CE. Alternatively, SR-BI and ABCA1 may co-operate in cholesterol efflux, since SR-BI performs not only CE flux but also contra-directional efflux of free cholesterol. Different substrates may be then utilised, ABCA1 acting on poorly lipidated apoAI and SR-BI in caveolae/rafts acting on small discoidal HDL particles or HDL3, especially when the cholesterol status of cells is high (Tall 2002).

Regulation of ABCA1 activity. Cholesterol is a potent inducer of ABCA1 expression. Among the primary mediators in this regulation are the liver X receptors (LXR) $\alpha\beta$ and retinoid X receptor (RXR) α . LXR and RXR are activated by oxysterols and retinoids respectively, form heterodimer and bind to response element within the ABCA1 gene promoter (Costet 2000).

ApoAI activates ABCA1 phosphorylation through the cAMP/protein kinase A (PKA)-dependent pathway; apoAI-mediated cAMP production required high expression of functional ABCA1; and Tangier disease mutants (see below) have defective apoAI-mediated cAMP signalling. These three points suggest that apoAI may activate cAMP signalling through G protein-coupled ABCA1 transporter (Haidar 2004). If PKA stabilises ABCA1 and does not influence apoAI binding, Janus kinase 2, in contrast, has a severe influence on apolipoprotein interaction with ABCA1 (Tang 2004). Protein kinase C alpha (PKC) phosphorylates and stabilizes ABCA1. PKC is activated by apoAI via phospholipase C generation of diacylglycerol. This may be initiated by the removal of cellular sphingomyelin (Yamauchi 2003). Also apoAI prevents ABCA1 calpain-mediated degradation (Arakawa 2002).

It has been reported that polyunsaturated fatty acids can modulate ABCA1 expression by the LXR pathway, acting as antagonists to oxysterol binding (Ou 2001). Additionally, unsaturated fatty acids (USFAs) markedly inhibit ABCA1-mediated cholesterol and phospholipid efflux from macrophages in vitro, when ABCA1 was induced by a cAMP analog, since USFAs reduce macrophage ABCA1 content by enhancing its degradation rate (Wang 2002). Native LDL itself elevates ABCA1 in both protein and mRNA levels through the LXR/RXR (Liao 2002).

Finally, regulation of the ABCA1 activity may be done via influencing sphingomyelinase. The majority of sphingomyelin exist in the plasma membrane, but roughly 25% of cellular sphingomyelin is contained in the lysosomes, endosomes and Golgi combined. By modulating sphingomyelin content, cholesterol could either be made available to or sequestered from ABCA1. Furthermore, the ceramide released from an interaction with sphingomyelin is potent in increasing cell surface level of ABCA1 protein (Witting 2003).

Tangier disease

It was widely believed that HDL protects against arteriosclerosis by clearing excess cholesterol from cells of the artery wall, particularly macrophages. However, the mechanisms by which HDL accomplishes this function were hotly debated for two decades until the end of 90's breakthroughs in understanding the physiology of reverse cholesterol transport were made. Using a graphical linkage exclusion strategy, Rust *et al.* assigned the Tangier disease (TD) genetic locus to a 7 cM region of chromosome 9q31 (Rust 1998). Subsequently, several groups independently identified the TD gene to be an ABCA1 transporter (Brook-Wilson 1999, Bodzioch 1999, Rust 1999).

Tangier disease is an autosomal recessive metabolic disorder. The most striking feature in Tangier patients is the almost complete absence of plasma HDL (hypoalphacholesterolemia), low serum cholesterol levels and a markedly reduced efflux of both cholesterol and phospholipids from cells (Francis 1995). Cholesteryl ester accumulation in tissue macrophages of classical Tangier patients leads to splenomegaly, enlarged tonsils and lymph nodes. Peripheral neuropathy has also been reported in some TD individuals (Assmann 1985). The low HDL level seen in TD is mainly due to an enhanced catabolism of HDL precursors (Bojanovski 1987). Human TD fibroblasts were the first experimental model to study ABCA1 function in HDL metabolism, as well as Wisconsin Hypoalpha Mutant chicken – naturally occurring animal model and the later designed mouse ABCA1 knockdown (Oram 2002, Schmitz 2001).

Animal models for studying ABCA1 in HDL metabolism

Mice with a targeted inactivation of ABCA1 display morphologic abnormalities and perturbations in their lipoprotein metabolism concordant with TD: decreased body weight, splenomegaly, enlarged tonsils and fat-soluble vitamin deficiency (Orso 2000). Normal placenta expresses high level of ABCA1 (Langmann 1999). Therefore, in *abca1*^{-/-} females a severe malformation of this organ results in a strongly reduced ability to bear young has been observed. However, a peripheral sensory neuropathy present in TD patients could not be detected in ABCA1 knockout mice, indicating some influence of other human gene loci (Christiansen-Weber 2000).

Structural and functional abnormalities in caveolar processing and the trans-Golgi secretory pathway indicate that the process of lipid export involved vesicular

budding between the Golgi and the plasma membrane are severely disturbed in fibroblasts lacking functional ABCA1 (Orso 2000). Like in human patients with TD, fibroblasts from *abca1*^{-/-} mice display an almost complete absence of apoAI-dependent efflux of CH and PL, suggesting that the co-transport of both lipid classes is facilitated by ABCA1 (Christiansen-Weber 2000). Furthermore, it was anticipated that overexpression of ABCA1 might result in an increased efflux. In support of this, stable expression of murine wild type ABCA1 in HEK293 cells significantly enhanced apoAI specific docking and cholesterol and phospholipids efflux (Wang 2000).

Next ABCA1 overexpressing models were constructed. Transgenic mice had equal hepatic and macrophage expression of human ABCA1; enhanced macrophage cholesterol efflux to apoAI; increased plasma CH, CE, FC, PL, HDL cholesterol; and increased levels of apoAI and apoB. ABCA1 overexpression results in a delay of apoAI catabolism in both liver and kidney, leading to increased plasma apoAI levels (Vaisman 2001).

Few studies have shown that adenoviral-mediated liver specific overexpression of ABCA1 in mice leads to a phenotype similar to ABCA1 transgenic. Interestingly, overexpression of transporter by only the liver contributes to the apoAI dependent cholesterol efflux the same as all tissues do in ABCA1 transgenic model (Wellington 2003, Basso 2003). However, it was remarkable that ABCA1 pathway in peripheral macrophages in mice made only a minor contribution to HDL formation. It was nearly impossible to restore normal HDL phenotype in *abca1*^{-/-} recipient mice by donating them ABCA1 expressing macrophages via bone marrow transplantation from wild type animals (Haghpasand 2001). These examples both imply that liver ABCA1 is responsible for generating most of the plasma HDL and that the major cause of the HDL deficiency in TD patients and ABCA1 knockout mice is an impaired liver ABCA1 pathway.

1.3. Post-transcriptional gene silencing – RNA interference

A heritable change in gene expression that cannot be explained by changes in gene sequence (mutations, rearrangements *etc.*) is an epigenetic regulation mechanism. It can result in the repression (silencing) or activation of gene expression. Until the end of the 1980s, only modifications of DNA (methylation) or proteins that lead to transcriptional repression or activation, or to the formation of prions, were classified as epigenetic (Lewin 1998). During the 1990s, however, a number of gene-silencing phenomena that occurred at the post-transcriptional level were discovered in plants, introducing the concept of post-transcriptional gene silencing (PTGS) or RNA silencing. PTGS results in the specific degradation of a population of homologous RNAs. It was first observed after introduction of an extra copy of an endogenous gene (or of the corresponding cDNA under the control of an exogenous promoter) into plants. Because RNAs encoded by both transgenes and homologous endogenous genes were degraded, the phenomenon was originally called co-suppression (Napoli 1990). Post-transcriptional gene silencing in plants is an epigenetic regulatory mechanism.

PTGS greatly reduces mRNA accumulation in plant cytoplasm but does not affect transcription (van Blokland 1994). Detailed analysis of RNA content in plants exhibiting PTGS has revealed the presence of discrete RNA degradation intermediates. For example, in glucanase (trans)-genes, both longer and smaller RNAs were found. The longer RNAs result from aberrant processing, whereas the smaller RNAs correspond to subfragments of the mRNA, which suggests that degradation starts with an endonucleolytic cleavage followed by exonuclease digestion (van Eldik 1998).

In higher plants, a natural role of RNA silencing appears to be a defence mechanism against viruses, since PTGS is activated by viral RNAs, which replicate via double-stranded intermediates (Covey 1997, Waterhouse 1998). However, it is also possible that ssRNA is converted to dsRNA by an RNA-dependent RNA polymerase (RdRP) (Lindbo 1993). In support of this hypothesis, the activity of a putative RdRP encoding locus is required for RNA silencing in *Arabidopsis* (Mourrain 2000). A similar phenomenon in the fungus *Neurospora crassa* was named quelling (Romano 1992).

Phenomenon and mechanism of RNA interference in animals.

In 1998 Fire *et al.* reported on potent and specific genetic interference by double-stranded RNA in *C. elegans* (Fire 1998). This phenomenon was called RNA interference (RNAi) and is naturally involved in the timing of larvae development. RNAi can spread within the individual and can be transmitted to offspring, moreover only a few molecules of dsRNA are sufficient to trigger RNAi. These suggest the presence of catalytic and amplification components in the interference process. RNAi occurs at the post-transcriptional level since dsRNA fragments corresponding to promoter and intron sequences do not activate the classical RNAi pathway. RNAi is a highly specific process: the injection of dsRNA homologous to particular gene eliminates or decreases the corresponding mRNA only.

Further experiments with *C. elegans* showed that the RNAi can be initialised by: micro-injection of dsRNA into the cytoplasm of the intestinal cells, feeding the worms on engineered *E. coli* producing dsRNA against the target gene and even simply soaking the worms in dsRNA solution (Fire 1998, Timmons 1998, Tabara 1999).

Biochemical studies in fruit fly embryo lysates helped to postulate the mechanism by which RNAi works (Tuschl 1999).

- 1) RNAi is initiated by an ATP-dependent, processive cleavage of dsRNA into 21 to 23 nt small interfering RNAs (siRNAs) by the enzyme Dicer, a member of the RNase III family of dsRNA-specific endonucleases (Hammond 2000, Bernstein 2001).
- 2) These native siRNA duplexes containing 5'-phosphate and 3'-hydroxyl termini are then incorporated into a protein complex called RNA-induced silencing complex (RISC) (Hammond 2000).
- 3) ATP-dependent unwinding of the siRNA duplex generates an active complex, RISC* (the asterisk indicates the active conformation of the complex) (Nykanen 2001).
- 4) Guided by the antisense strand of siRNA, RISC* recognises and cleaves the corresponding mRNA (Elbashir 2001b) (fig. 2).

Elbashir *et al.* have demonstrated that RNAi can be induced in numerous mammalian cell lines by introducing synthetic 21 nt siRNAs (Elbashir 2001a). By virtue of their small size, these siRNAs avoid provoking a cellular interferon response in mammalian cells on a foreign dsRNA (Stark 1998). Functional studies with synthetic siRNA in *Drosophila* cell lysates have demonstrated that each siRNA duplex cleaves its target RNA at a single site. The 5'-end of the guide siRNA sets the rule for defining the position of target RNA cleavage. Mutation studies have shown that a single mutation within the centre of a siRNA duplex discriminates between mismatched targets (Elbashir 2001c). A more stringent requirement has been shown to be for the antisense strand of the trigger dsRNA as compared to the sense strand (Chiu 2002).

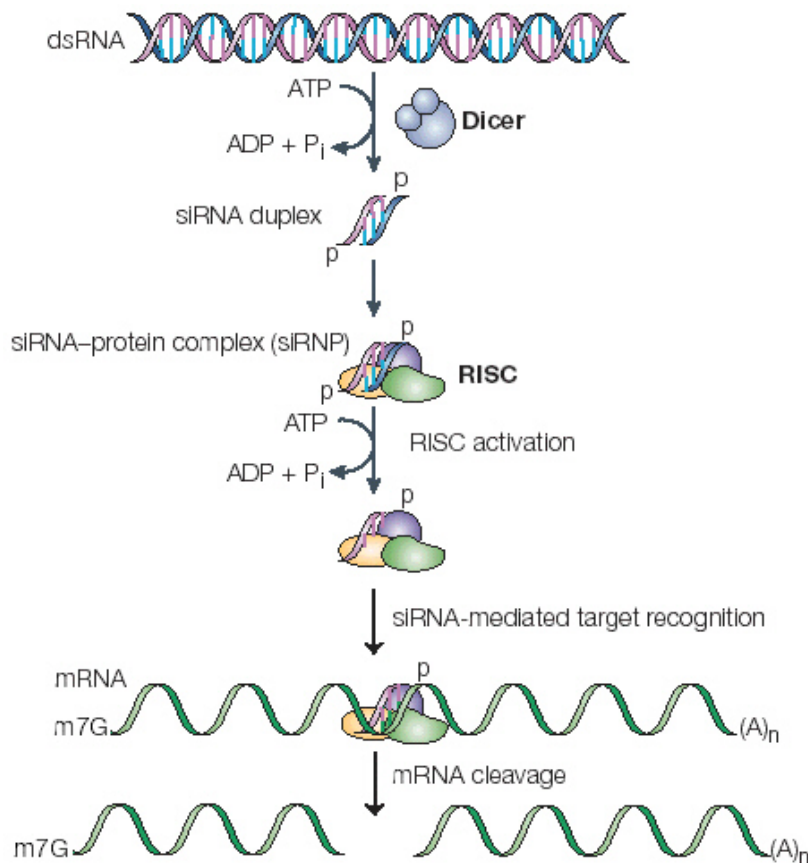


Figure 2. Schematic overview of possible RNA interference pathway in animals

Double strand (ds) RNA is processed by the ATP dependent RNase DICER to small interfering (si) RNA, RNA inducible silencing complex (RISC) is formed with siRNA After ATP dependent siRNA unwinding RISC attacks the target mRNA using the anti-sense siRNA as a guide, leading to the degradation of the mRNA (Dykxhoorn 2003).

Some particularly fascinating aspects of RNAi are its extraordinary efficiency and time-dependent effect. It has been estimated that in *Drosophila* embryos, ~35 molecules of dsRNA can silence a target mRNA thought to be present at >1000 copies per cell (Kennerdell 1998). RNAi reaches its maximum activity only 42 hours after transfection of synthetic siRNA. That may reflect a time lag between target mRNA degradation and the half-life of the existing protein expressed from the target gene as well as a need for the siRNAs to be processed or assembled into an active complex (Chiu 2002).

Stable expression of small interfering RNAs for functional gene knockdown.

The discovery of the potency of the synthetic 21 nt siRNAs to specifically suppress the expression of the endogenous and heterologous genes in different mammalian cell lines has opened a broad gate for analysis of gene function and gene-specific therapy (Elbashir 2001a). The disadvantages of this approach were the high costs and technical inconvenience of RNA work.

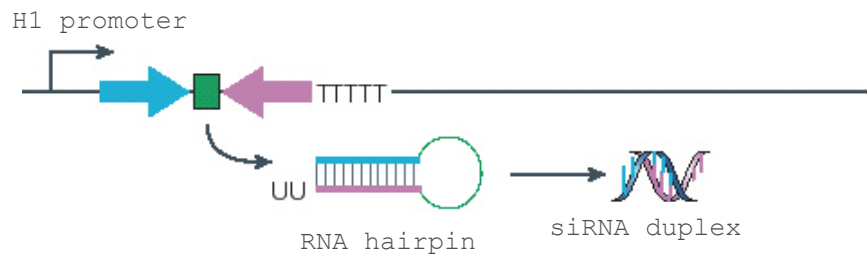


Figure 3. Technical approach utilising siRNA phenomena

Transcription of the self-palindromic RNA from the DNA source (plasmid, viral vector *etc.*) results in small hairpin RNA formation (loop in green). Dicer cleaving the loop produces a small RNA duplex (sense and antisense molecules are in blue and red respectively).

Brummelkamp *et al.* proposed a much easier system allowing siRNA expression from a DNA vector as a small hairpin RNA precursor (shRNA), which is processed into the active siRNA by the cellular machinery (Brummelkamp 2002).

Basically, the H1 RNA promoter was used to generate shRNAs. The H1 promoter drives the expression of a unique gene encoding H1 RNA, the RNA component of the human RNase P. The H1 RNA gene is transcribed by RNA

polymerase III into a small RNA transcript. This promoter is highly permissive for the nucleotide at the +1 position, which is originally an A. The gene specific shRNA contains a 19 nt sequence derived from the target transcript, separated by a short spacer (5-9 nt) from the reverse complement of the same 19 nt sequence. The resulting transcript is predicted to fold back on itself to form a 19 nt stem-loop structure (fig. 3). The termination sequence consists of a stretch of 5 thymidines. The cleavage of the transcript after the termination signal occurs after the second uridine generating a 2 nt 3' overhang (Baer 1990).

Finally, the aforementioned siRNA expressing vector was transferred into an adenoviral delivery system and retroviral vector, making RNA interference a more useful tool for broad spectrum of *in vitro* and *in vivo* biomedical research (Shen 2003, Stewart 2003, Liu 2004).

1.4. Adenoviral vectors and gene delivery

Adenoviruses were first discovered half a century ago in adenoids of humans with acute respiratory illness (Hillemann 1954, Rowe 1953). It was found that adenoidal tissue containing these agents underwent spontaneous degeneration after surgical removal. Currently about 200 adenoviral species, which infect birds, many mammals, and man, are organised into three genera: *atadenovirus*, *aviadenovirus* and *mastadenovirus*. There are 50 independent human pathogens classified into 6 serological classes (A – F). Most adenovirus infections in humans involve either the respiratory or gastrointestinal tracts or the eye. Adenovirus infections are very common, often are asymptomatic. Most people have been infected with at least one type of virus at the age of 15 and generated an immunity (Modrow 1997).

Structure and function of humane adenovirus serotype 5

Human adenovirus serotype 5 (*mastadenovirus*, human adenovirus C) is perhaps the best described and may be taken as a “typical” adenovirus.

It has a non-enveloped, icosahedral protein capsid, ~80 – 90 nm in size and consists of 252 capsomers: 240 “hexons” and 12 “pentons” at vertices of an icosahedron. The hexons consist of a trimer of polypeptide II with a central pore, and polypeptides VI, VIII and IX as minor components, which are thought to be involved in

stabilisation and/or assembly of the particle. The pentons are more complex; the base consists of a pentamer of peptide III and 5 molecules of IIIa. The pentons have a toxin-like activity, purified pentons causing cytopathic effect (c.p.e.) in the absence of any other virus components. The thin glycoprotein fibre (IV) protrudes from the centre of each penton. The core of the particle contains the terminal proteins covalently attached to the 5'-end of each DNA strand, and peptides V and VII – basic proteins, similar to histones, which are non-covalently associated with the viral chromosome forming a “chromatin-like” substance (fig. 4).

Adenovirus genome is a double stranded, linear, non-segmented DNA and it is ~36 kb in size. The terminal sequences of each strand (102 bp) are inverted repeats, hence the denatured single strands can form "panhandle" structures (Chroboczek 1992). The adenovirus packaging signal is located at the map units 0.5 – 1.1 of the genome. It is ~500 bp in length and has about 5 individual functional units and is absolutely necessary for the packaging of viral DNA into capsids (Grable 1992, Grable 1990, Hearing 1987).

Depending on the timing of the protein appearance during the infection cycle, encoded genes are divided into immediate early (E1A), early (E1B, E2, E3, E4) and late (L1-L5) groups. Products of the immediate early genes regulate expression of the early genes. This protein is a trans-acting transcriptional regulatory factor. Early genes are mostly responsible for viral DNA replication. They are encoded at various locations on both strands of the DNA. Multiple protein products are made from each gene by alternative splicing of mRNA transcripts – splicing was first discovered in adenoviruses (Berk & Sharp 1977). The assembly of viral particles occurs in the nucleus. At the late infection stage, synthesized viral proteins may interfere with the host immune system as factors of cytotoxicity. (Shenk 1996). Virions leave the infected cell by active lysis mainly with the “adenovirus death protein” E3 – 11,6 K (Tollefson 1996).

A new infection cycle starts when the adenovirus particle adheres and is internalised by the cell. At least two pairs of interacting molecules are involved in this process. First, the adenoviral fiber protein binds to the cell surface coxsackievirus and adenovirus receptor (CAR), then internalisation occurs only after contact between viral penton base protein and cellular integrin $\alpha_v\beta_5$ molecule (Bergelson 1997, Wickham 1993). Integrins and the penton base are thought to assist the acid-stimulated

virus release from early endosomes, ~15 min after internalisation (Greber 1993). By active lysing the endosome, virus passes to the cytosol. Next viral particle moves along the linear tracks of microtubules towards the nucleus. Penton base–integrin interactions together with reducing agents in endosomes also reactivate the viral cysteine protease L3/p23 inside the capsid. L3/p23 then degrades the internal protein VI (Greber 1996). This step thus weakens the capsid for final dissociation and DNA import into the nucleus.

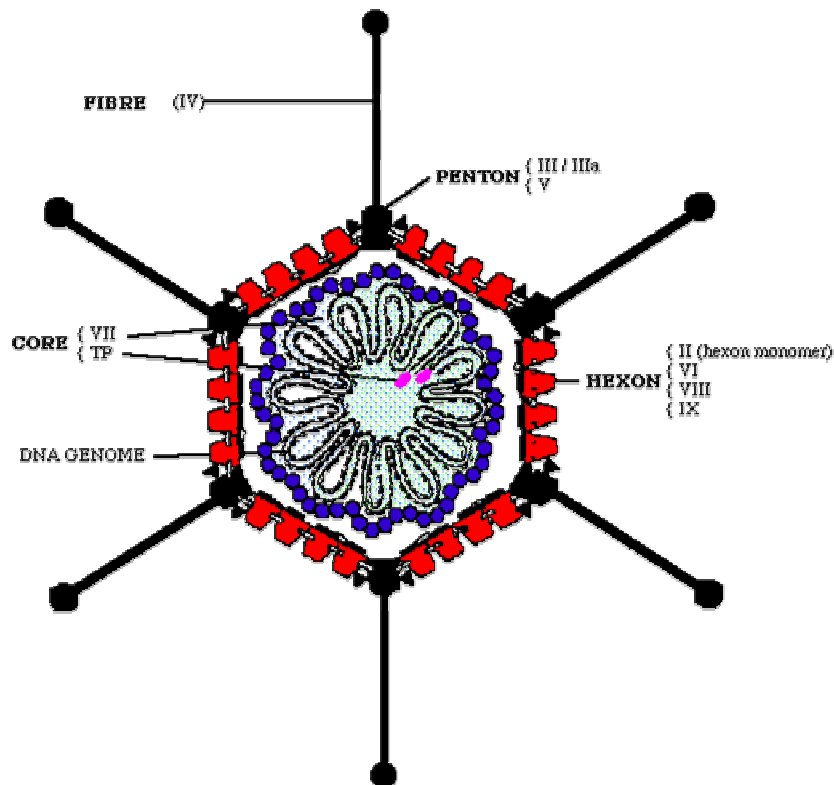


Figure 4. Schematic view of the human adenovirus particle, serotype 5 (Modrow 1997)

Recombinant adenovirus for in vitro and in vivo biological studies

Twenty-five years ago Graham *et al.* successfully immortalised human embryo kidney (HEK) cells by transfection of fragments of the adenoviral genome (Graham 1977). The adenoviral E1 region was responsible for this transformation. The E1A and E1B genes of this region is a transcriptional activator for various adenoviral and host cell genes and is absolutely required for productive infection. The deletion of the E1 region resulted in replication-defective adenoviral vectors, which were first constructed 20 years ago (Yamada 1985). Therefore, the cell line HEK293 contains integrated virus region E1 and provides it for virus replication in *trans-*

-complementation. Since the beginning of vector development, there were several attractive characteristics of the adenovirus based system. In contrast to retrovirus, adenoviruses infect non-dividing cells and have broad spectrum of infectivity. Adenoviruses can easily be concentrated to 10^{12} pfu/mL and have capacity for transgenes up to 5 kb (Romano 2000). The first application of adenovirus vectors in gene therapy clinical trials were conducted in the early 1990s for the treatment of patients with cystic fibrosis (Zabner 1993). Now, adenoviral vectors are employed in human cancer gene therapy (Roth 1997).

In addition, adenoviral vectors based on serotype 5 are excellent liver-directed gene transfer systems, as the adenovirus serotype 5 is preferentially localised in the liver of rodents after the intravenous injection (Jaffe 1992, Prevec 1989). An impressive breakthrough in the adenoviral vectors development field was made recently, when Xia *et al.* were able to show that siRNA expressed from adenoviral vectors *in vitro* and *in vivo* specifically reduces expression of stably expressed plasmids, endogenous genes and transgenes in mice (Xia 2002).

1.5. The aim of the study

The aim of the dissertation was to study the role of hepatic ABCA1 cholesterol transporter for HDL metabolism *in vivo*. It had been shown that ABCA1 is responsible for the HDL formation in plasma and therefore directing excess of cholesterol from peripheral tissues to the liver (reverse cholesterol transport). Recently some controversial data were obtained: first, it was shown that ABCA1 expressed in macrophages alone does not significantly contribute to the plasma HDL concentration, and second, it was discovered that liver specific overexpression of ABCA1 leads to a remarkable increase of HDL in plasma.

The aim of the study was to show directly if functional knockdown of hepatic ABCA1 alters HDL metabolism in steady state conditions in mice (*Mus musculus*).

The following steps were done to prepare this study:

- a) Establishment of an overexpression system to study ABCA1 in cell culture
- b) Development and construction of an original DNA vector for shRNA-mediated targeting of ABCA1 *in vitro*
- c) Real-time RT-PCR, Western blotting and immunofluorescence analysis of RNA interference efficiency *in vitro*
- d) Construction of a recombinant adenovirus for *in vivo* shRNA delivery
- e) Conducting of an animal study, which will employ FPLC analysis of plasma lipoproteins, liver mRNA determination and measurement of membrane proteins involved in the lipid metabolism.

These experiments should show, whether hepatic ABCA1 is responsible for HDL plasma concentration *in vivo*.

2. Methodological considerations

2.1. Materials

Diluents, solutions and buffers

All solutions were made with deionised water. In order to prevent DNA-contamination all solutions for molecular biology were autoclaved. For PCR reactions sterile water for injections was used. Methanol, ethanol, isopropanol (Merck), phenol and chloroform (Roth) were of molecular biology grade.

Chemistry, proteins and enzymes

All chemicals were from Merck, Roche, Roth, Serva, and Sigma companies.

Restriction endonucleases (*PacI*, *BseRI*, *AvaI*, *EcoRI*, *XhoI*, *SalI*, *SpeI*, *XbaI*, *PflMI*, *BamHI*, *SnaBI*, *SphI*, *NotI* and *NheI*) as well as CIP and T4 DNA ligase all were from New England Biolabs.

M-MLV Reverse Transcriptase and placenta RNase inhibitor both were from Invitrogen.

Kits

Adeno-X rapid titre, BD biosciences, K1653-1

DNA molecular weight marker, Fermentas, SM0333

Enzymatic colorimetric test for cholesterol, Roche, 1489437

Enzymatic colorimetric test for triglyceride, Roche, 1488899

Enzymatic colorimetric test for phospholipids, Roche, 1485424

NucleoSpin[®] extract, Macherey-Nagel, 740590

NucleoSpin[®] plasmid, Macherey-Nagel, 740588

NucleoSpin[®] RNA II, Macherey-Nagel, 740955

Protein assay Bradford reagent, Biorad, 500-0111

SYBR[®] Green PCR Master Mix, Applied Biosystems, 4309155

Primers

All primers were designed using software “Primer Designer” for Windows (version 3.0) and synthesised by MWG – Biotech AG. Sequences, size, melting temperature, location in correspondent cDNA and its accession number in [NCBI](#) is shown below, (FP – forward primer, RP – reverse primer, C – complementary strand)

Sequencing primer for shRNA insert into pALsh vector

seqALsh ACAGCTATGACCATGATTAC (20 bp, position 62 (C) in plasmid pALsh ([Laatsch 2004](#)))

Cloning primers for anti-ABCA1 small hairpin RNAs, symmetry axis of shRNA is indicated by vertical line, nucleotides in antisense to the ABCA1 mRNA are underlined.

ABCA1III GGTCTTGTTACCTCAGCCA|TGGCTGAGGTGAACAAGACCTT (42 bp,
position 1502 in [NM013454](#))

ABCA1III GAGGGGCATTGACCGGCTCA|TGAGCCGGTCAATGCCCTCTT (42 bp,
position 2221 in [NM013454](#))

ABCA1IV CCTGGCAGCAGCCTGTGGGGG|CCCCACAGGCTGCTGCCAGGTT (44 bp,
position 2547 in [NM013454](#))

ABCA1V GCCACAGGAGACAGCAGGCTAG|CTAGCCTGCTGTCTCCTGTGGCTT (46 bp,
position 2652 in [NM013454](#))

ABCA1VII TTGCACATATCCCAGACAAAA|TTTGTCTGGGATATGTGCAATT (44 bp,
position 5421 in [NM013454](#))

qRT-PCR primers

Human origin

hGAPDH-FP ACTGCCACCCAGAAGACTGT (20 bp, $T_m = 71$ °C, position 619 in [NM002046](#))

hGAPDH-RP ACCACCTTCTTGATGTCATCATA (23 bp, $T_m = 70$ °C, position 860 (C) in
[NM002046](#))

hABCA1-FP ACTCTTAAACGCCCTCACCAAAGAC (25 bp, $T_m = 76$ °C, position 4522 in
[NM005502](#))

hABCA1-RP	GTCTGGGGAAGCTGGGGCAGT (20 bp, $T_m = 77^\circ\text{C}$, position 4644 (C) in NM005502)
hLRPFP	CATGCTGCCTTCAGGGAGAC (20 bp, $T_m = 75^\circ\text{C}$, position 14313 in NM002332)
hLRPRP	GGAGAGCCTTGCAAGGTGT (20 bp, $T_m = 73^\circ\text{C}$, position 14447 (C) in NM002332)
Mouse origin	
mABCA1FP	GACGGAGCCGGAAGGGTTTC (20 bp, $T_m = 78^\circ\text{C}$, position 4339 in NM013454)
mABCA1RP	CCCAGCCAAGCAAGGGGTAT (20 bp, $T_m = 76^\circ\text{C}$, position 4613 (C) in NM013454)
mPGK1FP	TGTGAATCTGCCACAGAAGG (20 bp, $T_m = 71^\circ\text{C}$, position 556 in NM008828)
mPGK1RP	GATGTGCCAATCTCCATGTT (20 bp, $T_m = 70^\circ\text{C}$, position 789 (C) in NM008828)
mB2MFP	GGCCTGTATGCTATCCAGAA (20 bp, $T_m = 70^\circ\text{C}$, position 103 in NM009735)
mB2MRP	TGCAGGCGTATGTATCAGTC (20 bp, $T_m = 69^\circ\text{C}$, position 355 (C) in NM009735)
mApoA1FP	AGGTCACCCACACCCTTCA (19 bp, $T_m = 73^\circ\text{C}$, position 28 in NM009692)
mApoA1RP	TCCAGGAGATTCAGGTTTCA (20 bp, $T_m = 69^\circ\text{C}$, position 260 (C) in NM009692)
mApoEFP	TGACCAGGTCCAGGAAGAG (19 bp, $T_m = 70^\circ\text{C}$, position 207 in BC028816)
mApoERP	GTTGCGTAGATCCTCCATGT (20 bp, $T_m = 69^\circ\text{C}$, position 414 (C) in BC028816)
mCyp7a1FP	CACCATTCCTGCAACCTTCT (20 bp, $T_m = 72^\circ\text{C}$, position 927 in NM007824)
mCyp7a1RP	CCGGATATTCAAGGATGCAC (20 bp, $T_m = 72^\circ\text{C}$, position 1152 (C) in NM007824)
mSR-BIFP	TCTTCACTACGCGCAGTATG (20 bp, $T_m = 69^\circ\text{C}$, position 1512 in NM016741)
mSR-BIRP	GGCTGGTCTGACCAAGCTAT (20 bp, $T_m = 71^\circ\text{C}$, position 1775 (C) in NM016741)
Universal primers	
uABCA1FP	AACAACACTACAAAGCCCTCTTTG (22 bp, $T_m = 69^\circ\text{C}$, position 1295 in NM005502)
uABCA1RP	TTGTTTACCTCAGCCATGAC (20 bp, $T_m = 70^\circ\text{C}$, position 1515 (C) in NM005502)
EAFFPF	GCGCTACCGGACTCAGATCTCG (22 bp, $T_m = 75^\circ\text{C}$, position 595 in pEGFP-N1)
EAFPRP	ATGGTGGCGACCGGTGGAT (19 bp, $T_m = 73^\circ\text{C}$, position 680 (C) in pEGFP-N1)
Oligo(dT)₁₂₋₁₈	100 µg/mL in TE (pH 8.0), Invitrogen, 18418-012

Antibodies

α Hexon, murine anti-Hexon, 1:1000 for adenovirus titration, in Adeno-X rapid titre kit, BD.
 α FLAG, murine, monoclonal IgG, 1:2500 for IMF, Sigma.
 α ABCA1, rabbit, polyclonal IgG, 1:250 for Western, Biocompare.
 α SR-BI, rabbit, polyclonal IgG, 1:30000 for Western, a gift from J.C. Fruchard, France.
 α ApoA1, mouse, monoclonal IgG, 1:1000 for Western, BD.
 α ApoCIII, rabbit, polyclonal IgG, 1:1000 for Western, Bidesign.
 α ApoE, rabbit, polyclonal IgG, 1:2000 for Western, DAKO.
 α LDLR, chicken, polyclonal IgY, 1:250 for Western, Progen.
 α LRP-377, rabbit, polyclonal IgG, 1:10000 for Western, a kind gift from J. Herz, USA.
 α M-Cy3, donkey anti- mouse IgG Cy3 conjugated, 1:500 for IMF, Jackson.
GAMPO, goat anti-mouse IgG HRP conjugated, 1:5000 for Western, Jackson.
GARPO, goat anti-rabbit IgG HRP conjugated, 1:5000 for Western, Jackson.
RACPO, rabbit anti-chicken IgY HRP conjugated, 1:2500 for Western, Jackson.
 α Mouse, rat anti-mouse IgG HRP conjugated, 1:500 for Ad. titration, in Adeno-X rapid titre kit, BD.

Plasmids, adenovirus, bacteria strains, cells and animals lines

Plasmids used in the this study for details see also appendix.

pALsh, 3.2 kb, Amp, ([Laatsch 2004](#))
pcDNA3.1-mABCA1-FLAG, 12 kb, Amp, obtained from Dr. F. Rinninger (Wang 2000)
pE1.1, 2.7 kb, Kan, from O.D.260 Inc., www.od260.com (Danthinne 2001)
pEGFP-N1, 4.7 kb, Kan, Clontech, 6085-1 (Cormack 1996, Chalfie 1994)
pAdenoQuick1.1, 39 kb, Amp, from O.D.260 Inc., www.od260.com (Danthinne 2001)

Adenovirus:

Ad-EGFP, $1.2 \cdot 10^{11}$ mL⁻¹, kind gift from Dr. R. Vogel (Max-Planck-Department for structure biology, Hamburg, Germany)

Bacteria:

E.coli DH5 α F', genotype: [F'/endA1 hsdR17 (r_K⁻m_K⁺) glnV44 thi-1 recA1 gyrA (Nal^r) relA1 Δ (lacIZYA -argF)U169 deoR (ϕ 80 dlac Δ (lacZ)M15)], subclonig efficiency, GibcoBRL, 18265-017 (Crowther 1989)

Eukaryotic cell lines:

HEK293 – human embryo kidney, transformed by adenoviral E1 region, passage 20-30 (Graham 1977).

HuH7 – human hepatoma cell line, UKE, Hamburg, Germany (Nakabayashi 1982).

Mice:

C57BL6/1 – wild type, from UKE animal facility, Hamburg, Germany.

Cell culture materials

Dulbecco's MEM with Glutamax-1, Gibco, 31966-021

RPMI-1640 with Glutamax-1, Invitrogen, 61870-010

PBS, Dulbecco's complete, pH 7.4, Gibco, 14190-094

Trypsin-EDTA, Gibco, 25300-054

Trypan Blue, Sigma, T8154

Foetal Bovine Serum (FBS), Gibco, 10106-169

Penicillin-Streptomycin (10000 U/mL), Gibco, 15140-122

2.2. Methods

Bioinformatics

All information concerning DNA and protein sequences was obtained from public database at www.ncbi.nlm.nih.gov. Sequence alignments were done using BLAST-2-sequences service at the same Internet site.

Directional cloning into plasmid vectors

Directional cloning requires that the plasmid vector be cleaved with two restriction enzymes that generate incompatible termini and that the fragment of DNA to be cloned carries termini that are compatible with those of the doubly cleaved vector.

Materials

TE (10 mM TRIS-Cl; 1 mM EDTA; pH 8.0)

10x T4 DNA ligase reaction buffer (500 mM TRIS-HCl; 100 mM MgCl₂; 10 mM ATP; 100 mM DTT; BSA 250 μ g/ml; pH 7.5)

CIP – alkaline phosphatase, calf intestinal; bacteriophage T4 DNA ligase; restriction endonucleases; vector DNA (plasmid); target DNA fragment

Method (Ish-Horowicz 1981)

1. The vector (10 μg) and foreign DNA were digested with appropriate restriction enzymes.
2. Vector DNA was treated with CIP to avoid recircularisation.
3. DNA fragment was separated by agarose gel electrophoresis (see below). The vector DNA was purified by spin-column chromatography followed by elution with TE buffer.
4. DNA concentration was measured photometrically (see below) and calculated in pmol/ml, assuming that 1 bp has a mass of 660 Daltons.
5. The digested vector and insert were mixed at the molar ratio approx. 1:3 in the ligation reaction and the final DNA concentration was approx. 10 ng/ μl .

Then next components were added together:

10x ligation buffer	1 μL
Bacteriophage T4 DNA ligase	100 U
DNA insert	
DNA vector	
H ₂ O	to 10 μL

6. The reaction mixture was incubated over night at 16 °C or for 4 hrs at 20 °C.
7. Competent *bacteria* were transformed with 1 μL of ligation mix (see below).

Bacterial transformation

(Heat-shock transformation)

Materials

Subclone efficiency bacteria DH5 α

SOC (Tryptone, 20 g; Yeast extract, 5 g; NaCl, 3 g; H₂O, to 1000 mL; pH 7.0)

LB agar (Tryptone, 10 g; Yeast extract, 5 g; NaCl, 5 g; H₂O, up to 1000 mL; pH 7.5;

Agar-agar 15 - 30 g) *autoclaved*, with antibiotic for plasmid selection

Plasmid DNA (~1 ng/ μL), ligation mixture

Method

1. 30 μL to 50 μL of competent bacteria were taken from $-70\text{ }^{\circ}\text{C}$, placed into 1.5 mL tube and slowly refrozen on ice.
2. Approx. 1 ng of plasmid DNA (for retransformation) or 1 μL of ligation mix were added to bacteria suspension, carefully mixed and incubated on ice for 15-30 min.
3. Heat shock was performed by incubating the bacteria at $42\text{ }^{\circ}\text{C}$ for 1 min and then immediately placing on ice for 2 min.
4. After heat shock 300 μL of SOC-medium without any antibiotic was added. Cell suspension was incubated at $37\text{ }^{\circ}\text{C}$ for ~ 1 hr.
5. Transformed bacteria were plated on LB-agar plates with corresponding antibiotic and incubated at $37\text{ }^{\circ}\text{C}$ over night.

Glycerol stock of transformed bacteria

Materials

Glycerol stock-media (Glycerol, 65 mL; 1 M MgSO_4 , 10 mL; 1 M TRIS-HCl 2.5 mL; H_2O , up to 100 mL; pH 8.0), *sterilised through 0.2 μm filter*

Method

200 μL of bacterial culture at the logarithmic phase of growth were mixed with the equal volume of glycerol stock-media and immediately frozen at $-80\text{ }^{\circ}\text{C}$

Preparation of plasmid DNA

Plasmid DNA was isolated from small-scale (1 - 2 ml) bacterial cultures by treatment with alkali and SDS.

Materials

Alkaline lysis solution I (50 mM Glucose; 25 mM TRIS-Cl; 10 mM EDTA; DNase free RNase A 0.1 mg/mL; pH 8.0)

Alkaline lysis solution II (0.2 N NaOH (*freshly diluted from a 10 N stock*); 1% (w/v) SDS)

Alkaline lysis solution III (5 M potassium acetate, 60 mL; Glacial acetic acid, 11.5 mL; H_2O , 28.5 mL; pH 5.2)

Solutions I – III are part of NucleoSpin[®] plasmid kit

Antibiotic for plasmid selection: ampicillin 100 µg/mL, *to prevent satellite colonies at LB-agar up to 200 µg/mL*; kanamycin 50 µg/mL

Ethanol

Phenol-chloroform (1:1, v/v)

TE (10 mM TRIS-Cl; 1 mM EDTA; pH 8.0)

LB (Tryptone, 10 g; Yeast extract, 5 g; NaCl, 5 g; H₂O, up to 1000 mL; pH 7.5), *autoclaved*, with antibiotic for plasmid selection

Method (Birnboim 1979)

1. 2 mL of LB medium containing the appropriate antibiotic were inoculated with a single colony of transformed bacteria, incubated over night (not more than 16 hrs) at 37 °C with vigorous shaking (~250 rpm).
2. 1.5 mL of the culture were taken into an eppendorf tube, centrifuged at maximum speed for 30 sec at 4 °C in a bench centrifuge. The unused portion of the original culture was stored at 4 °C.
3. The medium was removed by aspiration, leaving the bacterial pellet as dry as possible.
4. The bacterial pellet was resuspended in 100 µl of ice-cold alkaline lysis solution I by vigorous vortexing.
5. For bacteria lysis, 200 µl of alkaline lysis solution II was added to each bacterial suspension and the content was mixed by rapid inverting the tube (vortexing is not allowed!). The tube might be stored on ice.
6. 150 µl of ice-cold alkaline lysis solution III was added mixed and incubated on ice for 3-5 min.
7. The bacterial lysate was centrifuged at maximum speed for 5 min at 4 °C in a bench centrifuge. Supernatant was taken into a fresh tube.
8. An equal volume of phenol-chloroform was added, organic and aqueous phases were mixed by vortexing and then emulsion was centrifuged at maximum speed for 2 min at 4 °C in a bench centrifuge. The aqueous upper layer was transferred to a fresh tube.

9. Nucleic acids from the supernatant were precipitated by adding 2 volumes of ethanol at room temperature, mixed and kept for 2 min at RT.
10. The precipitated nucleic acids were collected by centrifugation at maximum speed for 5 minutes at 4 °C in a bench centrifuge. The supernatant was removed.
11. The pellet was washed in 1 mL of 70% ethanol and dried at room temperature.
12. The nucleic acids were dissolved in 50 µL of TE (pH 8.0). The DNA solution was stored at -20 °C.

In order to obtain higher quality for sequencing or transfection, plasmid DNA in mini scale was purified using chromatographic columns from NucleoSpin[®] plasmid kit accordingly to manufacture recommendations.

Agarose gel electrophoresis

Materials

DNA staining solution (Ethidium bromide 10 mg/mL)

Electrophoresis buffer

50x TAE (TRIS base, 242 g; Glacial acetic acid, 57.1 mL; 0.5 M EDTA, 100 mL; H₂O, up to 1 L; pH 8.0), or

10x TBE (TRIS base, 54 g; Boric acid, 27.5 g; 0.5 M EDTA, 20 mL; H₂O, up to 1 L; pH 8.0)

Agarose solutions in electrophoresis buffer

6x Gel-loading buffer (0.25% (w/v) Bromophenol blue; 0.25% (w/v) Xylene cyanol FF; 30% (v/v) Glycerol in H₂O) *Store at 4 °C*

DNA samples, DNA molecular weight markers

Method (Aaij 1972, Sharp 1973)

1. For DNA separation, agarose to the final concentration of 0.5 - 2%* was melted in 1xTAE or 1xTBE buffer**.
2. Then agarose solution was cooled down to ~50 °C and ethidium bromide to the final concentration 0.1 µg/mL was added.
3. Up to 1 µg of the DNA probe was applied on a gel in loading buffer, as well as DNA fragment size standards and were separated at constant power ~100 V for 30 - 60 min.

4. The DNA-ethidium bromide fluorescence was recorded at UV light ($\lambda = 302$ nm) after completing of the separation.

* Range of separation in cells containing different amounts of standard agarose:

Agarose concentration w/v, %	Range of separation of linear DNA fragments, kb
0.3	5 – 60
0.6	1 – 20
0.7	0.8 - 10
0.9	0.5 - 7
1.2	0.4 - 6
1.5	0.2 - 3
2.0	0.1 - 2

** TBE buffer is more suitable if small fragments are separated

DNA purification

DNA fragments were purified using chromatographic columns from “NucleoSpin[®] Extract” kit accordingly to the manufacture protocol.

Spectrometric determination of DNA concentration

To determine DNA concentration in aquatic solutions absorption was measured at $\lambda=260$ nm (Biophotometer, Eppendorf) (50 μ L cuvettes with 10 mm optical path) and calculated as following $c = 0.05 \mu\text{g} \cdot \mu\text{L}^{-1} \cdot E_{260} \cdot d^{-1}$ (where **d** is dilution factor from 0 to 1, recalculation factor for DNA is 0.05).

DNA sequencing

All sequencing was done at MWG – Biotech AG, using “ValueRead” parameters and customer primers. 1.5 μ g of column purified DNA were taken as template.

Total RNA extraction

Materials

Cell culture or animals tissues

Total RNA extraction kit NucleoSpin[®] RNA II

2-mercaptoethanol

Method (Ausebel 1994)

1. Cells from 6-well plate (alternatively animals tissues up to 30 mg) were directly homogenised in guanidinium thiocyanat-mercaptoethanol buffer accordingly to the manufacturer's recommendations.
2. Total nucleic acids were precipitated, bind to silica column and washed with supplied buffers.
3. DNA was digested on a sorbent by adding RNase free DNase I, then column was washed again and pure RNA eluted in 60 µL of sterile RNase-free H₂O.
4. Quality of RNA extraction was proved by agarose gel (1%) electrophoresis in TBE buffer.
5. RNA concentration was determined photometrically (see above, recalculation factor for RNA is 0.04), stored until use at -80 °C.

Generating of cDNA by reverse transcription

Materials

10x M-MLV RT buffer (500 mM KCl; 100 mM TRIS-Cl; 15 mM MgCl₂; pH 8.3)

Autoclaved, store at -20 °C.

20 mM dNTP containing all four dNTPs (pH 8.0)

100 mM DTT

Reverse transcriptase (M-MLV RNA-dependent DNA polymerase) 100 units/µL

Placental RNase inhibitor 20 units/µL

Template RNA 100 µg/mL in H₂O

Oligo(dT)₁₂₋₁₈ 100 µg/mL in TE (pH 8.0)

Method (Sambrook 1989)

1. 1 µg of total RNA in a fresh eppendorf tube was denatured by heating at 75 °C for 5 min in 10 µL volume, followed by chilling on ice.

2. To the denatured RNA the following was added:

10x M-MLV RT buffer	2 µL
100 mM DTT	2 µL
20 mM dNTPs	1 µL
oligo(dT) ₁₂₋₁₈	1 µL
Placental RNase inhibitor	1 µL
Reverse transcriptase	1 µL
H ₂ O	to 20 µL

Mix was incubated for 1 hr at 37 °C.

3. In parallel negative control reaction was set up, including all components of the first-strand reaction except the reverse transcriptase.

4. Synthesised cDNA was stored at –20 °C until use.

Quantification of cDNA

Materials

2x SYBRgreen[®] reaction master mix

cDNA 1 to 500 dilution in H₂O

Gene-specific oligonucleotides, 10 µM in H₂O

Method (Foley 1993, Jones 1993, Liss 2002)

1. Prior to the real time PCR quantification itself, gene-specific primers (see above) were designed in order to fulfil the following requirements:

- a) Be unique for the gene
- b) Discriminate genomic and cDNA by introne spacing
- c) Have the same annealing temperature
- d) Have identical PCR efficiency

All this parameters were verified using the same SYBRgreen[®] master mix as for RNA quantification. Thermocycle was set up with various annealing

temperatures and respective amplification products were analysed by agarose gel (Rychlik 1990).

2. The following components of quantitative real time-PCR were mixed on ice:

Template (cDNA in 1:500 dilution)	5 µL
2x SYBRgreen [®] master mix	15 µL
10 µM primers (each)	0.6 µL
H ₂ O	to 30 µL

3. For tissues' analysis each quantification was supplied with two normaliser genes (PGK1 and B2M), for cell culture only one – GAPDH, as well as no-RT control.
4. Every reaction was set up in triplicates in optic tubes and placed into MX400 real time PCR machine (Stratagene, controlling software version 3.01).
5. The following thermal cycle was performed:

<u>Number of cycles</u>	<u>Denaturation</u>	<u>Annealing – Polymerisation</u>
1	10 min at 95 °C	
40	30 sec at 94 °C	60 sec at 60 °C

6. Since thermostable *Taq* DNA polymerase used in this reaction has processivity ~600 bp/min at 60 °C it was possible to establish two step PCR where annealing and polymerisation occurs at the same temperature.
7. Fluorescent data were recorded automatically at each cycle, amplification curves were built with MX4000 (analysis software version 3.01) and specific Ct parameter were taken for every PCR sample. Ct means cycle of amplification when the fluorescence signal is crossing threshold line (background) – set up identically for all experiments.
8. All calculations were done as following:

$$\mathbf{RE}(\text{goi}) = \mathbf{Ef}(\text{goi})^{\mathbf{Ct}(\text{goi})} / (\sum(\mathbf{Ef}_n(\text{norm})^{\mathbf{Ct}_n(\text{norm})}) / \mathbf{N})$$

Where is: **RE** – relative expression

Ef – efficiency of PCR amplification, for each amplicon were obtained by MX4000 software, and based on amplification pattern of correspondent cDNAs at different dilutions (d = 1, 4, 16, 64).

Ct – threshold crossing cycle

goi – gene of interest

norm – normaliser gene

N – number of normalising genes

9. For every experimental measurement the standard deviation in triplicates was not bigger than 0.16Ct, which is equal to 10% of relative units of expression.

Protein extraction

Extraction of proteins from cell culture and animal tissue.

Materials

Homogenisation buffer (20 mM TRIS-HCl; 2 mM MgCl₂; 0.25 M Sucrose; pH 7.4)

PIC – protease inhibitor cocktail (10 mM Antipain; 10 mM Chymostatin; 10 mM Leupeptin; 1 mM Pepstatin; 50% DMSO)

Cell lysis buffer (50 mM TRIS-HCl; 2 mM CaCl₂; 80 mM NaCl; 1% (v/v) Triton-X-100; pH 8.0)

Method

1. All procedures were accomplished on ice. Directly before use both homogenisation and cell-lyses buffers were completed with PIC (v/v, 1:1000).
2. For hepatocytes membrane preparation 1 ml of the homogenisation buffer was added to 50-100 mg liver tissue and was disintegrated with Ultraturrax.
3. The homogenate was centrifuged twice for 15 min at 4 °C with 4000 rpm (~800 g, bench centrifuge) and supernatant was reused.
4. The supernatant was centrifuged with a Beckman TL-100 ultracentrifuge in a TLA-100.2 fixed angle rotor for 1 hr at 4 °C with 55000 rpm (~100000 g).
5. The pellet containing plasma membranes was taken into 200 µL of cell lysis buffer with 0.1% SDS. Protein concentration was determined by SDS Lowry (see below) and solution stored at –80 °C until use.
6. Alternatively, cultured cells were directly disrupted in cell lysis buffer (~100 µL per each 50 cm²). Lysate was centrifuged at 4 °C with 800 g for 15 min and concentration of the proteins in the supernatant was determined by SDS-Lowry.

Determination of the protein concentration by SDS-Lowry

Materials

0.1 M NaOH

Bovine serum albumin standard solution, Pierce, 23210

Lowry solution A (2% Na₂CO₃ in 0.1 NaOH)

Lowry solution B (1%CuSO₄ in H₂O)

Folin's phenol reagent

Method (Lowry 1951)

1. Protein containing solution was normally diluted 1:5 in 0.1 M NaOH and 100 µL was used. Lowry working solution was prepared by mixing 49 mL of solution A with 1 mL of solution B. 1 mL of ready Lowry solution was mixed with 100 µL of protein probe and incubated for 10 min at room temperature.
2. Folin's phenol reagent was diluted in water 1:1 prior to use. 100 µL of diluted Folin's reagent was added to the reaction and further incubated in darkness at room temperature for 30 min
3. After incubation the optical density was determined. For that 300 µL of reaction mixture was measured at 760 nm using ELISA-reader (Dynatech Laboratories, MRX software version 1.12). To determine concentration in absolute values, a standard curve (0-2,5 µg/mL) was generated using bovine serum albumin.

SDS-PAGE

Separation of the proteins in polyacrylamid gel according to Nevill.

Materials

11x Protein gel loading buffer (Glycerol, 8.8 mL; Bromphenol blue, 8 mg; H₂O, up to 10 mL)

40% (w/v) Acrylamide/N,N'-Methylenbisacrylamide = 75/2, BioRad, 161-0148

TEMED

10% (w/v) APS

BSA 1 mg/mL

Broad range molecular weight marker, Rainbow marker, BioRad ,161-0317

Anode buffer (TRIS base, 258.5 g; H₂O, up to 5 L; pH 9.5)

Cathode buffer (TRIS base, 24.8 g ; Boric acid, 12.4 g; SDS, 5 g; H₂O, up to 5 L; pH 8.6)

Method (Neville 1971)

1. For separation of the proteins polyacrylamide gel was based on TRIS-buffer system pH 9.5 (anode buffer) using different concentration of polymer (8–12%) with 2/75th part of co-polymer. Polymerisation was catalysed by adding 1/200th volume of APS and initiated by 1/800th volume of TEMED.
2. To focus proteins on the border of the separating gel, 3% stacking gel was made on top using 50 mM TRIS-buffer system pH 6.8. Polymerisation of the stacking gel was initiated as above.
3. Protein samples were mixed with 11x protein loading buffer (10:1 w/w) and supplied with SDS up to 1% of final concentration. If necessary, samples were reduced with 1% 2-mercaptoethanol at 96 °C for 15 min. Gel of 1 mm thickness was normally loaded with 10–50 µg of the proteins. One extra line was always used for 3–5 µL of broad range protein molecular weight marker.
4. Electrophoresis was carried out at 30 mA for focussing and at 60 mA for separating of the proteins. For upper and lower electrode chamber of the electrophoresis device (mini protean, power supply pac200, BioRad), cathode and anode buffer were used correspondingly.

Western blot

Proteins separated by SDS-PAGE were transferred onto nitrocellulose membrane and detected with antibodies followed by chemifluorescence visualisation.

Materials

Blotting buffer (TRIS base, 12.1 g; Glycin, 56.2 g; 20% Methanol; H₂O, up to 5 L)

0.2% Ponceau solution in 3% Trichloroacetic acid

Wash buffer A (TRIS base, 12.1 g; NaCl, 45 g; Tween 20, 5 g; H₂O, up to 5 L; pH 7.4)

Wash buffer B (TRIS base, 12.1 g; NaCl, 45 g; Tween 20, 5 g; SDS, 5 g; Sodium desoxycholat, 12.5 g; H₂O up to 5 L; pH 7.4)

ECL-solution, Amersham

Solution A (0.1 M TRIS-HCl 10 mL; 250 mM Luminol, 50 μ L; 90 mM Cumarin-3-carbonacide, 25 μ L; pH 8.5)

Solution B (0.1 M TRIS-HCl 10 mL; 30% H₂O₂, 3 μ L; pH 8.5), mix equal volumes of A and B solutions just before use.

1° antibodies

2° antibodies conjugated with HRP

Method

1. The proteins isolated in the SDS-PAGE were transferred in the blotting buffer on the nitrocellulose membrane by electro-blotting at 4 °C over night with 0,7 mA/cm.
2. For the loading and transfer control the membrane was coloured for 10 min with Ponceau solution after the blotting, cut in appropriate fragments for antibody incubation and decolourised in PBS.
3. Membrane was incubated for 2 hrs in block solution (5% BSA, 10% milk-powder in wash buffer A), and rinsed twice in wash buffer A.
4. Blot was incubated over night at 4 °C with first antibody solution (5% BSA in wash buffer A) at a given concentration.
5. Blot was washed 1 min in wash buffer A, 15 min in wash buffer B and again 1 min in wash buffer A.
6. Appropriate secondary antibodies coupled to HRP were given to the blot in 5% BSA-wash buffer A for 2 hrs.
7. Then blot was washed again as in p.5, incubated for 1 min with ECL solution and exposed to the black-&-white negative photo material.

Indirect immunofluorescence

Materials

PBS (2.7 mM KCl; 8.1 mM KH₂PO₄; 137 mM NaCl; 1.5 mM Na₂HPO₄; pH 7.4)

4% (w/v) PFA in PBS

Glycin/Saponin (Glycin, 5 g; Saponin, 500 mg; PBS pH 7.4, up to 1 L)

1% (w/v) PPD

Mowiol[®]

5 μ M DAPI in PBS

1° antibodies

2° antibodies conjugated with fluorescent group

Method

1. Cells for immunostaining were seeded on cover slips under standard condition (see below)
2. For fixation cells were washed with PBS and incubated in 4% PFA/PBS. Then, cells were washed 5 times in PBS for 5 min and permeabilised in glycin/saponin buffer for 5 min.
3. Unspecific binding sites were blocked by adding 80 μ L blocking solution (2% BSA in glycin/saponin buffer). The cells were incubated for 30 min at 37 °C.
4. Primary antibody was given in blocking solution for 1 hr at 37 °C. Cover slips were washed two times in glycin/saponin buffer.
5. Secondary antibodies were given s. p. 4. Cells were washed five times in PBS, for nucleus DNA visualisation stained with DAPI (\sim 5 μ M in PBS) for 3 min. The cells were embedded with 5 μ L PPD/Mowiol[®] (25 μ L 1% PPD + 225 μ L Mowiol[®]) using nail lack.
6. Confocal images were taken using a Zeiss LSM 510 Meta (software version 3.0) and oil immersion objectives.

Adenoviral culture

Materials

HEK293 cells

CsCl solution $\rho = 1.2411$ g/L (32.27% w/v, $\eta_{20\text{ }^\circ\text{C}} = 1.3572$) (CsCl, 26 g; H₂O, 74 g)

CsCl solution $\rho = 1.3393$ g/L (45.54% w/v, $\eta_{20\text{ }^\circ\text{C}} = 1.3666$) (CsCl, 34 g; H₂O, 66 g)

CsCl solution $\rho = 1.4525$ g/L (61.00% w/v, $\eta_{20\text{ }^\circ\text{C}} = 1.3771$) (CsCl, 42 g; H₂O, 58 g)

All CsCl solutions sterilised through 0.2 μ m filter

Adenoviral storage buffer (NaCl, 3.94 g; KCl, 0.11 g; 1 M MgCl₂, 0.5 mL; Glycerol, 50 mL H₂O, up to 500 mL; pH 8.0) *sterilised through 0.2 μ m filter*

NAP25 column, Amersham

4% (w/v) Agarose in PBS; pH 7.4

Plasmid encoding adenoviral genome in TE buffer

Transfection reagent FuGene6[®], Boehringer-mannheim, 1 814 443.

PacI endonuclease

Complete cell culture medium (DMEM with Glutamax-I supplied with 10% (v/v) FBS and 1% (v/v) Penicillin/Streptomycin)

Method

Generation of adenoviral vector

1. 2 µg of the adenoviral encoding plasmid were digested with restriction endonuclease *PacI* to release the viral backbone in 30 µL reaction volume for 1 hr.
2. Endonuclease was heat inactivated by incubating at 65 °C for 15 min.
3. HEK293 cells competent in trans-complementation were transfected using linearised adenoviral genome supplied with 10% of tracking plasmid (pEGFP, served as transfection control) with help of FuGene6[®] reagent. For a 60 mm dish, 5×10^5 cells were seeded one day before transfection. When cells reached 50% of confluence, they were transfected with 1 µg DNA in 3 µL of transfection reagent.
4. 24 h after adenoviral genome transfection, the cell monolayer was covered with 1% agarose gel. Therefore 4% agarose solution in PBS was sterilised by autoclaving. Melted agarose was equilibrated at 40 °C for at least 1 hr. Three volumes of complete DMEM were mixed with one volume of 4% agarose solution, medium was aspirated from the cells and immediately substituted by 1% melted agarose.
5. Cells were incubated at 37 °C and observed during 7-10 days post-transfection in order to detect adenoviral plaque formation.

Propagation of adenoviral vector

6. Infectious material from 2-3 single plaques was collected in 200 µL volume and subjected for independent propagation.

7. Prior to each amplification step, productive cells were frozen-thawed three times to release adenoviral particles from the cell nuclei. For propagation one half of the lysate was used for next infection (see below). The remaining aliquot was stored at -80°C .
8. Infection was propagated by passaging cell cultures in 12 well plate, T25 cell culture flask, T300 and finally 20 x T300. For every passage HEK293 cells were infected at $\sim 80\%$ confluence. Infection took place in complete DMEM in a 25% of regular volume in CO_2 incubator for 4 hrs.
9. Cells at the last step of virus amplification were harvested at the second day post infection ($\sim 50\%$ of cells were round and detached from the plastic) by centrifugation at 4°C for 10 min at 500 g. Cell debris was resuspended in 10 mL of complete DMEM and three cycles of freezing-thawing in liquid nitrogen were performed. Cell lysate was purified by centrifugation at 5000 g for 15 min at 4°C and subjected to ultracentrifugation.

Concentration and purification of adenoviral vector

10. A discontinuous CsCl gradient was prepared as followed: to the bottom of the ultracentrifuge tube 1 mL of CsCl solution ($\rho = 1.2411\text{ g/L}$), 2 mL of solution ($\rho = 1.3393\text{ g/L}$) and 2 mL of solution ($\rho = 1.4525\text{ g/L}$) were added to underlay one each other. 5 mL of cell lysates were applied on top of the gradient ($\rho = 1\text{ g/L}$) containing adenoviral particles. Two tubes were equilibrated with accuracy of 1 mg and ultracentrifuged at 30000 rpm ($\sim 100000\text{ g}$) for 20 hrs at 10°C using a swing-out rotor (SW-41, Beckman). Normally, two adenoviral bands are formed after centrifugation: the upper contains defective particles at the low density and lower band representing more dense particles.
11. The lower adenoviral band was collected with a 1 mL syringe in $\sim 1\text{ mL}$ volume. Gel filtration column NAP25 was equilibrated with 25 mL of adenovirus storage buffer. To remove CsCl, viral particles were applied onto column and eluted by storage buffer. First 2.5 mL were discarded (dead volume of the column) and desalted viral particles were collected in the next 2 mL volume.
12. Adenovirus stock was aliquoted and stored at -80°C until use.

Adenoviral titration

Identification of infected cells using an adenovirus-specific-antibody.

Materials

Dulbecco's PBS

Methanol

1% BSA in PBS

Complete DMEM (see above)

Method

1. HEK293 cells (5×10^5) were seeded in each well of a 12 well plate in complete DMEM.
2. Using Dulbecco's PBS as diluent, 10-fold dilutions from 10^3 to 10^8 -fold of the viral stock-solution were prepared.
3. 100 μ L of viral dilution were added into 500 μ L of medium drop-wise to each well. To provide accurate calculations the infection was set up in duplicates.
4. Cells were incubated at 37 °C in 5% CO₂ for 48 hrs.
5. Afterwards the medium was aspirated and the cells dried for 5 min.
6. To fix cells, 1 mL ice-cold 100% methanol was added very gently to each well.
7. The plate was incubated at -20 °C for 10 min, and methanol was aspirated.
8. Wells were gently rinsed three times with 1 mL of 1% BSA in PBS. Mouse anti-hexon antibody in 1:1000 dilution in PBS with 1% BSA were made.
9. Wells were incubated with 0.5 mL of anti-hexon antibody dilution for 1 hr at 37 °C.
10. 1° antibody was aspirated and the wells were gently rinsed three times with 1 mL of 1% BSA in PBS.
11. Rat anti-mouse antibody (HRP) in 1:500 dilution in PBS with 1% BSA was prepared.
12. Final rinse from the wells was aspirated and 0.5 mL rat anti-mouse antibody (HRP) dilution added to each well. Cells were incubated for 1 hr at 37 °C on an orbital shaker.

13. Prior removing of the 2° antibody, DAB working solution was prepared by diluting 10x DAB substrate 1:10 with 1x stable peroxidase buffer. Before use DAB working solution was adjusted to RT.
14. 2° antibody dilution was aspirated and wells were gently rinsed three times with 1 mL of 1% BSA in PBS. After removing the final rinse, 500 µL of DAB working solution were added to each well and incubated at RT for 10 min. DAB was aspirated and 1 mL of PBS added.
15. Hexon-positive cells were counted under microscope at magnification x20 and infectious titre calculated as following: $\text{ifu/mL} = \text{N} \cdot \text{D} / \text{V}$ (ifu ~ pfu)

Where: **N** is a total number of hexon-positive cells in one well.
 V [mL] – volume of diluted viral stock solution taken for infection.
 D – dilution factor of adenoviral stock solution.

Cell culture

Materials

Trypan blue (0.5% in isotonic saline solution)

Complete DMEM (see above)

Trysin-EDTA

Dulbecco's PBS

Method

1. All work was accomplished sterile under the “clean bench”. The incubation of the cells took place at 37 °C and 5% CO₂ in a humid incubator. All used media and solutions were kept in the water bath at 37 °C prior to use.
2. Cells were split depending upon the cell density every three to five days. For this the cells were washed with PBS and incubated briefly with Trypsin-EDTA. The cells were separated from the cell culture bottle by knocking and resuspended in the new cell culture medium.
3. To determine the cell number a Neubauer's cell chamber was used. Dead cells were stained before with trypan-blue (0,5% in isotonic saline solution).

Transfection of mammalian cells

Materials

Transfection reagent FuGene6[®], Boehringer-mannheim, 1 814 443.

Dulbecco's PBS

Plasmid DNA at 0.1 - 1 µg/µL in TE buffer

Complete DMEM (see above)

Method

1. Cell for transfection were seeded in standard cell culture plastic ware in order to reach ~80% of confluency on the day of transfection. Complete medium was always used.
2. 1 µg of DNA was mixed with 3 - 4 µL of FuGene6[®] reagent, as recommended by the producer. For 60 mm cell culture dish 2 µg of plasmid DNA was used.
3. DNA-transfection reagent complex was added to the cells in complete medium, incubated overnight and then medium was replaced. Normally, cells were harvested after 2 - 3 days post-transfection.

Adenoviral infection of mammalian cells

Materials

Adenoviruses in storage buffer

Dulbecco's PBS

Complete DMEM (see above)

Method

1. HuH7 cells became transduced by Ad-EGFP or Ad-anti-ABCA1 in 6-wells. $2 \cdot 10^5$ cells were seeded one day prior infection using complete DMEM.
2. Adenoviral stock solution was taken from -80 °C storage, slowly thawed on ice and diluted in complete DMEM to desirable MOI (multiplicity of infection) normally from 1 to 100 viral particles per cell.
3. Only 500 µL of infection solution was used in each 6-well. Infection took place in CO₂ incubator at 37 °C, every half an hour cells were carefully agitated. After

4 hrs of incubation, medium was exchanged to 2 mL of complete DMEM. Depending on the experiment, cells were incubated for 2-3 days.

4. Prior to harvest cells were washed two times with PBS and total RNA was isolated as described above.

Animal husbandry

For all experiments wild-type C57BL/6 male mice were used at the age of 12 weeks. Animals were maintained on a regular chow diet and held under controlled conditions: 20 °C, 50% air humidity, 14/10 hours of light-darkness rhythm, food and water *ad libitum*. The animal care department of the University Clinic Eppendorf, Hamburg, Germany, took care for the mice. The bioassays were accomplished with the permission of the health authority Hamburg, Germany.

Adenoviral administration into the animals

Adenovirus in storage buffer was injected into tail vein of the mice. The injection volume was always adjusted to 200 µL with Dulbecco's PBS at RT.

Blood puncture

Materials

Heamatocrite capillaries

0.5 M EDTA; pH 8.0

Method

Every blood puncture was done after a 4 hr fasting period (only water was available). Blood was taken from orbital plexus using heamatocrite capillary. 150-200 µL of blood was immediately supplied with 1/100 volume of 0.5 M EDTA and kept on ice. Plasma was separated by centrifugation at maximum speed (bench centrifuge) at 4 °C for 10 min. Plasma pools were made by mixing equal amounts of plasma from each animal in the same experimental groups.

Organs withdrawal

Materials

Liquid nitrogen

Tissue-Tek[®] O.C.T. compound, Sakura, 62550

Solution for narcosis (Ketanest 6 mg/mL; Rompun 1.6 mg/mL; in 0.9% NaCl)

PBS

Method

Animals received 100 μ L of narcosis solution per 10 g of weight. After anesthetizing, mice were fixed on a preparative table, abdomen and thorax were opened, then right atrium was cut with the scissor and perfusion was performed by injection of 20 mL of PBS into left ventricle until liver became blood-free. Well-perfused organs (lung, liver and spleen) were taken for protein or RNA extraction (frozen in liquid nitrogen) and for histological investigation (embedded into Tissue-Tek[®] O.C.T. compound), see below.

Histology

Materials

PBS

4% (w/v) PFA in PBS

1% (w/v) PPD

Mowiol[®]

5 μ M DAPI in PBS

Method

1. Tissue pieces were frozen into Tissue-Tek[®] compound in liquid nitrogen and stored at -20 °C until use. Cryoblocks were cut into 10 μ m thick slices with knife angle ~ 4 ° using a cryotome HM560 (Leica).
2. Slices were maintained on glass plates. Dried briefly on air at RT, fixed in 4% PFA in PBS for 3 - 5 min, washed 5 times in PBS for 5 min.
3. To stain nuclei, slices were incubated with DAPI (~ 5 μ M in PBS) for 3 min and embedded with 5 μ L PPD/Mowiol[®] (25 μ L 1% PPD + 225 μ L Mowiol[®]) using nail lack.

4. Confocal images were taken using a Zeiss LSM 510 Meta (software version 3.0) and immersion objectives.

Plasma lipoproteins separation and lipid determination

A. Gel filtration of plasma lipoproteins – FPLC

Materials

FPLC buffer (1 mM TRIS-HCl; 10 mM NaCl; 1 mM EDTA; pH 8.0)

Method (Rudel 1986)

1. Fresh plasma was always used for lipoprotein separation. From each experimental group (7 animals) ~35 μ L of plasma were taken to generate plasma pools. FPLC (Pamp500, Pharmacia) was loaded with 200 μ L of plasma and lipoproteins were separated using a S6-sepharose column at 4 °C.
2. First 10 mL of eluate was discarded and then 40 fractions with each 500 μ L were collected. If necessary individual fractions were kept for few days at 4 °C until analysis.

B. Enzymatic determination of the lipids

Materials

Precipath[®] L, Roche, 1285874

Cholesterol determination reagent

Phospholipids determination reagent

Triglyceride determination reagent

2 M CaCl₂

Method (Carr 1993)

1. Cholesterol, triglycerides and phospholipids concentrations were determined in FPLC plasma fractions using enzymatic colour test. In 96-well, 100 μ L of the FPLC probe was mixed with 200 μ L of the reagent. Reaction developed at 37 °C for 10 min. Then OD was measured at 550 nm using a micro-titre plate reader.

2. To determine lipid concentrations in absolute values, a standard curve (0 - 20 µg/mL) was generated using Precipath® at different dilution in FPLC buffer.
3. Since Ca²⁺ ions are essential for phospholipids test, the method was slightly modified. To overcome 10 mM EDTA in FPLC buffer, reaction was supplied with 5 µL of 2 M CaCl₂ – a ten times molar excess of Ca²⁺ on EDTA.

Flow cytometry

Preparation of the single cell suspension from murine liver

Materials

Erythrocytes lyses buffer (0.5 M EDTA, 1 mL; NH₄Cl, 4.01 g; K₂CO₃, 0.69 g; H₂O up to 500 mL; pH 7.4) *sterilised through 0.2 µm filter*

CHD-enzymatic mix (Collogenase IV, Sigma, C5138, 450 µL; Desoxyribonuclease I, Sigma, D5025, 450 µL; Hyaluronidase V, Sigma, H6254, 450 µL; RPMI-1640 medium with Glutamax-1, up to 9 mL)

Dulbecco's PBS pH 7.4

Solution for narcosis (Ketanest 6 mg/mL; Rompun 1.6 mg/mL; in 0.9% NaCl)

Medium RPMI-1640 with Glutamax-1

Method

1. Animals were anaesthetised with Ketamin-Rompun mix (see above).
2. Liver tissues (~400 mg) were cut into small parts (~1 mm) with a scalpel in ice cold PBS.
3. Tissue pieces were incubated with 1.5 mL of CHD-enzymatic mix for 1 hr at RT on an orbital shaker.
4. Digested cells were pressed through the nylon filter with 50 µm pore size, (Falcon). That allows recovering of a single cell suspension.
5. Cells were washed twice with PBS by centrifugation for 5 min at 4 °C with 200 g.
6. In order to lyse erythrocytes, cell pellet was briefly resuspended (vortex) in 2 mL of ice-cold erythrocytes lyses buffer. Adding 3 mL of ice-cold PBS immediately stopped lysis reaction.

7. Hepatocytes were harvested by centrifugating for 5 min at 4 °C with 200 g and resuspended in 1 - 2 mL of PBS.
8. Cell suspension was analysed by flow cytometry (Givan 2001), Cytomics FC 500, (Beckman Coulter). To detect EGFP fluorescent signal specially designed optic filter set was used. Cells were kept on ice until use.

Safety and waste disposal

In all work with chemicals “R- und S-Sätze” – German safety law was considered (<http://www.chemlin.de/chemikalien/r-s-saetze.htm>). Organic solvents were disposed separately according to halogen-containing and halogen-free, into the appropriate collectors. Solutions, gels and disposable material contaminated with ethidium bromide were disposed separately. Biological and infectious material (virus, bacterial cultures *etc.*) and anything contaminated with this (pipette tips, agar plates *etc.*) were autoclaved and afterwards discarded.

Software and statistic

The evaluation and representation of acquired data was performed with the help of Microsoft® Excel2000 software. In each case the average values, as well as the standard errors of the measurement (\pm SEM) are represented. With the help of the Student's t-test for independent samples the significances of two groups of data were examined. Difference of two groups were estimated as statistically significant, if the probability of a mistake $p < 0.05$.

3. Results

The aim of this study was to investigate the role of hepatic ABCA1 cholesterol transporter for plasma HDL metabolism. Therefore, vectors were designed to target murine and human ABCA1 expression by RNA interference. The efficiency of siRNA-mediated down regulation of ABCA1 *in vitro* was judged by real time RT-PCR, immunofluorescence and western blot analysis. A recombinant adenovirus was constructed from the most effective vector. Adenovirus was used to down-regulate ABCA1 expression exclusively in liver. Subsequent to the animal infection expression, patterns of proteins involved in lipid metabolism as well as lipoprotein plasma profiles were analysed.

3.1. ABCA1 knockdown mediated by RNA interference *in vitro*

Transient overexpression of murine ABCA1 in cell culture

To establish RNAi mediated murine ABCA1 knockdown *in vitro*, first an over-expressing system for ABCA1 was generated. Human embryonic kidney 293 cell line can be transfected efficiently, but has extremely low endogenous ABCA1 expression level. The transporter protein was not detectable in immunofluorescence analysis with available antibodies. Only the trace amounts of respective mRNA were measured by RT-PCR. The plasmid pcDNA3.1-mABCA1-FLAG (further reference to as pmABCA1-FLAG; donated by Prof. Rinninger) was used to generate overexpression of murine FLAG-tagged ABCA1 transporter in human cells (Wang 2000).

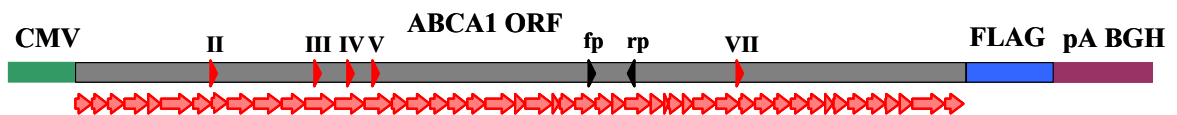


Figure 5. Murine ABCA1-FLAG expressing cassette in pcDNA3.1 plasmid

Murine cholesterol transporter ABCA1 expressed from the pcDNA3.1 under CMV promoter and bovine growth hormone polyadenylation signal (blue). Protein ORF linked to FLAG antigen-expressing sequence (green). Forty-seven exons are indicated below (red arrows). Positions of the mice specific PCR forward (fp) and reverse (rp) primers are shown with black triangles. Roman numbers are designated positions of anti-ABCA1 RNA interference-target regions (red triangles).

This plasmid is a derivative from common expression vector (pcDNA3.1) and contains the murine ABCA1-ORF fused to the FLAG antigen under control of CMV promoter and polyadenylation signal of bovine growth hormone. The nucleotide sequence of that plasmid was also taken to design primer pairs for quantitative real time PCR determination of the transcript. Figure 5 shows a scheme of the overexpressed gene including the primers used for RT-PCR and target regions for RNA interference.

To be able to detect the murine transgenic mRNA on a human background two discriminative primer pairs were chosen from the mouse and human cDNA sequence, respectively. In general, cDNAs from these two species have ~88% identity, therefore for specificity reasons areas with highest diversity were taken.

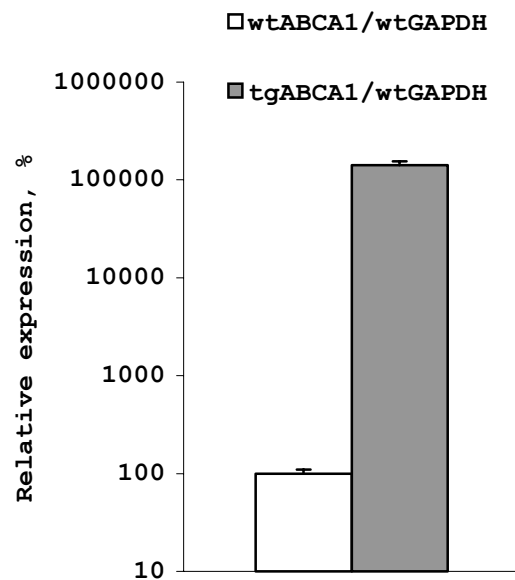


Figure 6. ABCA1 expression in human cell culture

GAPDH-normalised transcriptional level of the overexpressed murine ABCA1 transporter is shown (right) in percents to constitutive expression of the homologues human gene (left) *in vitro*. HEK293 cells were transfected with mock or ABCA1 plasmid, respectively. Two days after transfection total RNA was isolated and reverse transcription following the quantitative real time-PCR was performed. Two different PCR primer pairs (hABCA1 and mABCA1, see methodological considerations) were used to discriminate between human endogenous and murine transgenic transcripts respectively. Measurements were done in triplicates.

The plasmid pmABCA1-FLAG was used in co-transfection experiments with green fluorescent protein-expressing plasmid pEGFP-N1 (Clontech). This plasmid served as transfection control and provided EGFP mRNA for normalisation of transgenic transcript in qRT-PCR.

After transfection of murine ABCA1 cDNA into human cells qRT-PCR was performed. Human GAPDH transcript was used as an endogenous normalising gene. The transcriptional level of transgenic cholesterol transporter was then ~1000 times higher compared to constitutive expression, if judged two days after transfection (fig. 6).

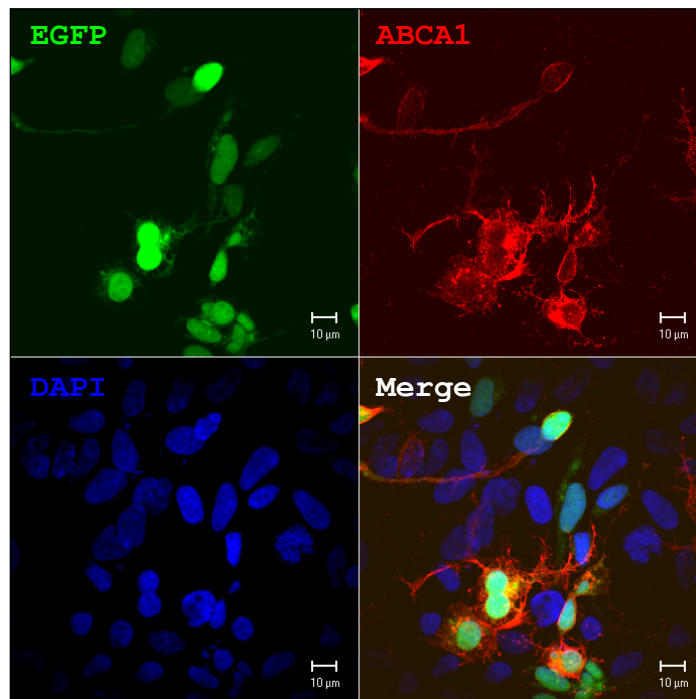


Figure 7. Immunofluorescence of HEK293 cells overexpressing murine ABCA1-FLAG

Human embryonic kidney cells 293 were transfected with plasmids expressing EGFP protein and murine ABCA1 transporter linked to FLAG antigen. After 48 hr cells were fixed and detection was performed using a monoclonal anti-FLAG antibody (mouse origin, 1:2500). ABCA1 protein was visualised with Cy3 conjugated antibodies against mouse IgG (1:500). Cy3 fluorescence is in red, EGFP in green and DAPI for nuclear DNA staining in blue. Bars are 10µm.

Since ABCA1-ORF is tagged to FLAG epitop it was possible to utilise anti-FLAG antibody for immunofluorescence detection of overexpressed protein in cell culture. Again HEK293 cells were co-transfected with pEGFP-N1 (10% of total DNA used). Generally, all cells exhibiting an EGFP fluorescence were also FLAG positive (fig. 7). Laser scanning confocal microscopy became a technique of choice to localise

transporter. ABCA1 protein was found predominantly on a cell membrane surface and a typical “dendritic” structure of overexpressing cells as previously described was observed (Wang 2000).

This overexpressing system was used to test ABCA1 siRNA-expressing constructs *in vitro*.

Cloning of small interfering RNA-expressing vector for murine ABCA1 targeting

The original plasmid pALsh was developed in our laboratory (Laatsch 2004) and was taken for vector construction. This vector contains the H1 promoter – region, which promotes the expression of small RNA molecules. Furthermore it consists of two non-palindromic endonuclease sites (*Bse*RI) and a termination penta-T motive, which provides precise transcription stop without following polyadenylation (fig. 8).

```

1gaacgctgacgtcatcaaccgctccaaggaatcgcgggccagtgctactagggcggaacacccagcgc
>>.....>

71gctgctgcccctggcaggaagatggctgtgaggacaggggagtgccgcccctgcaatatttgcattgctgct
>.....H1promoter.....>

141atgtgttctctgggaaatcaccataaacgtgaaatgtctttggatttgggaatcttataagtctgtatgag
>.....>

      start                stop
      ↓                    ↓
      BseRI BseRI
      -----
211accacagatccaattgaggagctcctcggtttttcgacctcgagggggggcccgggtaccagcttttgtt
...>>

281cccttagtgagggttaattccgagcttggcgtaatacatgggtcatagctgttctctgtgtgaaattgtta
<<...seqALsh...<<
  
```

Figure 8. Nucleotide sequence of H1 promoter region and *Bse*RI cloning sites in the plasmid pALsh

Transcription start and termination positions are indicated in red. Sequencing primers in reverse orientation are located at 312-331 nucleotide. Two non-palindromic *Bse*RI endonuclease sites allow cleavage exactly at the start and stop positions.

From the ABCA1-ORF five regions 21-23 nt in size with TT extinction at the 3'-end were chosen as RNAi target sequence: II, III, IV, V and VII (these roman numbers would further designate all corresponding derivatives) (fig. 5). Sequences became the 3'-part of the synthesised oligodeoxynucleotides, while the 5'-part was created as a palindromic counterpart without 5'-AA. These oligonucleotide molecules were self-annealed producing double strand DNA with TT-3'-overhang and directly

cloned into *Bse*RI digested pALsh plasmid (fig. 9A). This system does not contain any of stem-loop structure-forming nucleotide. Target sequences were derived from cDNA areas with 100% identity between murine and human ABCA1 genes, thus this siRNAs should equally silence both murine and human transporter genes.

The cloning results were confirmed by *Ava*I digestion since this site flanks the H1 promoter region and the stop-motive. Correct cloning results in an increase of the size of the small DNA fragment, which is released by the endonuclease digest (fig. 9B). Oligonucleotide insertion into the plasmid pALsh was also checked by direct sequencing from the reverse primer seqALsh (supplements, fig. 33). Sequences of palindromic region appeared to be a difficult task, only one clone out of five has been successfully analysed. Because of possible mistakes in primer synthesis and not resolved primary structure of cloning products, the exact sequences of the constructs, apart from clone II, remain enigmatic.

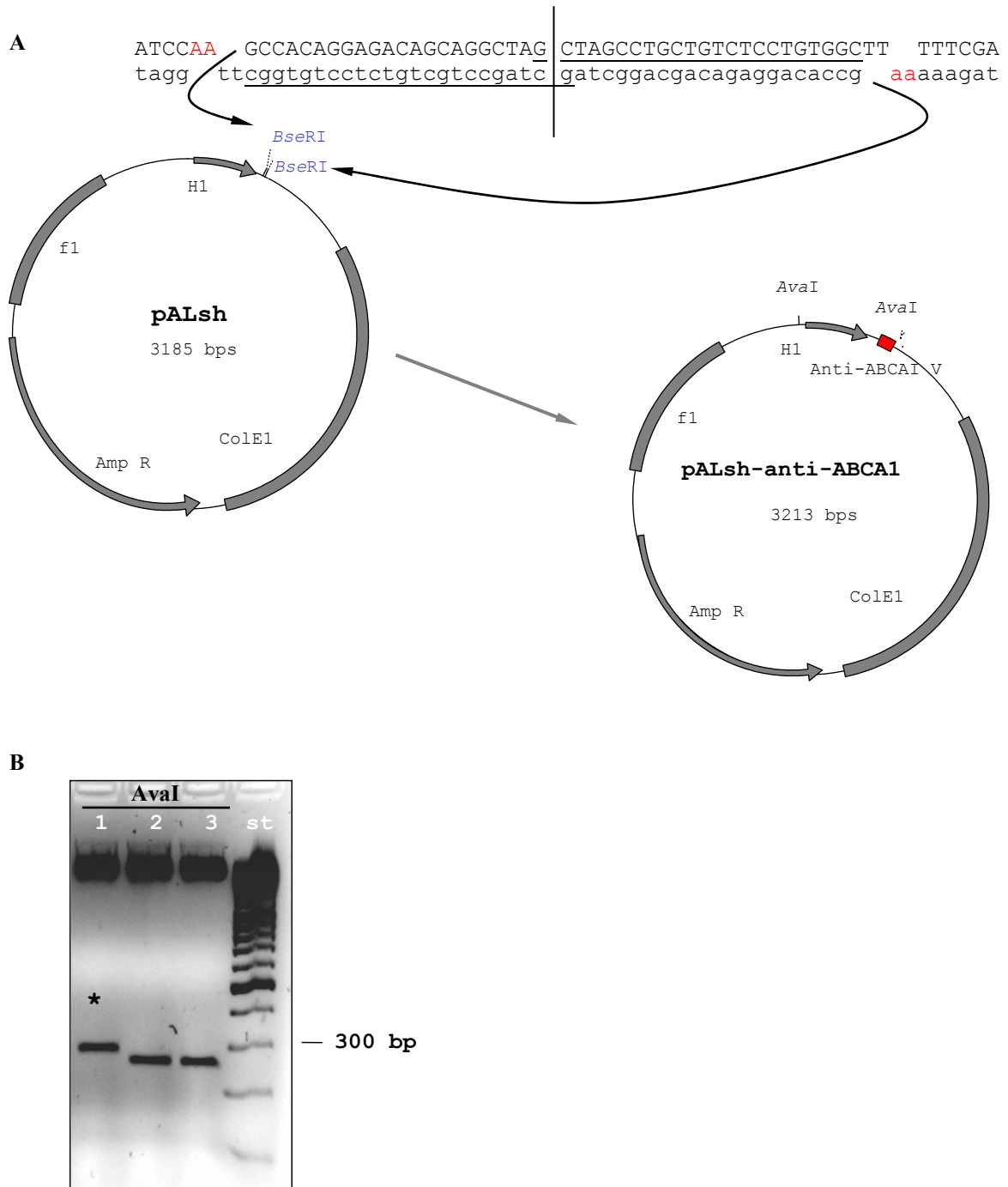


Figure 9. Cloning of anti-ABCA1 siRNA-expressing vector

One step cloning to generate pAL-anti-ABCA1 vectors. (A) Schematic view of the cloning. The plasmid pALsh was digested at *Bse*RI sites (blue) to generate 5'-end AA-extension (red). The underlined palindromic oligonucleotides (vertical line indicates symmetry axis) correspond to the targeted region within the ABCA1 mRNA and were cloned downstream of the H1 promoter into the plasmid pALsh. AmpR: ampicillin resistance gene – β -lactamase; ColE1: minimal *E.coli* origin; f1: origin of single strand DNA replication of the filamentous phage F1; complementary strand shown in lower case. (B) Control digestion of the resulting clones with *Ava*I endonuclease. Correct insertion (clone 1) leads to an increase of the fragment size released by *Ava*I (asterisk) in contrast to clone 2 and to the empty vector, lane 3. DNA molecular weight standard was from Fermentas.

Characterisation of anti-ABCA1 RNA interference in vitro

Five independent pAL-anti-ABCA1 clones targeting ABCA1 mRNA in different positions were taken for determination of their ability to knockdown ABCA1 expression in cell culture. These clones as well as empty vector were co-transfected into HEK293 cells with pEGFP and pmABCA1-FLAG expressing plasmids (fig. 10). Three days after transfection the relative level of ectopic ABCA1 mRNA was determined in total cellular RNA. Normalisation was performed using transgenic EGFP transcript. This approach circumvents all influences from variation in transfection efficiency. The pALsh-control was taken as a 100% reference. Only one clone was successfully suppressing the ABCA1 expression down to ~25% of over-expressed level – pAl-anti-ABCA1(V) (fig. 10, $p < 0.001$ column 1 vs. column 5). All other constructs did not significantly alter ABCA1 mRNA levels. Importantly, neither siRNA-expressing plasmids pALsh-anti-ABCA1(II-VII), nor the empty vector pALsh influenced the endogenous LRP expression, which was used as control protein and which was normalised to human GAPDH mRNA (fig. 10, column 7).

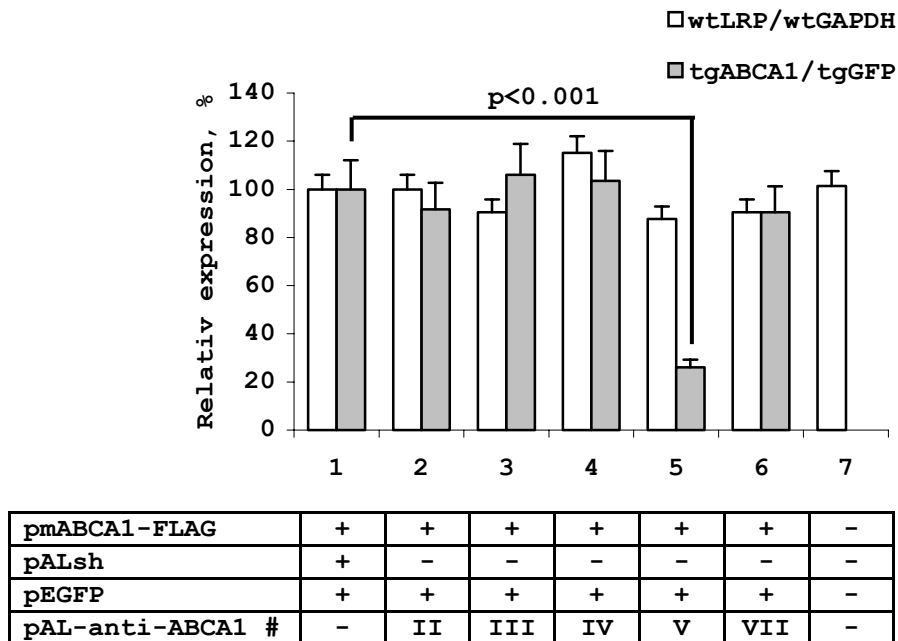


Figure 10. Relative expression of endogenous human LRP and transgenic murine ABCA1 in cells transfected with various constructs expressing anti-ABCA1 siRNAs

HEK293 cells were co-transfected with pmABCA1-FLAG, pAlsh, EGFP and pAL-anti-ABCA1 plasmids as indicated. Three days post-transfection cells were harvested, total RNA isolated and used for reverse transcription followed by quantitative RT-PCR. Relative amounts of wtLRP and tgABCA1 transcripts were normalised to wtGAPDH and tgEGFP mRNA, respectively. Data are calculated as percents of expression level of the cells transfected with the empty vector (first pair of columns). Error bars indicate standard deviation between triplicates for every measured point.

Furthermore, the capacity of the construct pALsh-anti-ABCA1(V) to inhibit transgenic ABCA1 expression *in vitro* was confirmed by protein quantification. Transfection of anti-ABCA1(V) construct resulted in almost complete block of the transgenic protein expression as judged by confocal microscopy. Cells were immunostained against FLAG antigen and visualised by Cy3-labelled secondary antibody. EGFP expressing cells were FLAG-positive only in pALsh control (fig. 11A), and no ABCA1 associated fluorescent signal was detected in cells co-transfected with anti-ABCA1(V) construct (fig. 11B).

In parallel experiments, cell lysates were subjected to SDS-PAGE, followed by fluorescence scan for EGFP detection. That insures equal protein load on a gel, as well as transfection accuracy (fig. 11C – lower panel). Subsequent Western blotting was performed with antibody detection against ABCA1 protein (recognising both murine and human antigen). In comparison to the pALsh control, pAlsh-anti-ABCA1(V) led to a drastic reduction of the tgABCA1 signal (fig. 11C, upper panel, lane 3 compared to lane 2). Due to the slightly different molecular weight wt- and tgABCA1 can be distinguished. Since the RNAi was designed not to discriminate between human and mice sources, it was remarkable that strongly expressed tgABCA1 under anti-ABCA1(V) siRNA treatment was reduced to a very faint band while the wild type product of the elevated molecular size vanished completely (fig. 11C, upper panel, lane 3 compared to lane 1).

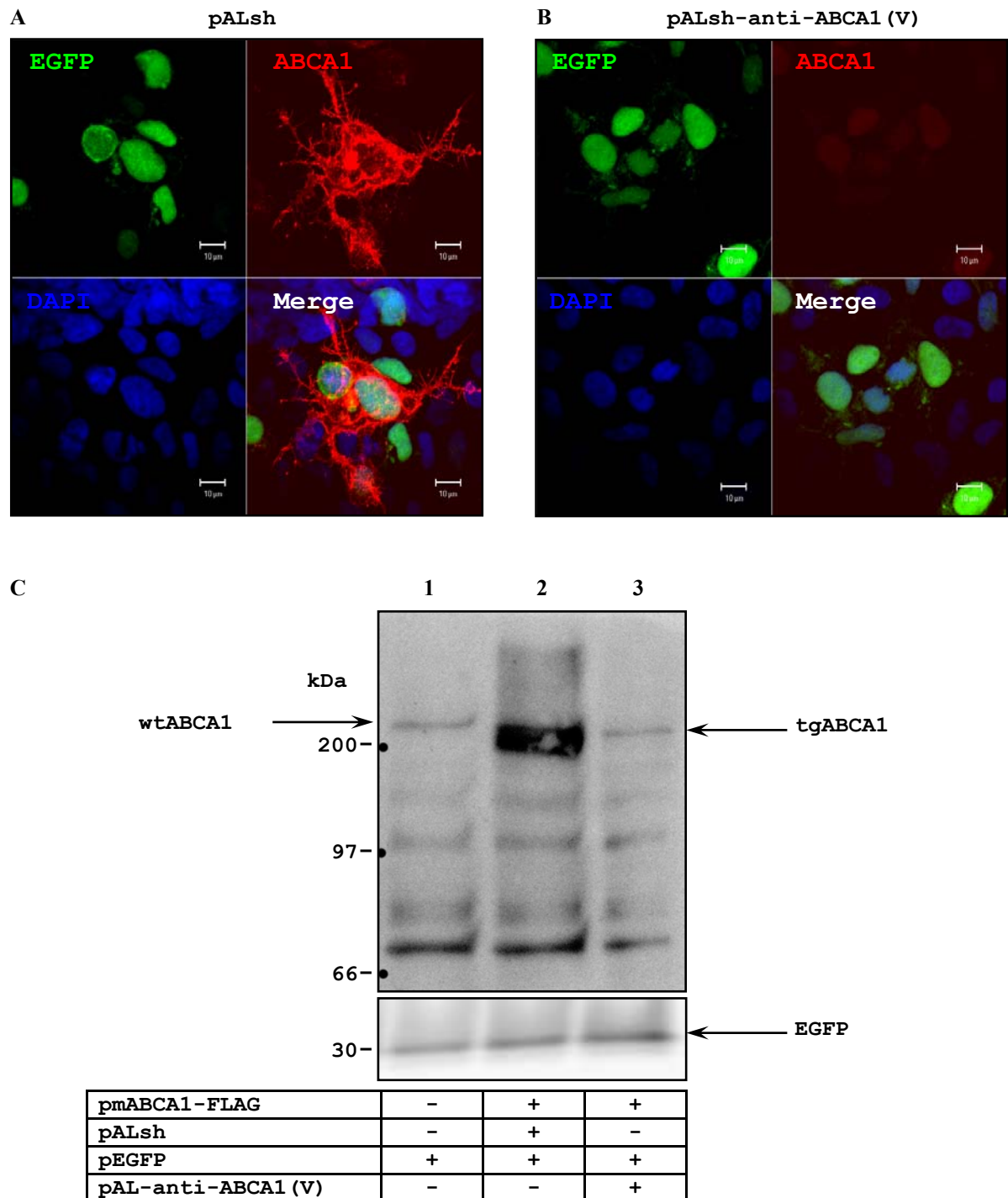


Figure 11. Effects of anti-ABCA1 siRNA on murine ABCA1 overexpression in vitro

HEK293 cells were co-transfected with murine ABCA1-FLAG cDNA, EGFP and either pALsh or pALsh-anti-ABCA1 clone V. (A, B) Three days post-transfection cell were fixed and immunostained (see fig. 7). (C) Cells were lysed and protein content used in SDS-PAGE and Western blot detection with polyclonal ABCA1 antibody (rabbit, 1:250) and visualised by GARPO (1:5000) and ECL (upper panel). EGFP fluorescence served as loading control (lower panel).

To study HDL metabolism *in vivo* it is necessary to knockdown ABCA1 protein expression for more than 5 days since HDL have a half-life longer than 1 day. Therefore, additional studies were performed on RNA interference itself to analyse its ability to down regulate ABCA1 expression *in vitro* for a longer period of time. The activity of siRNA at different time points is shown at fig. 12. Two observations have been made: first, the maximum level of tgABCA1 suppression was reached at relatively late time (at the third day post-transfection) and second, even on the fifth day of observation the residual ABCA1 mRNA level remains at ~25% of control (pALsh transfection).

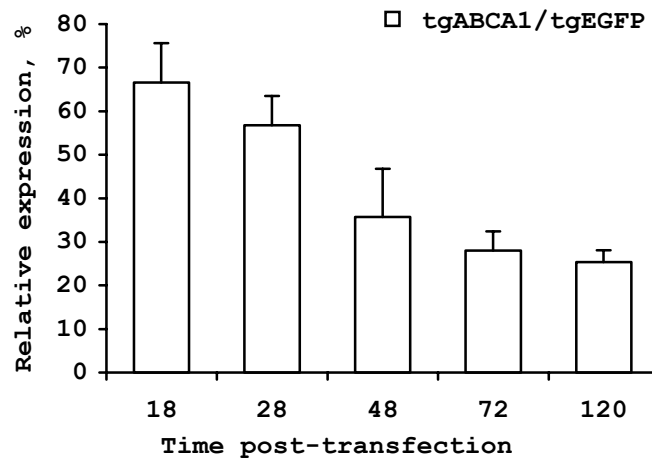


Figure 12. Ability of siRNA to suppress tgABCA1 mRNA at different time points

HEK293 cells were co-transfected with pmABCA1-FLAG, pEGFP and pALsh or pALsh-anti-ABCA1. At indicated time points post-transfection, cells were harvested, total RNA purified and tgABCA1 transcript amount was determined relatively to tgEGFP. Normalised ABCA1 expression in pALsh-anti-ABCA1-transfected cells was plotted in percents of control transfection (pALsh). Error bars indicate the standard deviation between triplicates for every measure point.

The capacity of the pALsh-anti-ABCA1(V) vector to silence transgenic murine ABCA1 expressed at various abundance was also checked. If human HEK293 cells were transfected with pmABCA1-FLAG in quantity ranging from 5 ng to 1.3 μ g, no significant difference in the efficiency of RNAi was observed (fig. 13).

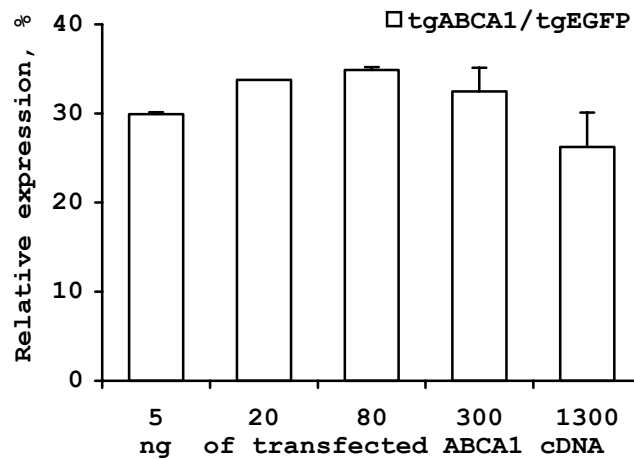


Figure 13. siRNA efficiency to inhibit transgenic ABCA1 expression from different amount of transfected cDNA

HEK293 cells were co-transfected with different amount of pmABCA1 as indicated, and constant amount of pEGFP and pALsh or pALsh-anti-ABCA1. Three days post-transfection tgABCA1 mRNA was normalised to EGFP and compared to pALsh transfected cells for different ABCA1 cDNA concentration. Plotted in percents. Error bars indicate standard deviation between triplicates for every measured point.

Construction and characterisation of adenoviral vector for anti-ABCA1 small interfering RNA delivery

The plasmid pAL-anti-ABCA1(V) expressing the siRNA, which was able to silence the murine cholesterol transporter ABCA1, was used to construct a recombinant adenoviral vector. The promoter region H1, oligonucleotide insertion together with penta-T termination motive was transferred into shuttle vector pE1.1 (see fig. 14). This plasmid contains 1% of 5'-end adenoviral genome and kanamycin resistance gene (see above). The insert was placed as one cassette downstream of this adenoviral sequence (fig. 14). The result was a new plasmid pE1.1-anti-ABCA1. The cloning procedure was proved by double digest with *SpeI* and *XbaI* endonucleases (fig. 15A). In a second step, the 1.5 kb fragment of the plasmid pE1.1-anti ABCA1 including KanR, 5'-end of adenoviral genome and H1-siRNA cassette was directly inserted into the *SfiI* digested plasmid pAdenoQuick1.1 (see above).

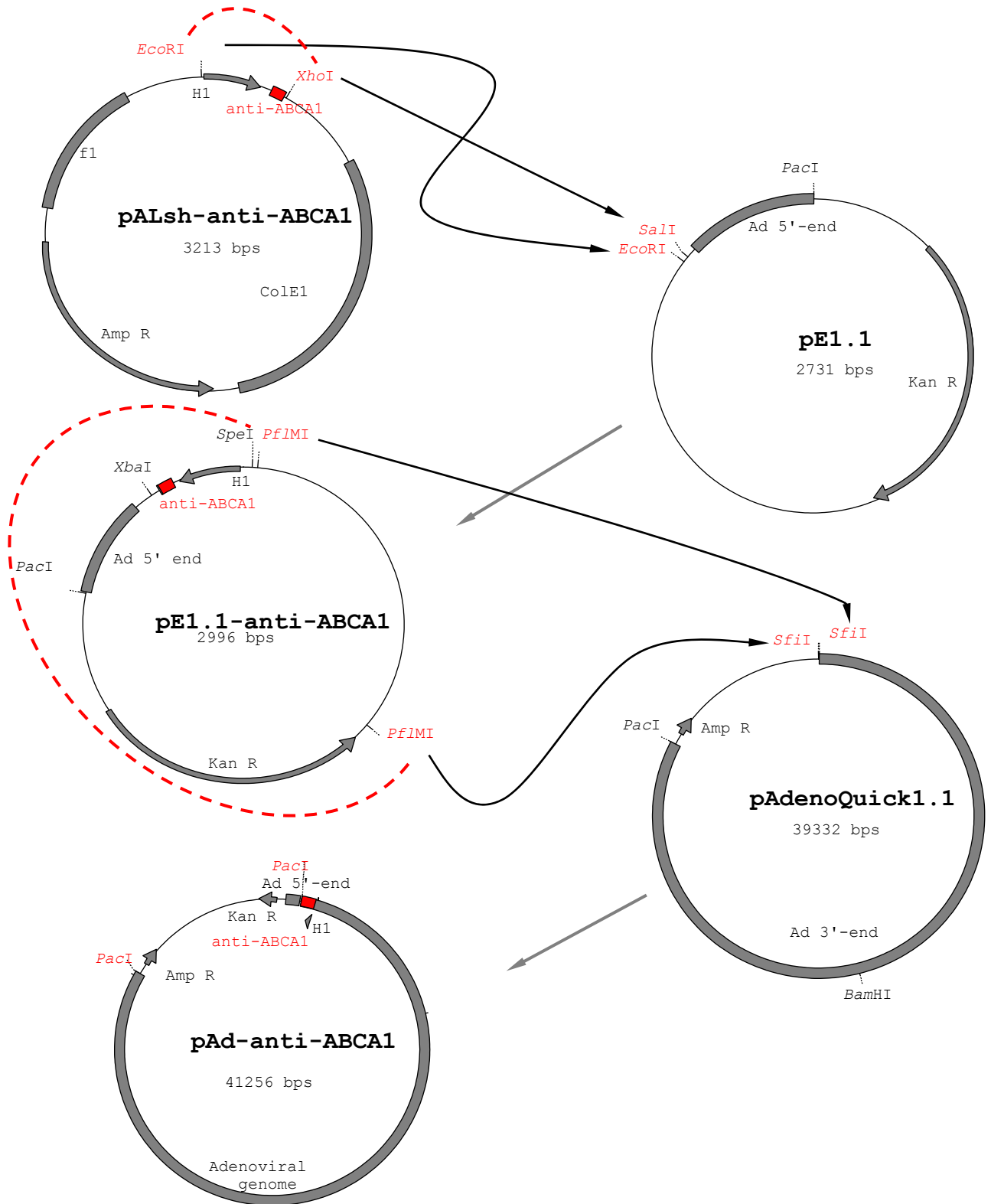


Figure 14. Cloning of anti-ABCA1 siRNA-expressing adenoviral vector

Two step strategy for pAd-anti-ABCA1 vector cloning. First, H1 promoter together with siRNA-expressing insert was recloned into the shuttle plasmid pE1.1. Second, the 5' region of adenoviral genome with downstream-located anti-ABCA1 insert was directly cloned into the plasmid pAdenoQuick1.1 encoding all viral genes minus E1 region. The resulting plasmid pAd-anti-ABCA1 carries complete genome of the 1st generation adenovirus with siRNA expressing cassette as a transgene. Amp^R: ampicillin resistance gene; Kan^R: kanamycin resistance gene; ColE1: minimal *E.coli* origin; f1: origin of single strand DNA replication of the filamentous phage F1.

The resulting plasmid pAd-anti-ABCA1 then included complete adenoviral genome minus E1 region, ampicillin and kanamycin resistance genes as well as anti-ABCA1(V) siRNA-expressing cassette. To generate this plasmid a non-palindromic *Sfi*I endonuclease restriction site was utilised, which is absent in adenoviral genome and also a special ligation temperature-profile was established (see discussion). The preciseness of cloning was checked by several digestion reactions, all of which should produce one unique DNA band specific for the newly created plasmid (fig. 15B).

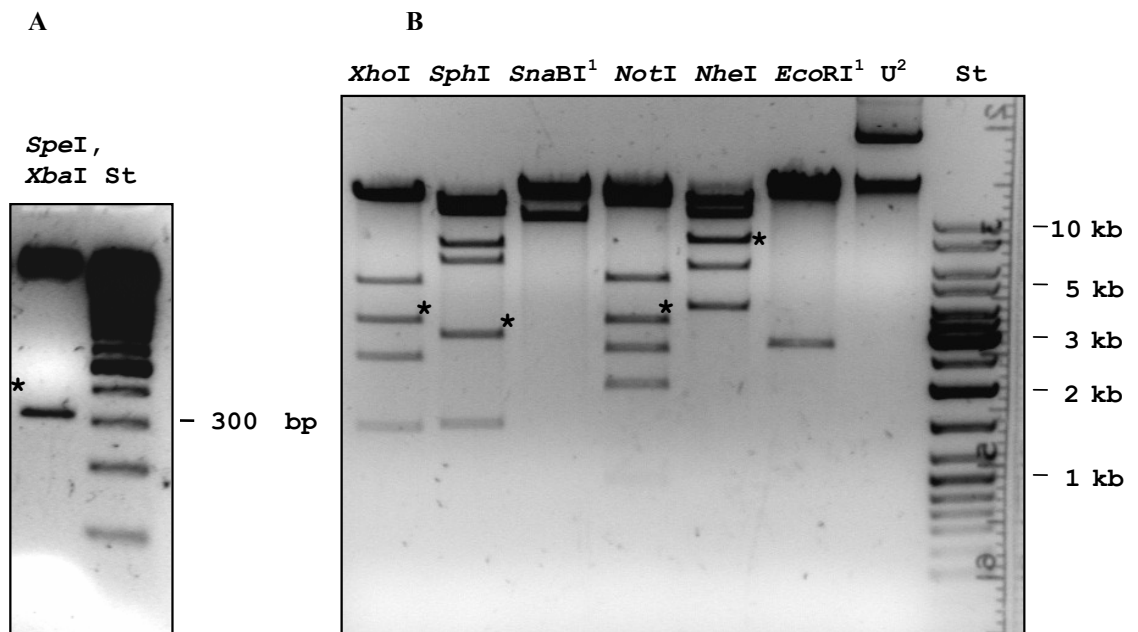


Figure 15. Cloning conformation for Ad-anti-ABCA1 adenoviral vector

(A) First cloning step checked by endonuclease release of a correct size insert (asterisk) from the intermediate plasmid pE1.1-anti-ABCA1. (B) Control digestion of the plasmid pAd-anti-ABCA1 with several endonucleases. Unique bands indicate correct clones are marked with asterisks. DNA molecular weight standard is from Fermentas. For exact fragment size please refer to the plasmid maps in appendix.

¹) *Sna*BI and *Eco*RI does not produce informative bands.

²) Indicates undigested plasmid.

To generate anti-ABCA1 adenovirus HEK293 cells were used. This cell line provides the E1 region (transcriptional activator), which is essential for adenoviral replication and is absent in 1st generation recombinant adenoviral genome. The constructed recombinant adenoviral genome was released from the plasmid by *Pac*I digest, purified by ethanol precipitation and transfected into HEK293 cells. At the ~7th day post-transfection few individual adenoviral plaques formed in cell culture (fig. 16AB).

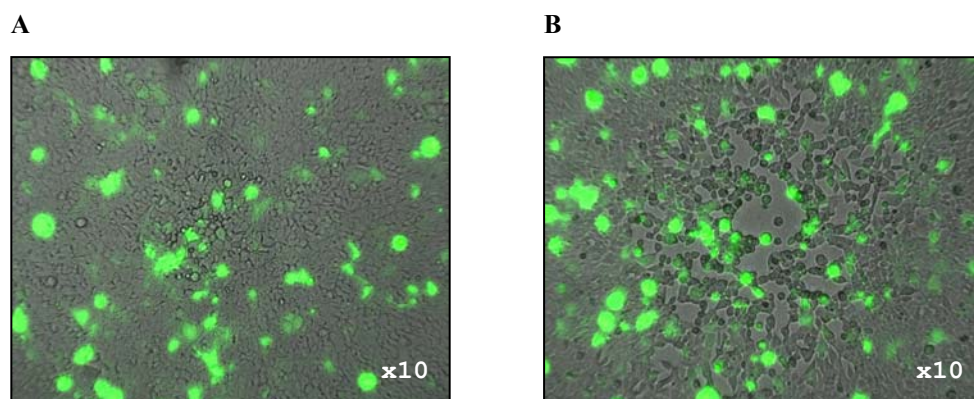


Figure 16. Adenoviral plaque formation

HEK293 cells were transfected with linear adenoviral genome. One day post-transfection cells were covered with agarose gel. (A) Initiation of the viral infection on the fifth day. (B) Two days later infection is spreading further in cell culture under the agarose. Merge of EGFP fluorescence and phase contrast.

Infectious material from a single plaque was used to propagate adenoviral culture to a big scale. Finally adenoviral particles were concentrated in CsCl density gradient (supplement, fig. 34) and CsCl was removed by NAP25 column gel filtration.

The generated stock of anti-ABCA1 adenovirus and EGFP-expressing adenovirus – Ad-EGFP was titered using “Adeno-X rapid titer kit” (BDbiosiences) under conditions recommended by the manufacture (supplements, fig. 35). Infectious titres are shown in table 4 and used for adenoviral dose calculation in all *in vitro* and *in vivo* experiments.

Table 4. Adenoviral titres

Adenovirus	Titre, mL ⁻¹
Ad-EGFP	1.2*10 ¹¹
Ad-anti-ABCA1	6.0*10 ¹⁰

Functional activity of Ad-anti-ABCA1 virus to down-regulate cholesterol transporter expression was tested in cell culture. Human hepatoma cell line – HuH7 was infected with Ad-anti-ABCA1 and Ad-EGFP at multiplicity of infection (MOI) from 1 to 100, shown in figure 17. Three days post-infection levels of human ABCA1 transcript were determined relatively to uninfected cells (wtGAPDH was used as normaliser gene). Infection with Ad-anti-ABCA1 resulted in a dose dependent degradation of wtABCA1 transcript. Already at a MOI of 10 more than 50% of the correspondent mRNA was degraded. It remained at ~25% of the expression level of untreated cells if MOI = 100 was used. Infection with EGFP-expressing adenovirus did not lead to a significant alteration of wtABCA1 mRNA level (Ad-EGFP vs. Ad-anti-ABCA1, $p < 0.01$).

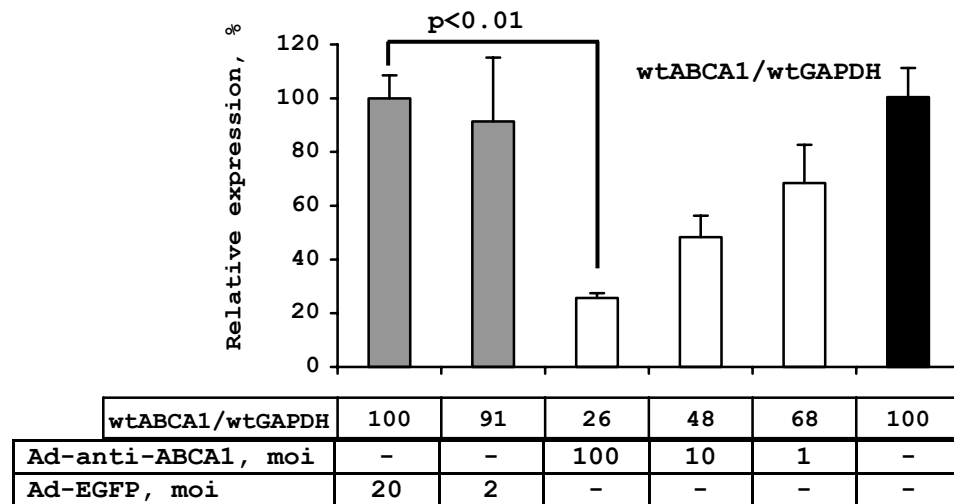


Figure 17. Adenoviral effects on the ABCA1 expression

Human hepatoma HuH7 cells were infected with Ad-EGFP (grey columns) and Ad-anti-ABCA1 (white) at various doses, as indicated. Three days post-infection cells were harvested, total RNA isolated and used for reverse transcription with consequent qPCR. The relative amount of wtABCA1 transcript was normalised to wtGAPDH and plotted as percents of its expression in the uninfected cells (black). Error bars are indicating the standard deviation between triplicates for every measure point, $n = 3$.

3.2. Liver specific ABCA1 knockdown in mice

Biodistribution of recombinant EGFP-adenovirus in vivo

Prior to analysing the *in vivo* effects of ABCA1 knockdown, it was important to verify adenoviral distribution in mice. The main target was to manage relatively high transduction in the liver tissue without any strong impact on other organs – especially lung and spleen. For this purpose wt mice were injected with low (2.5×10^8 ifu/animal) and high dose (2.5×10^9 ifu/animal) of Ad-EGFP. Three days post-infection animals were sacrificed, perfused with PBS and then the organs were extracted and investigated for EGFP-transduction ratio. The liver tissues were digested enzymatically to achieve single cell suspension. Then cells were counted by flow cytometry. Side and forward laser scattering were acquired as well as EGFP fluorescence. Laser scattering helps to identify hepatocytes according to size and surface structure of the counted particles. Detection of EGFP transduction is based on exciting the cells with the 480 nm spectral line of the argon laser and recording the emission at the 500-520 nm wavelength window. Fluorescence intensity is plotted in logarithmic scale from 1×10^{-1} to 1×10^3 relative units. Figure 18 represents histograms of EGFP fluorescence intensity distribution of the single cell suspensions of Ad-EGFP-transduced liver. The detector sensitivity was adjusted to gate all cells with fluorescence intensity less than 1.5 relative units as EGFP-negative. Cells with higher emitting signal were EGFP-positive.

At low infectious dose (2.5×10^8 ifu/animal) liver transduction failed. Only ~1% of cells expressed EGFP (fig. 18A), while at high adenoviral dose (2.5×10^9 ifu/animal) ~90% of hepatocytes were successfully transduced (fig 18B).

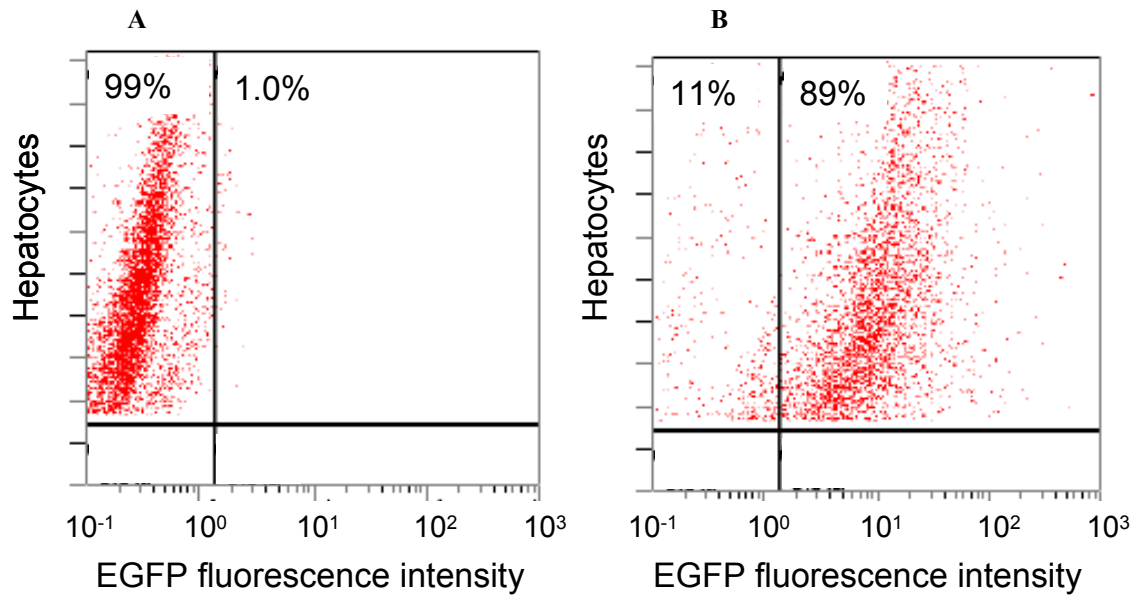


Figure 18. Detection of in vivo EGFP-transduction of mice liver cells with different adenoviral dose by flow cytometry

Mice C57Bl/6 were injected into the tail vein with low (2.5×10^8 ifu) and high (2.5×10^9 ifu) doses of EGFP-encoding adenovirus. Three days post-infection animals were sacrificed, a single cell suspension was prepared out of hepatic tissue and subjected to fluorescence flow cytometry. Fluorescence signal of EGFP was plotted against site scattering in logarithmic scale. Gate A2 represents portion of cells with EGFP fluorescence intensity higher than background. (A) Infection with low infection dose. (B) Liver EGFP-transduction with high adenoviral dose.

In parallel histological analysis of liver, spleen and lung tissues from the animal infected with high Ad-EGFP dose were performed. The majority of liver cells gave a bright EGFP signal all over the optic section, as judged by confocal microscopy. To localise individual cells nucleic DNA was stained with DAPI. In contrast, spleen and lung cells did not exhibit any clear bright fluorescence in the green channel at the same conditions (fig. 19, right). To ensure the absence of any EGFP expression in peripheral tissues, spectral characteristic (lambda stack) of the specimen was recorded using meta-detector (Carl Zeiss LSM 510 Meta, software version 3.0). Tissue slices were excited at 458 nm and emission intensity in a wavelength range from 480 nm to 560 nm (every 10 nm) was recorded in one data file (fig. 19, middle). The emission intensity data of the sample allows building its characteristic spectra (fig. 19, left). As expected, the recorded emission spectra from liver tissue were identical to EGFP characteristic spectrum, which was obtained from pEGFP transfected cell culture (supplement, figure 36). Spleen and lung had slight background green fluorescence, which is not similar to the EGFP spectrum.

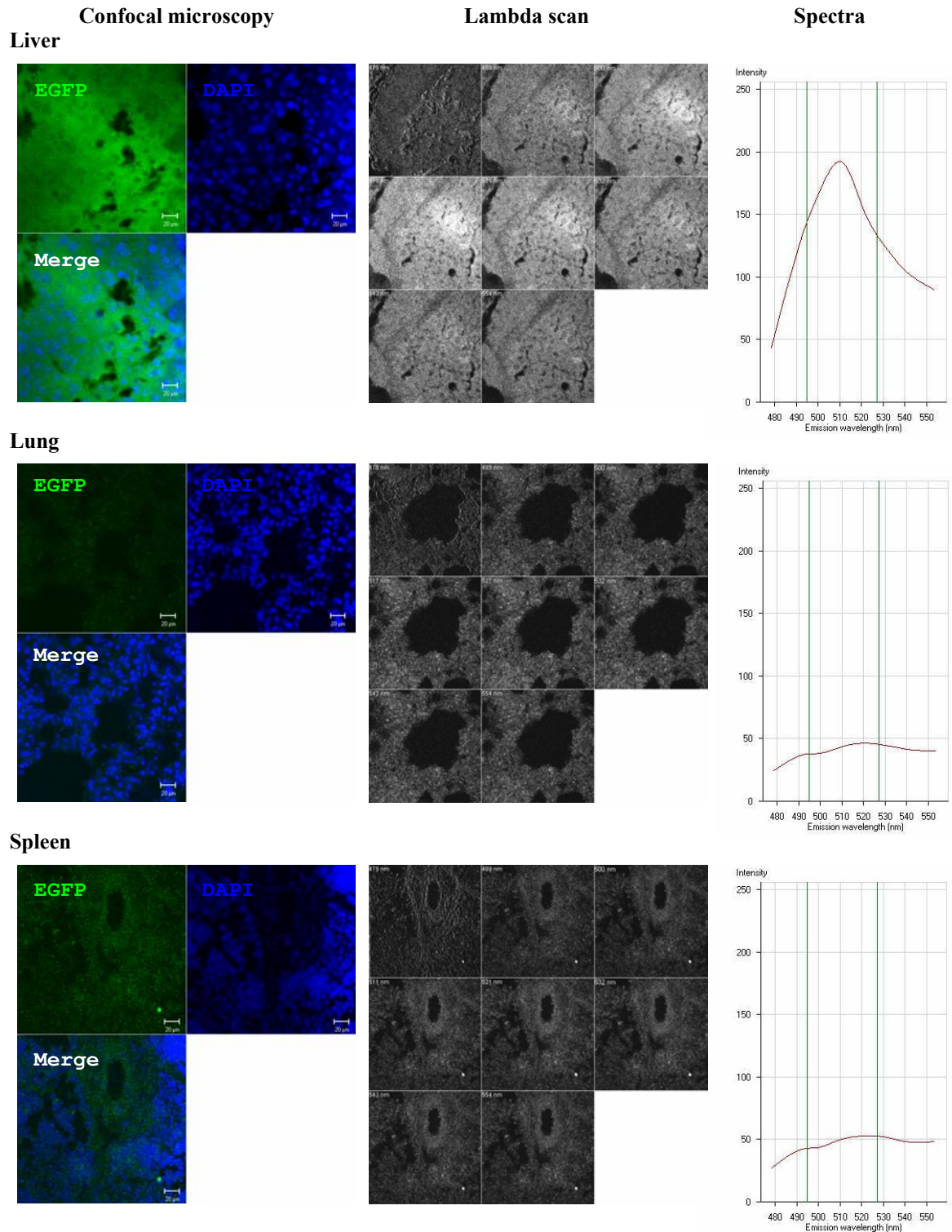


Figure 19. Biodistribution of adenoviral particles in mice organs

Liver, lung and spleen tissues from mice infected with high adenoviral dose (2.5×10^9 ifu) were cryocut, fixed in PFA and stained with DAPI. Confocal microscopy was performed, DAPI (blue) and EGFP (green) fluorescence recorded at equal conditions for all samples (right panel). Using the lambda scan mode, fluorescence intensity of the tissues at wavelength from 480 nm to 550 nm with step of 10 nm was recorded (middle). Characteristic spectral curve (left panel) helped to discriminate EGFP fluorescence from background. Bars are 20 μ m.

Expression of some proteins involved in lipid metabolism in mice liver

Wild type (C57Bl/6) male mice, 12 weeks of age were randomly organised into two groups (7 animals per each). After 2 days, blood puncture (day 0, fig. 20) was performed from the 4 hours fasted animals. Adenoviruses expressing EGFP or anti-ABCA1 siRNA were injected into the tail vein directly after the blood puncture. Plasma probes were also taken on the 5th and 7th day post-adenoviral administration.

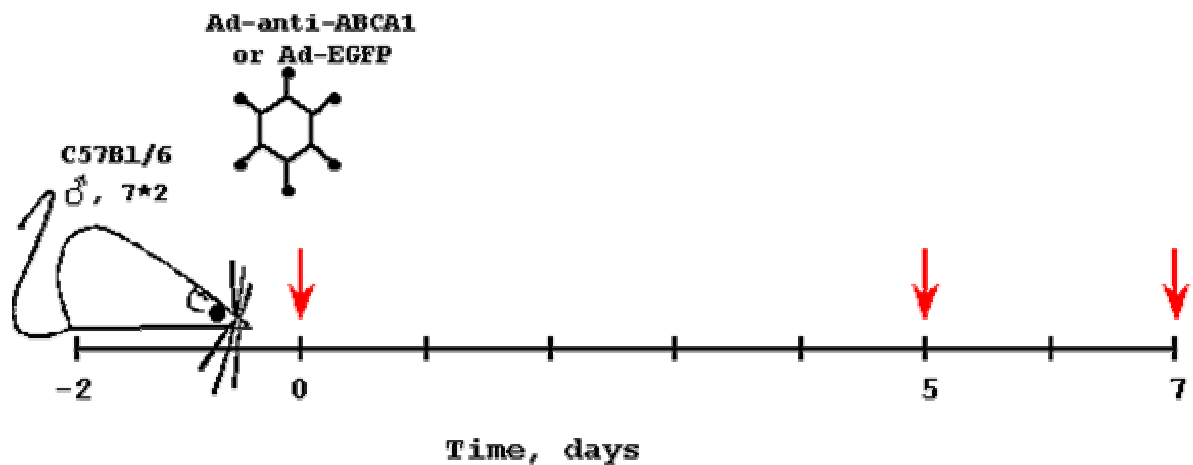


Figure 20. In vivo experimental set up

Fourteen wild type male mice were organised in two groups. Blood punctures were done before (day 0) and after (days 5, 7) Ad-EGFP or Ad-anti-ABCA1 viral administration. At the end of experiment animals were sacrificed and organs were taken for qRT-PCR and Western blot analysis.

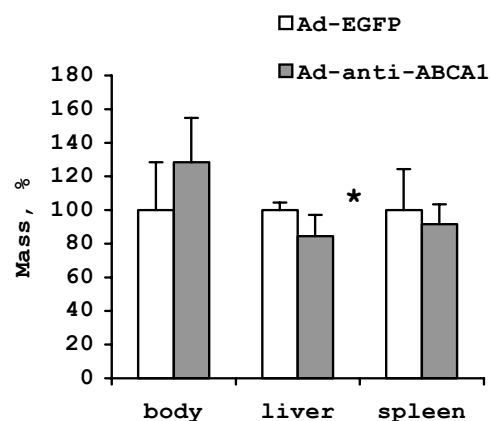


Figure 21. Relative body and organess weight

Before termination of the experiment animals from both groups were weighted alive. Liver and spleen was also weighted after perfusion (liver weight, * $p < 0.03$ Ad-EGFP vs. Ad-anti-ABCA1), $n = 7$.

On the 7th day animals were anaesthetised, sacrificed and perfused with PBS. Afterwards liver tissue sample was taken for quantitative real time-PCR and for SDS-PAGE, followed by Western blotting (fig. 20).

The figure 21 represents relative body mass as well as liver and spleen weight. On the 7th day post-infection total body weight increased on 20% as a respond on ABCA1 silencing, but high standard deviations made data not significant. In contrast, liver mass decreased significantly up to 20% in this experimental group vs. control, $p < 0.03$, $n = 7$.

In the figure 22 the relative expression of some genes in the liver are shown. The following mRNA were quantified: ApoAI, Cyp7a, SR-BI ApoE and ABCA1. GAPDH gene was not an appropriate normaliser since the mouse gene consists of only one exon, which makes no assurance for discrimination between cDNA and genomic GAPDH locus. For the normalisation of the mRNA levels two different housekeeping genes were used (PGK1 and B2M). All relative expressions were calculated using equilibrated “double-normaliser”. This approach ensures accuracy since theoretically the expression of any gene could be affected by adenoviral administration.

In the quantification experiment no difference in ApoAI and SR-BI mRNAs was found. Expression of Cyp7a mRNA was elevated 1.5 times in the Ad-anti-ABCA1 group compared with Ad-EGFP infected. However the standard deviation was relatively high. Expression of ApoE was significantly 1.4 times higher in Ad-anti-ABCA1 group ($p < 0.02$, $n = 3$). Surprisingly, no difference in cholesterol transporter transcript level was possible to detect. In both groups mRNA levels of ABCA1 appeared to be equal.

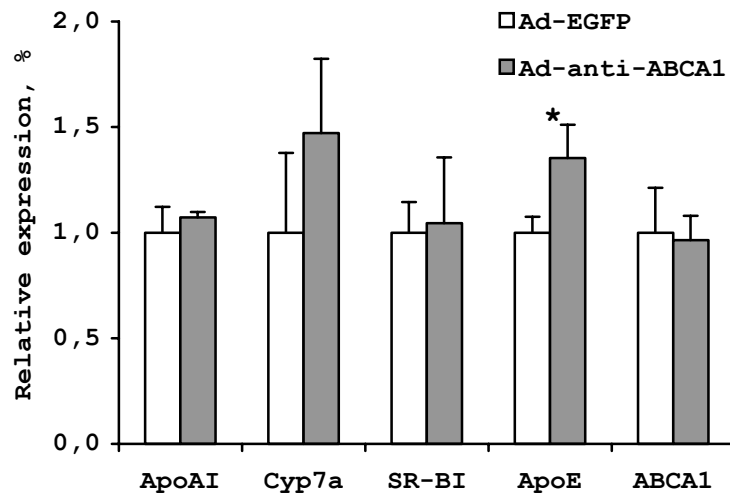


Figure 22. Comparison of mRNA levels in the liver

Liver total RNA was extracted, converted to cDNA and subjected to real time quantitative PCR. For standardisation one pair of house box genes (PGKI and B2M) was utilised. Tissues from three animals were used per group. Measurements were done in triplicates. Error bars indicate standard deviation inbetween animals in each group from two independent experiments (liver ApoE mRNA, * $p < 0.02$ Ad-EGFP vs. Ad-anti-ABCA1), $n = 3$.

Hepatocytes membrane proteins influenced by anti-ABCA1 RNA interference

Expression of some liver proteins involved in lipid metabolism in response to adenoviral administration was further investigated. On the 7th day after infection by Ad-EGFP or Ad-anti-ABCA1 mice were perfused, liver was extracted and homogenised. Plasma membrane proteins were separated in SDS-PAGE followed by Western blotting. The following proteins involved in lipid metabolism were detected with specific antibodies: ABCA1 cholesterol transporter, apolipoprotein E, LDL receptor, scavenger receptor class B type I and lipoprotein receptor related protein (fig. 23). ABCA1 protein expression was sufficiently downregulated by adenovirus mediating anti-ABCA1 RNA interference. In addition ApoE expression was slightly elevated as a response on Ad-anti-ABCA1 administration.

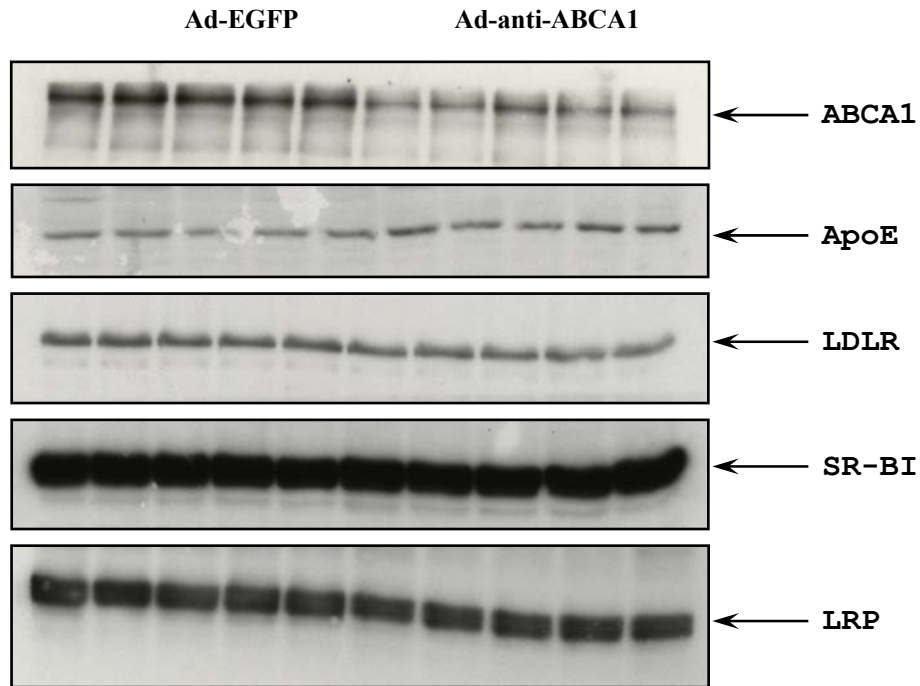


Figure 23. Expression of the liver proteins

Liver tissues were homogenised and plasma membranes were purified by ultra-centrifugation. Membrane proteins were solubilised and separated by SDS-PAGE following by Western blotting. Five animals per group were analysed. For the protein detection specific 1^o antibodies were used as indicated. Visualisation was performed using corresponding secondary antibodies conjugated with HRP and subsequent ECL detection.

In order to quantify protein abundance, Western blot membrane was digitally scanned and the optic density of each protein band was measured. After background subtraction, ABCA1 and ApoE signals were calculated in percents to Ad-EGFP infection. On the 7th day after anti-ABCA1 siRNA liver transduction liver membrane ABCA1 protein amount decreased two times vs control ($p < 0.001$, $n = 5$). Furthermore, ApoE protein increased 1.5 times when ABCA1 was down-regulated ($p < 0.003$, Ad-EGFP vs. Ad-anti-ABCA1, $n = 5$ (fig. 24A, B)). The expression pattern of the SR-BI, LRP and LDLR proteins remained similar in both groups.

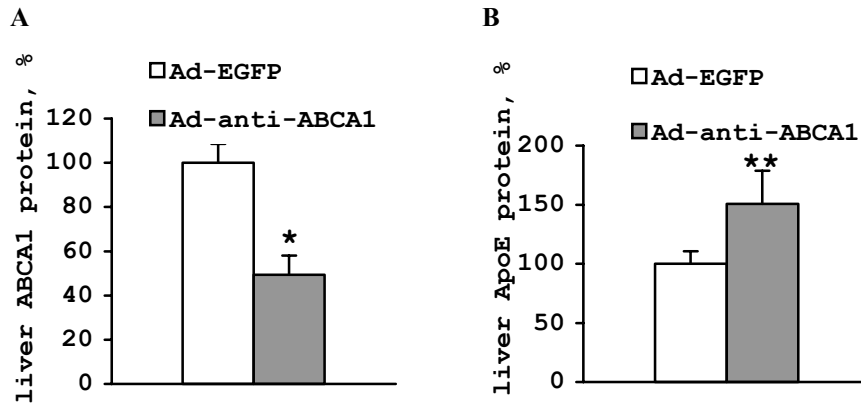


Figure 24. Quantification of the liver plasma membrane proteins

The quantification of the liver membrane ABCA1 transporter (A) and apoE (B) based on Western blot analysis (fig. 23). Chemifluorescence signals were scanned digitally for every protein band, after background subtraction relative units of intensity were averaged in each group and presented as percents to Ad-EGFP-treated group (* $p < 0.001$, ** $p < 0.003$ Ad-EGFP vs. Ad-anti-ABCA1), $n = 5$.

Plasma lipoproteins in mice

Plasma from individual blood samples ($n = 7$) was pooled into two groups according to viral administration. Immediately 200 μL of pooled plasma were separated by S6 gel-filtration chromatography and 500 μL fractions were collected. Cholesterol, phospholipids and triglyceride concentrations were determined in each of 40 FPLC fractions (fig. 25 and 28, upper diagrams always represent lipid profile after Ad-EGFP infection, lower – effects of adenoviral mediated anti-ABCA1 hepatic siRNA expression).

Plasma cholesterol profile had already changed significantly on the 5th day post-Ad-anti-ABCA administration *in vivo* (fig. 25B). This effect became more pronounced at the 7th day after infection. Seven days after Ad-EGFP injection no cholesterol profile alterations were detected as compared to the initial day of experiment (fig. 25A).

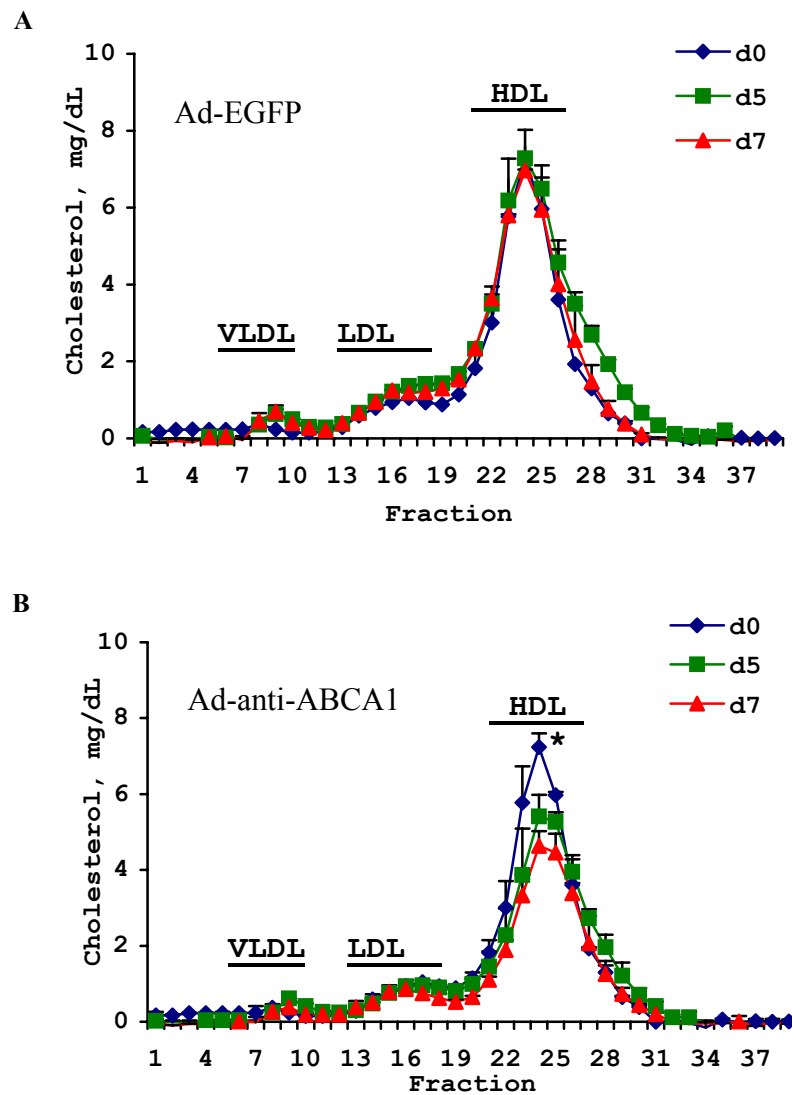


Figure 25. Cholesterol content of plasma lipoproteins fractionated by FPLC

Plasma samples were collected and pooled ($n = 7$) from C57Bl/6 mice before (blue) and 5 (green) or 7 days (red) after injection with 2.5×10^9 (ifu/mouse) of Ad-EGFP (A) or Ad-anti-ABCA1 (B). Gel-filtration of fresh plasma pools was done immediately. Cholesterol concentration was determined in each FPLC fraction (HDL-cholesterol, $*p < 0.02$ day 0 vs. day 7). VLDL-, LDL- and HDL-containing fractions are indicated. Fraction numbers are at the bottom.

To determine and compare lipoprotein concentration of different size, FPLC fractions from 7 to 11 were collected as VLDL-, from 13 to 17 – as LDL- and from 21 to 26 – as HDL-containing pools. The distribution of the cholesterol concentration through different lipoprotein containing pools is shown in figure 26. All changes in cholesterol content under anti-ABCA1 siRNA treatment were observed in HDL-containing fractions.

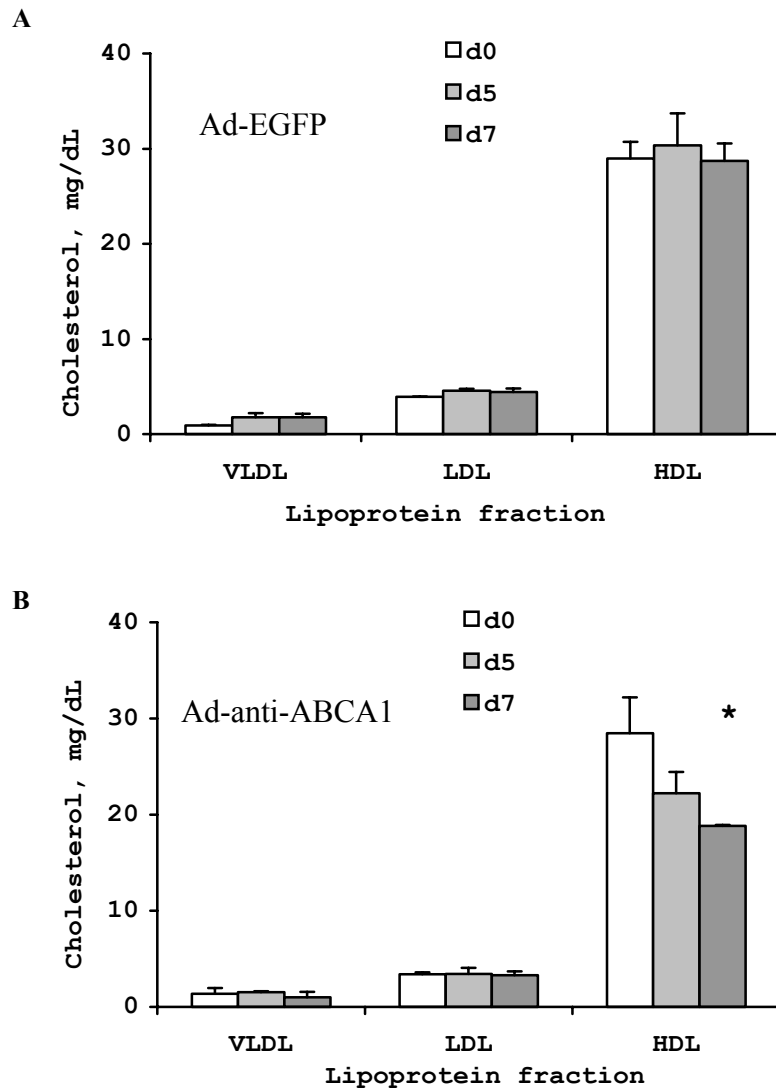


Figure 26. Plasma cholesterol concentration in different lipoprotein fractions

Cholesterol concentrations were determined in every FPLC fraction (see above) and integrated to calculate lipids amount in VLDL, LDL or HDL containing fractions. (A) Effects of Ad-EGFP administration. (B) Plasma cholesterol response on Ad-anti-ABCA1 injection (HDL-cholesterol, * $p < 0.009$ day 0 vs. day 7). Experiments were repeated twice, while plasma from seven animals was pooled each time.

There was a definite progressive decrease between pre-infection day and day 7 post-infection (fig. 26B) in contrast to Ad-EGFP infection (fig. 26A). It is important to note that neither Ad-EGFP nor Ad-anti-ABCA1 administration had a significant impact on VLDL- or LDL-cholesterol.

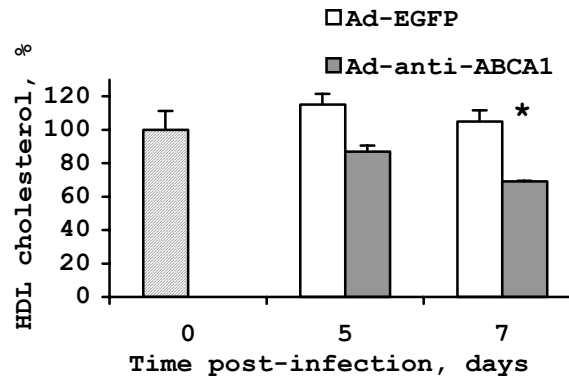


Figure 27. Cholesterol related to the plasma HDL particles

Plasma was separated by FPLC and fractions from 21 to 26 were pooled. The cholesterol concentration in HDL-containing fractions was determined for the Ad-anti-ABCA1 infection (grey columns) and for the reference infection with Ad-EGFP (empty columns) at the different time points and calculated in percents to the uninfected control (striped column). Average from two experiments (* $p < 0.009$, Ad-EGFP vs. Ad-anti-ABCA1).

Generally, HDL cholesterol dropped down to $\sim 60\%$ of the initial level on the 7th day after Ad-anti-ABCA1 infection compared to Ad-EGFP (fig. 27). The plasma phospholipids profile was stable in the control group (Ad-EGFP infected, fig. 28A) during the observed period. In contrast, plasma pools obtained from Ad-anti-ABCA1 infected animals showed a slight decrease in phospholipids in HDL containing fractions (fig. 28B) on the 7th day. Similar to cholesterol, figure 29 summarises phospholipids concentration in VLDL, LDL and HDL fractions. In the control group phospholipids in HDL show a little progression, and in Ad-anti-ABCA1 a slight decrease (fig. 29A and B). Therefore ABCA1 is also involved in phospholipids transfer. In contrast to cholesterol, phospholipids content did not change significantly (fig. 30) and on the 7th day after virus administration remained at $\sim 85\%$ of the initial level.

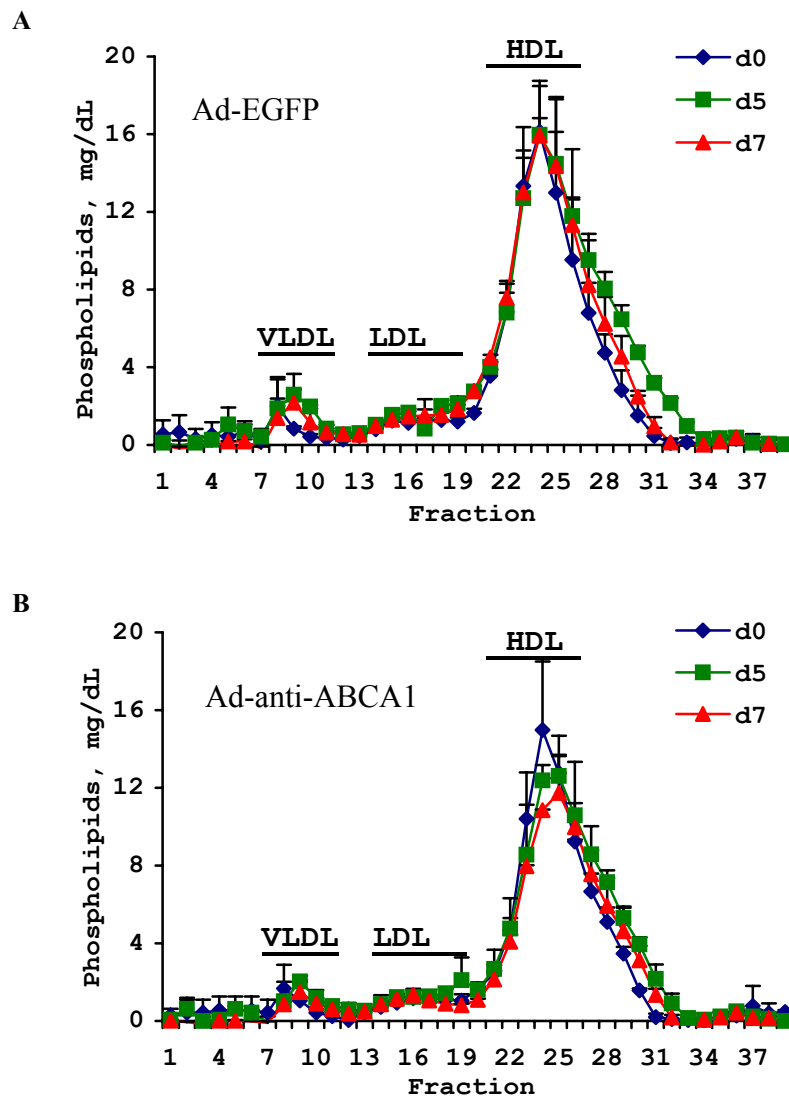


Figure 28. Phospholipids content of plasma lipoproteins fractionated by FPLC

Plasma samples were collected and pooled ($n = 7$) from C57Bl/6 mice before (blue) and 5 (green) or 7 days (red) after injection with 2.5×10^9 (ifu/mouse) of Ad-EGFP (A) or Ad-anti-ABCA1 (B). Gel-filtration of fresh plasma pools was done immediately. Phospholipids concentration was determined in each FPLC fraction. VLDL-, LDL- and HDL-containing fractions are indicated. Fraction numbers are at the bottom.

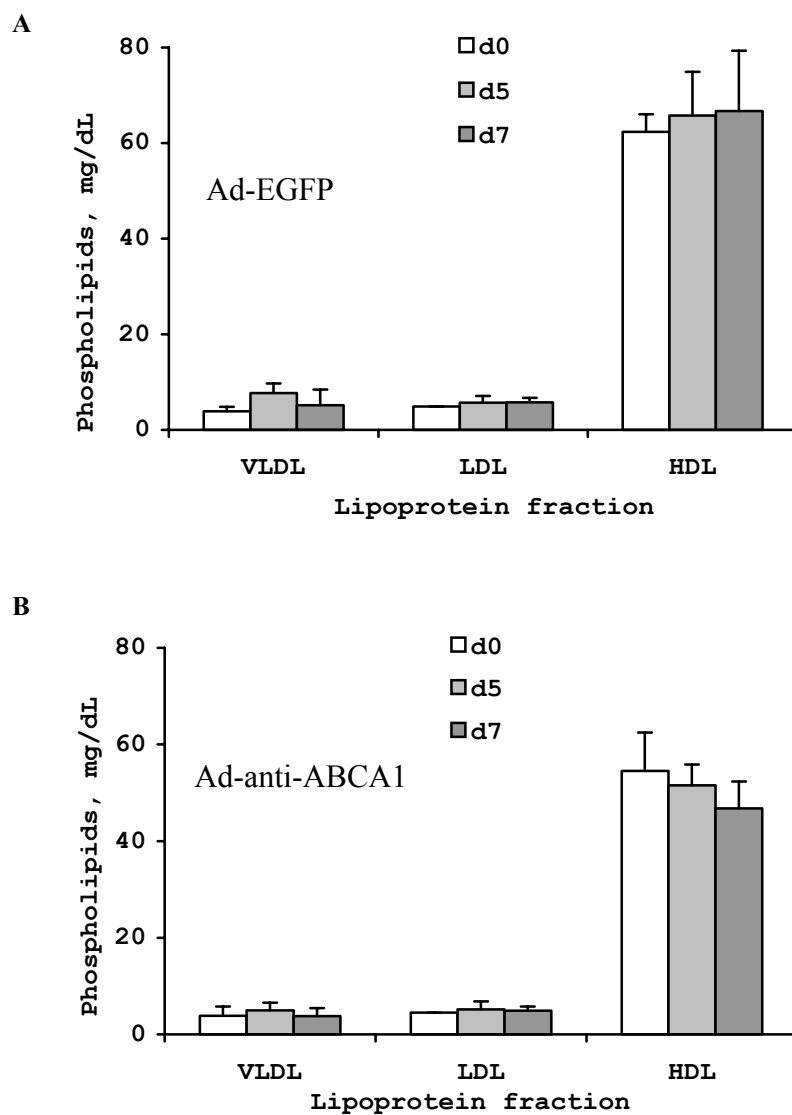


Figure 29. Plasma phospholipids levels in different lipoprotein fraction

The phospholipid concentrations were determined in every FPLC fraction (see above) and integrated to calculate lipids amount in VLDL, LDL or HDL containing fractions. Effects of Ad-EGFP administration (A) and Ad-anti-ABCA1 (B). The experiment was repeated twice, plasma from seven animals was pooled for each.

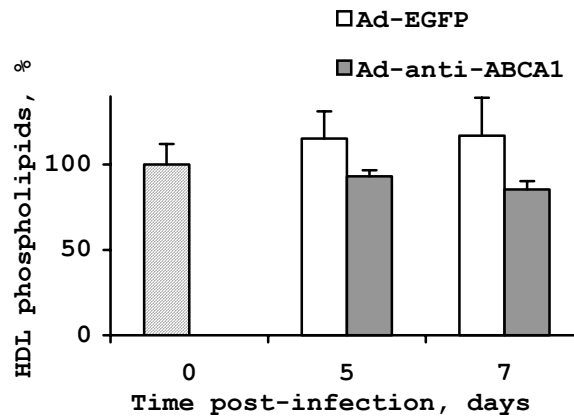


Figure 30. Plasma HDL-phospholipids levels

High density lipoprotein containing fractions were separated by FPLC and fractions 21-26 of adenoviral-infected mice ($n = 7$) were pooled. The empty columns represent control infection (Ad-EGFP) and grey columns - Ad-anti-ABCA1 infection. Phospholipids load of HDL at the different time point are presented in percents to the uninfected control – striped column. Average from two experiments.

The triglyceride FPLC profiles were obtained with much stronger variation between the different days analysed (supplements; fig. 38 and 39). Generally, there was no pronounced effect on triglyceride concentration in any lipoprotein fraction in respect to adenoviral mediated hepatic ABCA1 silencing (fig. 31).

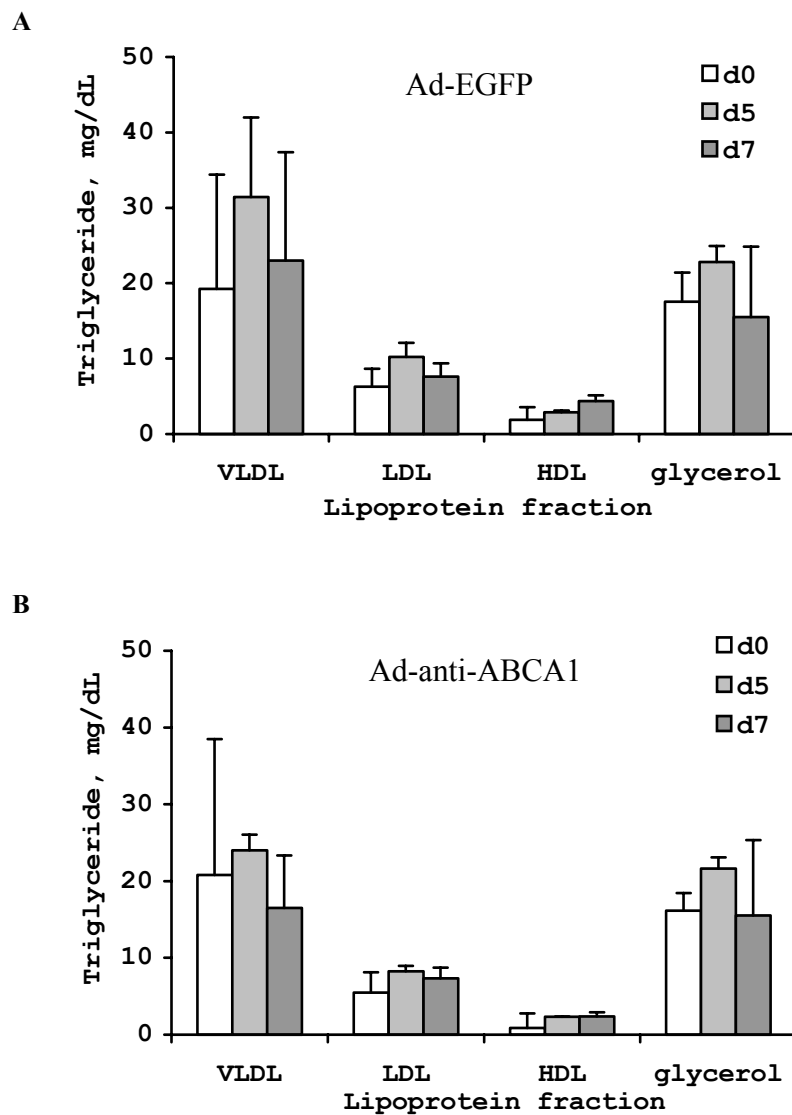


Figure 31. Plasma triglyceride levels in different lipoprotein fraction

Triglyceride concentration was determined in every FPLC fraction (see above) and integrated to calculate lipids amount in VLDL, LDL or HDL containing fractions. Effects of Ad-EGFP administration (A) and Ad-anti-ABCA1 (B). Experiments were repeated twice, while plasma from seven animals was pooled.

In addition to the lipid concentration, the amount of the most important HDL apoproteins was compared in the different HDL fractions. The proteins in the FPLC fractions 21 to 24 contained the highest amount of HDL. Apoproteins were separated in SDS-PAGE and apoproteins AI, E and CIII were detected with the respective antibodies. The plasma HDL associated apoAI amount decreased dramatically on the 7th day after anti-ABCA1 siRNA liver transduction as judged by Western blotting (fig. 32, below). Furthermore, the amount of apoE in the HDL also decreased significantly (fig. 32, above), while apoCIII remained at a constant level (supplement, fig. 37)



Figure 32. Plasma apolipoproteins 7 days post-infection

SDS-PAGE of HDL-containing FPLC fractions (as indicated) from pooled mice plasma (n = 7), 7 days post-injection with Ad-EGFP or Ad-anti-ABCA1. Western blot detection was done with anti-ApoE (1:2000) rabbit IgG and anti-ApoAI (1:1000) mouse IgG and visualised by GARPO (1:5000) and GAMPO (1:5000) respectively.

In conclusion, these experiments show that hepatic ABCA silencing mediated by adenoviral delivery of siRNA directly influences HDL cholesterol plasma level and HDL associated apoproteins concentration.

4. Discussion

In this study, RNA interference mediated gene silencing for endogenous and ectopically expressed ABCA1 was successfully established. A recombinant adenovirus carrying shRNA insert was constructed, which provides down regulation of ABCA1 expression exclusively in liver *in vivo*. The alteration of plasma HDL-cholesterol as well as the expression of apolipoproteins and liver proteins involved in lipid metabolism was observed over a one-week period after adenoviral administration.

4.1. RNA interference construction and *in vitro* studies

The overexpressing system was designed for *in vitro* testing of shRNAs. HEK293 cells were transfected with murine ABCA1 cDNA. This resulted in a ~1000x increase of specific mRNA production (fig 6). Furthermore, using confocal microscopy, ABCA1 protein was detected (fig. 7).

To design RNA interference for ABCA1 silencing the method previously established in our laboratory was utilized. The plasmid-based system contained the H1 promoter and a TTTTT sequence as a termination signal similar to the system, first described in 2002 (Brummelkamp 2002). The multiple cloning sites are replaced with asymmetric endonuclease restriction site *BseRI* (fig. 8). Furthermore, Laatsch *et al.* proposed to completely abandon an additional loop sequence, since up to now there is no evidence for the dicer-machinery to depend on certain loop structure. This solution helps to avoid a potential problem when siRNA of unpredictable length are formed after shRNA cleavage containing additional nucleotides from the loop region (Laatsch 2003). These are most likely not complementary to the mRNA sequence, thus disturbing the highly sequence-specific process of RNAi (Amarzguioui 2003). A new rule for target sequence selection was taken into account: target sequences should start with at least two nucleotides palindromic to their counterparts in the preceding mRNA sequence. There is a high likelihood that this will result in processed siRNA which is completely complementary to the mRNA sequence independent of the exact cleavage site.

Only unique target regions were taken for the molecular design of shRNA (fig.5, see also methods). No significant similarities between targets and any other sequences in human or mouse genome were detected by the BLAST search program. This ensured

specific ABCA1 down regulation by siRNA without any unwelcome influences on other mRNAs. The murine and human targeting sequences were identical.

To choose the most effective shRNA, clone cells were co-transfected with pmABCA1-FLAG, pEGFP and shRNA expressing vectors. EGFP mRNA was used as normaliser for the mRNA quantification. While in the protein detection experiments, EGFP fluorescence served as co-transfection control. Only one clone (V) was successful to mediate ABCA1 mRNA degradation (fig. 10) and effective to silence its protein as judged by IMF and western blotting (fig. 11).

Chiu and Rana have shown that RNA interference reaches its maximum at surprisingly late time – on the second day post siRNA transfection (Chiu 2002). In order to establish the reasonable time frame for *in vivo* experiments anti ABCA1 shRNA was studied *in vitro* in a time dependent manner. It was observed that the effect of RNA interference reaches its maximum on the third day post-transfection, and on RNA level stays stable until at least the fifth day (fig. 12).

4.2. Adenovirus vector for shRNA delivery

The first generation of adenovirus vector was used in this study. This system allows relatively easy and fast cloning and virus propagation. Insertion of shRNA expressing cassette has been performed by direct cloning into viral vector which has certain difficulties since vector is ~39 kb and the insert is just ~2 kb in size. To enrich successful clone outcomes, a special ligation protocol was designed for this study. Standard ligation procedure (see methods) was performed in PCR thermocycler blocks. In order to provide an optimal balance between high ligase enzymatic activity (approximating to the maximum at room temperature) and low motility of ligating DNA fragments (stopping their Brownian movement at 0°C) the reaction was exposed to temperature cycling between 5°C and 20°C and back to 5°C, with steps of 1°C. At each step, the ligation mixture was incubated for 0.5 min; the total number of cycles was 10. The initiation (fig.16), propagation and CsCl purification (fig. 34) of adenovirus was performed according to the established procedures in our laboratory. For titration, a commercial kit was used, which allows the determination of the number of infectious particles capable of penetrating HEK293 cells and initiating hexon protein synthesis (fig 35). The titration is based on an immunochemical reaction with hexon protein of

viral capsid. Adenoviral titre therefore was expressed as ifu – infection forming units per mL. Accordingly to the manufacturer report, ifu is a very similar value to pfu – plaque-forming unit and titres determined by this kit were about the same as those determined by measuring cytopathic effects using the limiting dilution method.

Adenovirus was injected in mice via tail vein. As shown by several studies, administration of the virus initiates transgene expression predominantly in the liver (Jaffe 1992, Zinn 1998, Awasthi 2004). The study conducted *in vivo* on adenoviral-mediated hepatic overexpression of human ABCA1 in mice showed firstly that after infusion of 1.5×10^9 pfu/animal into the tail vein there was still a dose-dependent increase of transgenic ABCA1 hepatic expression and secondly that at the given dose there was no detectable spleen infection (Wellington 2003). However, in the current study a higher dose was used (2.5×10^9 pfu/animal) since it is much more important for knockdown experiments to transduce total cell population than for overexpression experiments (fig. 18). It was preliminary revealed that a dose of 2.5×10^9 pfu/animal does not make significant gene delivery to spleen and lung as judged by EGFP fluorescence detection (fig 19).

Adenoviral infection itself may generally influence biological processes *in vivo* and liver lipid metabolism in particular. Therefore a control group of animals was obtained by administering EGFP expressing adenovirus at the same dose as anti-ABCA1 shRNA expressing virus.

Munehira *et al.* have reported that the turnover of ABCA1 transporter has a half-life of about 1 - 2 hours (Munehira 2004). Adenoviral-delivered transgenes in the liver normally reach expression maximum at the third day post-administration and stay for at least few weeks as an episomal genetic material in hepatocytes (Jaffe 1992). Finally, as HDL half-life is approximately 1 day, 5 - 7 days after viral injection was seen to be a reasonable time to begin observations (fig. 20).

4.3. Hepatic ABCA1 transporter and HDL metabolism

In this study plasma HDL level was reduced down to ~60% by *in vivo* liver transduction with siRNA-expressing adenovirus, targeting ABCA1 cholesterol transporter (fig 25, 26, 27). Also HDL phospholipids were decreased down to ~75% (fig. 28, 29, 30). Finally HDL apolipoproteins (apoAI and apoE) were down regulated

(fig. 32). In contrast triglyceride concentrations as well as other lipoproteins were not affected (fig. 31). This result was obtained by down regulation of liver ABCA1 protein content only to 50% of its physiological level (fig. 23, 24). Partial protein knock-down could be explained by a few factors:

a) RNA interference *in vitro* has never reached more than 70-80% efficiency (fig. 12 and 13)

b) No more than 90% of hepatocytes were successfully transduced even at the highest dose (fig. 18).

Taking these circumstances into account, it is possible to assume that hepatic ABCA1 cholesterol transporter is essential for the generation of 80% or more of the total plasma HDL particles.

The proposal that the liver itself generates the majority of the HDL only appears to be controversial – in fact it is not. This does not harm the general concept of reverse cholesterol transport but with slight modification incorporates previously discovered facts and helps to solve existing paradox.

Four points must firstly be considered:

It has been shown that only lipid-free apoAI is able to interact efficiently with ABCA1 *in vitro* (Denis 2004). This therefore forms a paradox with the findings that lipid-free-apoAI molecules are normally not present in significant quantities in plasma (Liang 1994, Asztalos 1995). So apoAI is only able to compose plasma HDL in the form it is never present in plasma.

The Wisconsin Hypoalpha Mutant chicken hypercatoblises apoAI and accumulates cholesteryl esters in hepatic parenchyma and intestinal epithelial cells (Oram 2002). This implies that unlipidated apoAI is rapidly cleared from the plasma, presumably by the kidney. So it is rather senseless to secrete apoAI directly to the plasma.

Banerjee *et al.* have shown that synthesised apoAI was rapidly transported from RER to Golgi complex, and that at steady state apoAI was predominantly localised in trans-Golgi network and derived primarily from biosynthetic and not from endocytic routes (Banerjee 1997).

ABCA1 transporter can shuttle between plasma membrane and late and early endosomes (Neufeld 2001, Neufeld 2002).

When mentioned above statements are taken together, the following hypothesis rises:

ApoAI, when synthesized by the liver, should be immediately lipidated via ABCA1 dependent phospholipids and cholesterol efflux to prevent its rapid degradation. Lipidation may happen not only on the surface of the hepatocytes but also in some endocytic compartments. By docking to the ABCA1, apoAI is capable of stabilizing the transporter and enhancing its expression. This post-transcriptional *in-situ* lipidation of apoAI leads to the formation of discoidal pre-HDL particles. Therefore cholesterol of nascent HDL originates exclusively from the liver.

This illustrates a primarily function of ABCA1 in plasma HDL.

Next, must be consider the following:

The very recent findings of Neufeld *et al.*, that cholesterol is retained in late endocytic compartments and that the motility of those compartments is impaired, suggests that the cellular cholesterol sequestered in TD fibroblast late endocytic vesicles impairs their movement toward the cell surface (Neufeld 2004). So ABCA1 is involved in the transportation of lipids to the plasma membrane.

ABCA1 can efflux phospholipids and cholesterol to apoAI either directly (Wang 2000) or indirectly – by creating lipid domains (Chambenoit 2001) from lipid rich tissues *in vitro*.

In monocytes/macrophages from TD patients, the basal as well as apoAI dependent cholesterol efflux is only moderately impaired. Additional mechanisms must be active to overcome the ABCA1 defect, which are not present in fibroblasts. It was speculated that members of the ABCB and ABCC families conduct this function (Klucken 2000). A most resent study revealed the crucial role of ABCG1 and ABCG4 for cholesterol efflux from macrophages to both smaller (HDL-3) and larger (HDL-2) particles (Wang 2004).

Studies with bone marrow transplantation in ABCA1 knockout mice have established that expression of ABCA1 in macrophages alone does not increase plasma HDL significantly (Joyce 2002, van Eck 2002, Haghpassand 2001).

Despite the already discussed essentiality of lipid-free apoAI for ABCA1 dependent cholesterol efflux, ABCA1 looks rather more like a secondary player in the process of cholesterol efflux from peripheral tissues and plasma HDL formation,

because it is dependent on pre-existing nascent HDL and could be competed by other mechanisms.

Furthermore, the accumulation of apoE in the liver (fig.) and the drastic decrease of HDL-derived apoE (fig.) imply an important role of intracellular apoE for the formation of mature HDL via ABCA1 *in vivo*. This hypothesis receives support from two recent studies with ABCA1 deficient mice with focus on the central nervous system (Wahrle 2003, Hirsch-Reinshagen 2004). The lack of ABCA1 resulted in considerably lower apoE levels in plasma, cerebrospinal fluid, an impaired lipidation of astrocyte-derived apoE (Wahrle 2003) and an intracellular lipid accumulation in astrocytes (Hirsch-Reinshagen 2004). Thus, the results are suggestive of an intracellular pathway existing in lipoprotein-synthesizing cells, in which apoE is tethered to lipids within endosomal compartments (Heeren 2003). These lipid-laden vesicles probably serve as a pool for the lipidation of extracellular apoA-I, in a process which is regulated by the gatekeeper ABCA1.

The other findings of this work were concerned with the apoE metabolism in response to ABCA1 functional knockdown. The amount of apolipoprotein associated with HDL was reduced. In contrast, levels of apoE in the liver increased by 50%, consistent with elevation of its mRNA expression level. This may be explained by the results of a study of apoE recycling in human fibroblasts and hepatocytes made by Heeren *et al.* This showed that recycling of TRL-derived apoE *in vitro* is stimulated by HDL-3 particles and associated with internalisation of HDL-3 derived apoAI and cholesterol efflux (Heeren 2003). The recycling of apoE results in the formation of cholesterol/apoE enriched HDL particles. In the light of these findings it was proposed that, at the cell surface, HDL (especially its apoAI component) could interact with ABCA1. This interaction may play a key role for binding, internalisation, lipidation and re-secretion of HDL derived apoAI during apoE recycling.

Thus, hepatic ABCA1 silencing might perturb apoE recycling. Elevation of apoE mRNA expression in the liver has probably happened to counteract the loss of apolipoprotein in the plasma since more and more of it becomes trapped in recycling endosomes of hepatocytes.

From this study it is not entirely assured if apoE recycling was primarily affected by the loss of either hepatic surface or endosomal ABCA1, or if it was an indirect effect

mediated by the decrease of plasma HDL. Finally, hepatic sequestration of apoE might be a cumulative effect as a smaller amount of plasma HDL has much smaller chance of activating apoE recycling via less abundant ABCA1.

Surprisingly, siRNA mediated ABCA1 mRNA degradation *in vitro* and *in vivo* was different. *In vitro* experiments were set up as method validation of RNA interference gene silencing and the protein expression was consequently reduced following a degradation of its messenger RNA (fig. 10 and 11). ABCA1 mRNA levels in mice liver were not altered after adenoviral mediated RNA interference (fig. 22). This is in contrast to a markedly reduced liver ABCA1 protein content (fig. 24A) and to physiological effects on HDL metabolism (fig. 27).

One possible explanation for the difference between mRNA and protein levels *in vitro* and *in vivo* could be given by the hypothesis proposed by Laatsch *et al.* (Laatsch 2003). Their findings suggest that shRNA targeting mRNA can also mediate post-transcriptional protein repression by blocking mRNA translation without messenger degradation – the so-called miRNA pathway (Grosshans 2002). Since the functional interconversion of siRNA- and miRNA-mediated protein repression was already demonstrated (Hutvagner 2002, Doench 2003) it was possible to hypothesise that siRNA-like mRNA degradation and miRNA-like translational repression may only be the extrema of a sterically regulated process. Haley and Zamore have shown that continuous, central A-form helix produced by mRNA and antisense siRNA is essential for RISC-mediated Mg^{2+} -dependent endonucleolytic cleavage of mRNA. If the central helix is disturbed, by wobble for example, mRNA could not be cleaved but translation would be reduced (Haley 2004). It is however possible that siRNA and miRNA mechanisms have different biochemical requirements or could be triggered by the host, since in this study *in vivo* and *in vitro* experiments have been done on mouse and human backgrounds respectively. From another point of view, if siRNA and miRNA do not require two independent molecular pathways, then the existence of a minimum unit of RNA interference may be revealed by the difference between mouse and human physiology, highlighting a situation where one process supports and/or mimics the other. In this case either human or mice model may be partially depleted in RNA interference machinery, which deserves additional study.

5. Summary

The role of the hepatic ABCA1 cholesterol transporter for HDL metabolism was studied in this dissertation using adenoviral-mediated RNA interference to target ABCA1. The influence of hepatic siRNA-mediated ABCA1 down-regulation on HDL plasma concentration *in vivo* was analysed. Five different plasmid-based siRNA vectors directed against sequences within the murine ABCA1 gene were generated. The efficiency of siRNA-mediated down-regulation of a co-transfected ABCA1 construct in HEK 293 cells was judged by RT-PCR, immunofluorescence and Western blot analysis. The recombinant adenovirus was constructed using the most effective plasmid, enabling down-regulation of ABCA1 expression exclusively in the liver. This anti-ABCA1 virus was administrated into the tail vein of C57Bl/6 male mice in the dose of 2.5×10^9 ifu. One week after injection, in comparison to the control group (administrated with EGFP expressing adenovirus), Western blot analysis of liver membrane preparations indicated a significant (~50%) down-regulation of endogenous ABCA1 protein in all Ad-anti-ABCA1 treated mice. Moreover, FPLC analysis of pooled plasma samples revealed that ABCA1 protein reduction was associated with an approximately 60% reduction of HDL cholesterol levels while other lipoprotein classes were not influenced.

As a secondary effect a 1.5 times elevation of apoE expression was observed in the liver as a response to ABCA1 down regulation, while other proteins involved in lipoprotein metabolism were not influenced.

In conclusion, the current study demonstrates that hepatic ABCA1 silencing mediated by adenoviral delivery of siRNA markedly reduced HDL cholesterol plasma levels in mice.

5. Supplements

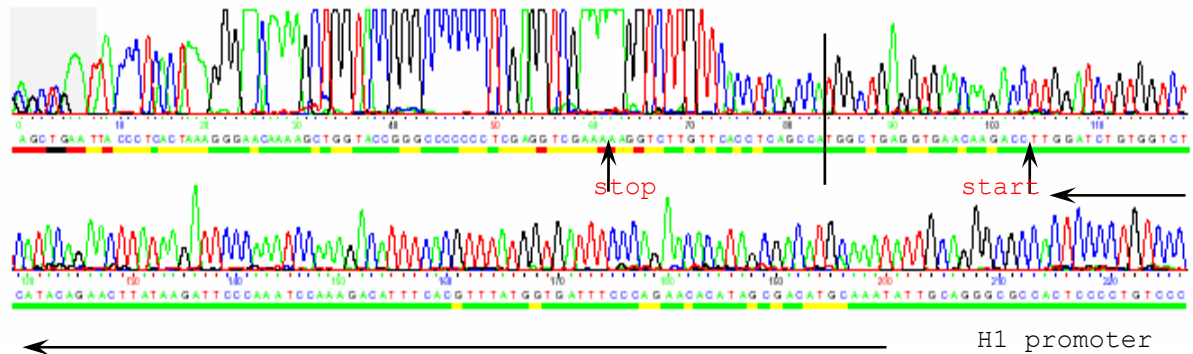


Figure 33. Sequence conformation of cloning anti-ABCA1(II) siRNA-expressing oligonucleotide into the plasmid pALsh

The plasmid pAL-anti-ABCA1 was sequenced starting from reverse primer seqALsh. Termination site penta-T motive and transcriptional initiation site (indicated with arrows) flanks palindromic oligonucleotide sequence encoding anti-ABCA1(II) siRNA (vertical line indicates symmetry position). Horizontal arrow – partial H1 promoter sequence.

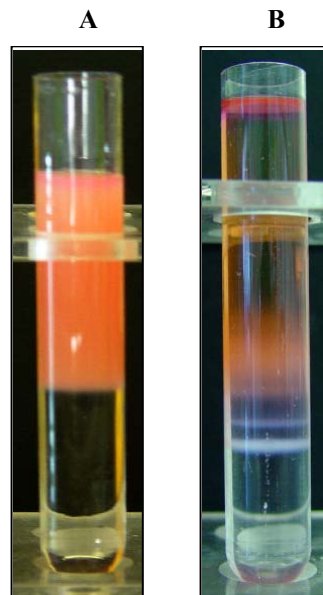


Figure 34. Concentration of adenoviral particles in CsCl density gradient

Cells with productive adenoviral infection were harvested and lysed by three cycles of freezing-thawing in liquid nitrogen. Lysate was loaded on CsCl density gradient and ultracentrifuged.

(A) before ultracentrifugation.

(B) After ultracentrifugation: two white bands formed, upper – defective viral particles at the lower density; lower band represents more dense particles.

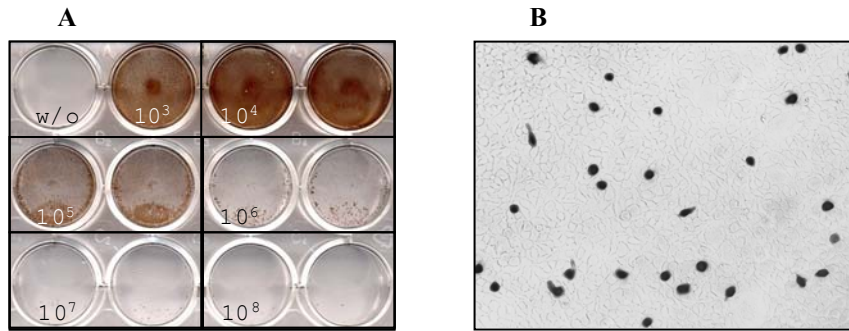


Figure 35. Adenoviral titretion

HEK293+E1 competent cells in 12-well plate were infected with different adenoviral dilutions as indicated. (A) Two days post-infection cells were fixed, immunostained with anti hexon-protein antibody (mouse, 1:1000) and visualised with HRP-conjugated anti-mouse IgG antibody (rat, 1:500) and DAB reaction. (B) Titre determination was done by counting hexon-positive cells at x20 magnification accordingly manufacturers recommendations.

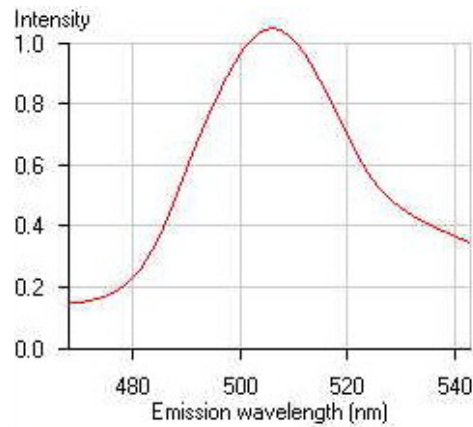


Figure 36. Reference EGFP fluorescence spectrum

Emission spectrum of pEGFP-transfected cell culture was recorded. Confocal microscopy, lambda scanning mode (wavelength window step = 10 nm). Excitation wavelength is 458 nm.

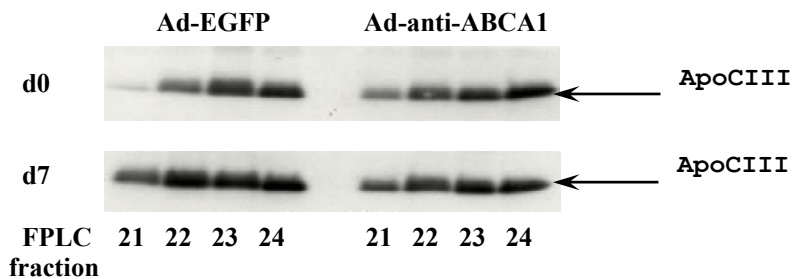


Figure 37. Plasma apolipoprotein CIII

SDS-PAGE of HDL-containing FPLC fractions from C57Bl/6 mice plasma (n = 7) before (above) and 7 days after (below) injection with 2.5×10^9 (ifu/mouse), of Ad-EGFP or Ad-anti-ABCA1. Western blot detection were done with apoCIII (1:1000) antibody and visualised by GARPO (1:5000) and ECL.

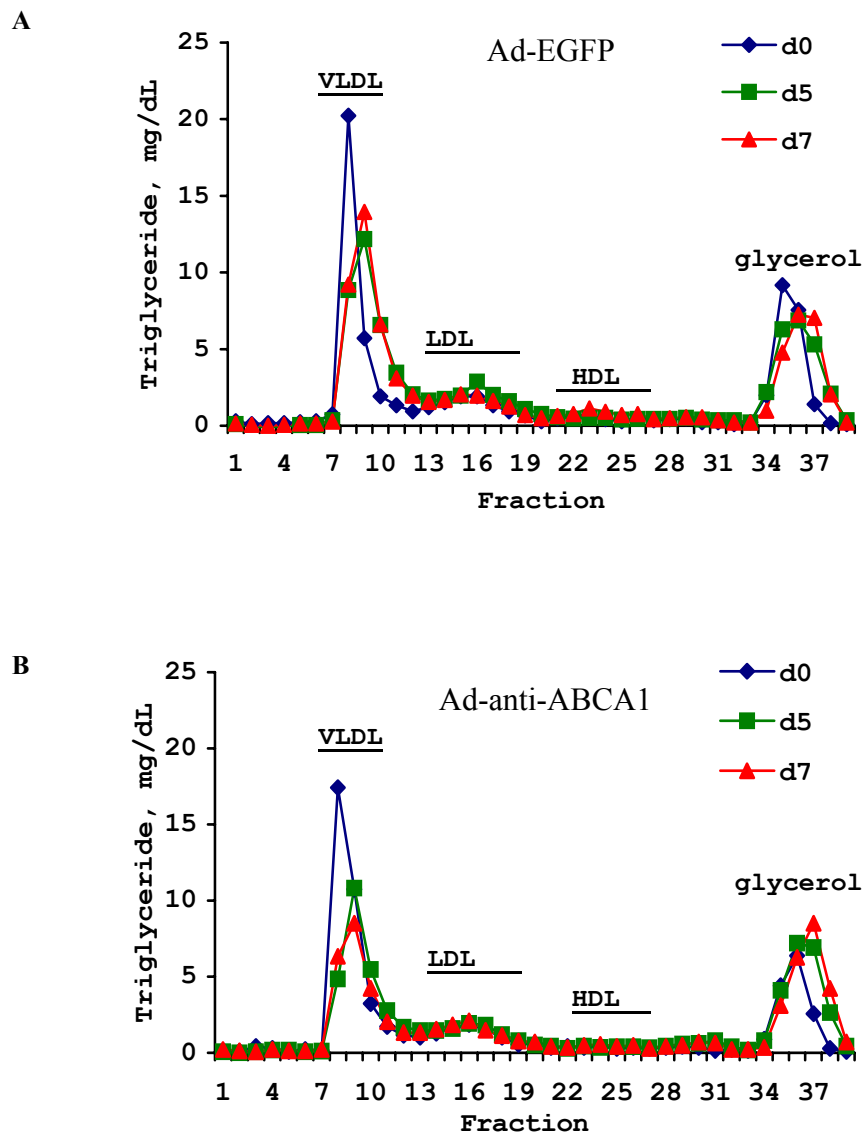


Figure 38. Triglycerides of plasma lipoproteins fractionated by FPLC

Plasma samples were collected and pooled ($n = 7$) from C57Bl/6 mice before (blue) and 5 (green) or 7 days (red) after injection with 2.5×10^9 (ifu/mouse) of Ad-EGFP (A) or Ad-anti-ABCA1 (B). Gel-filtration of fresh plasma pools were done immediately. Triglyceride concentration was determined in each FPLC fraction. VLDL-, LDL-, HDL- and glycerol-containing fractions are indicated. Fraction numbers are at the bottom.

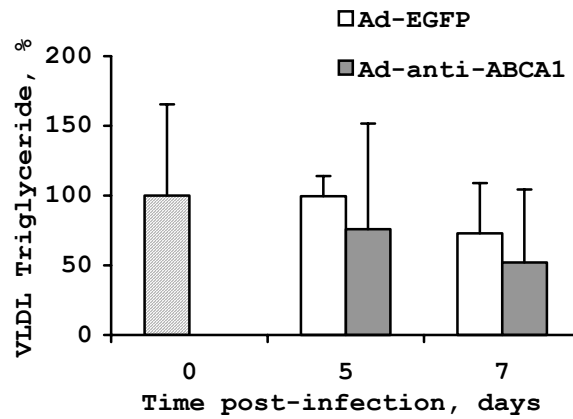


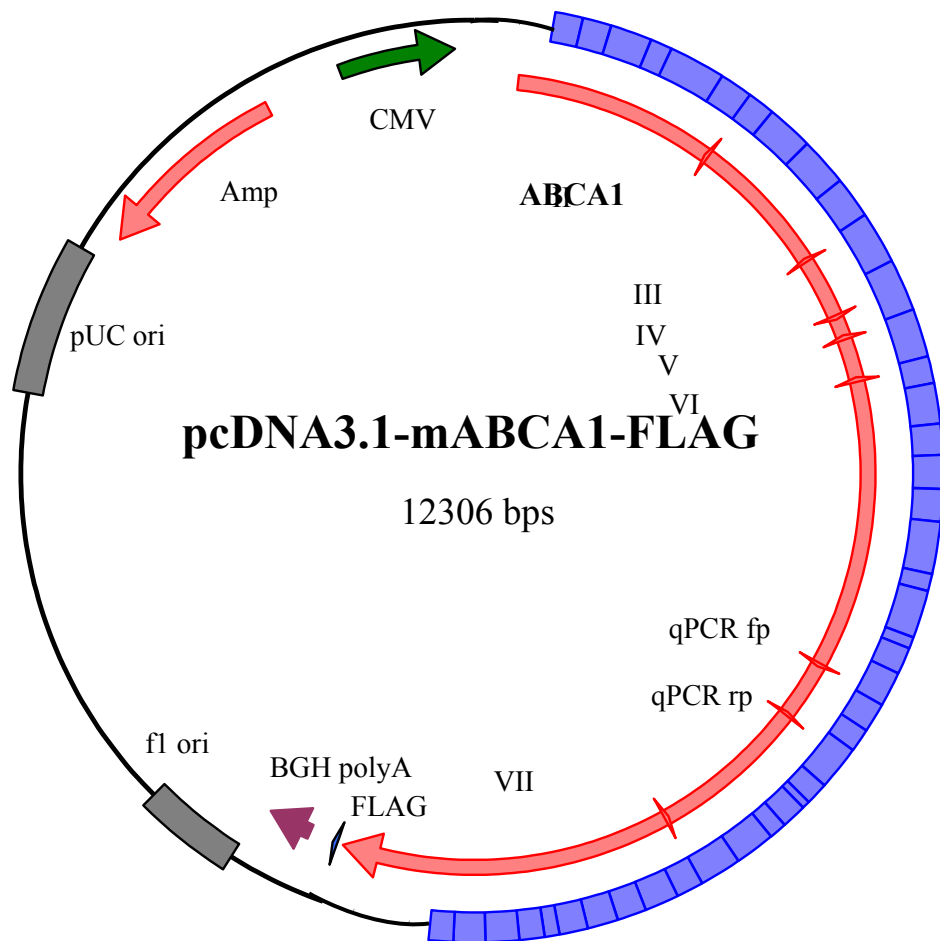
Figure 39. Plasma HDL-triglyceride levels

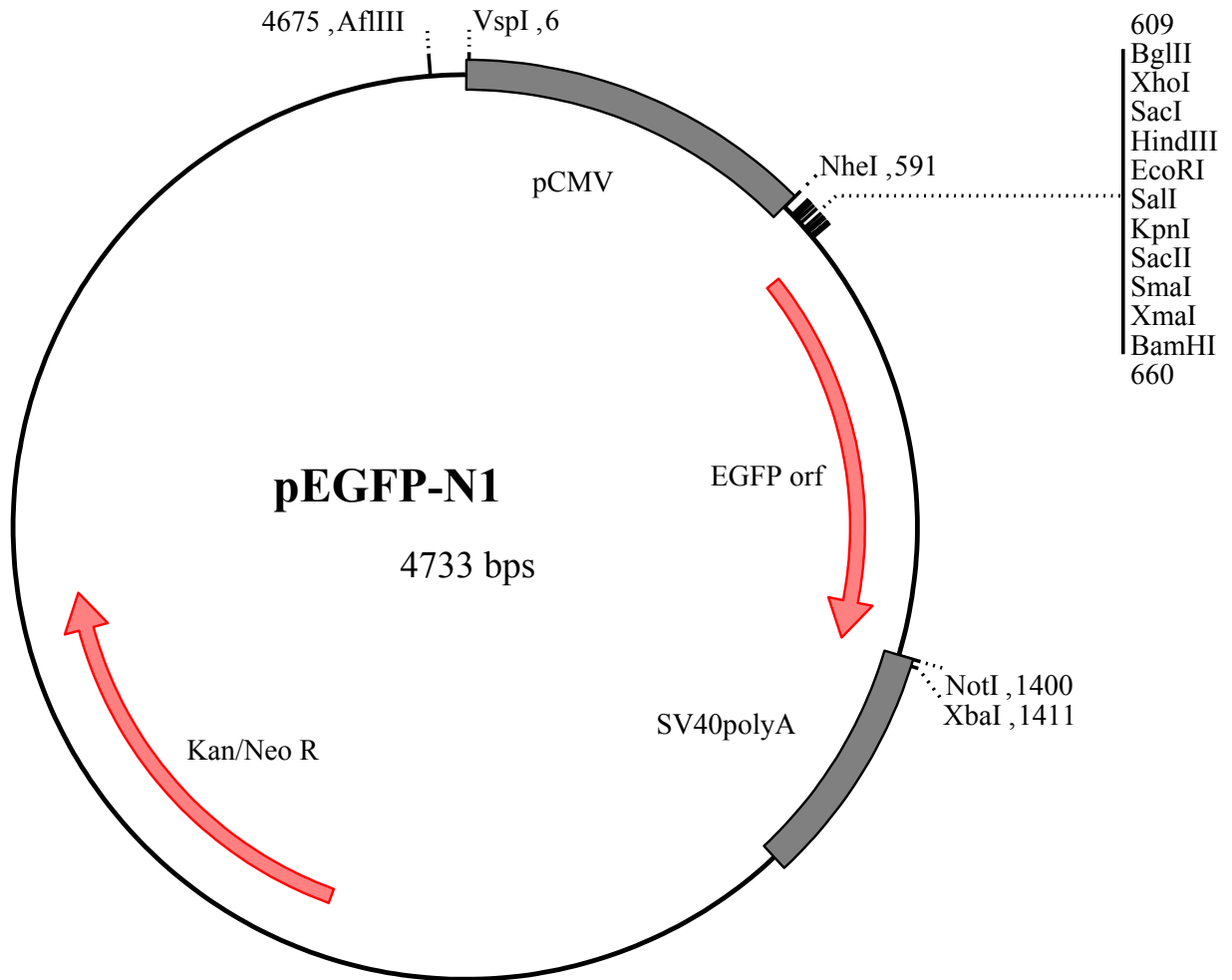
High density lipoprotein containing fractions separated by FPLC (21-26) from plasma pools of adenoviral infected mice (n = 7). Empty columns for control infection – with Ad-EGFP, grey columns for Ad-anti-ABCA1 infection. Triglyceride load of HDL at the different time point presented in percents to the uninjected control – striped column. Overage from two experiments.

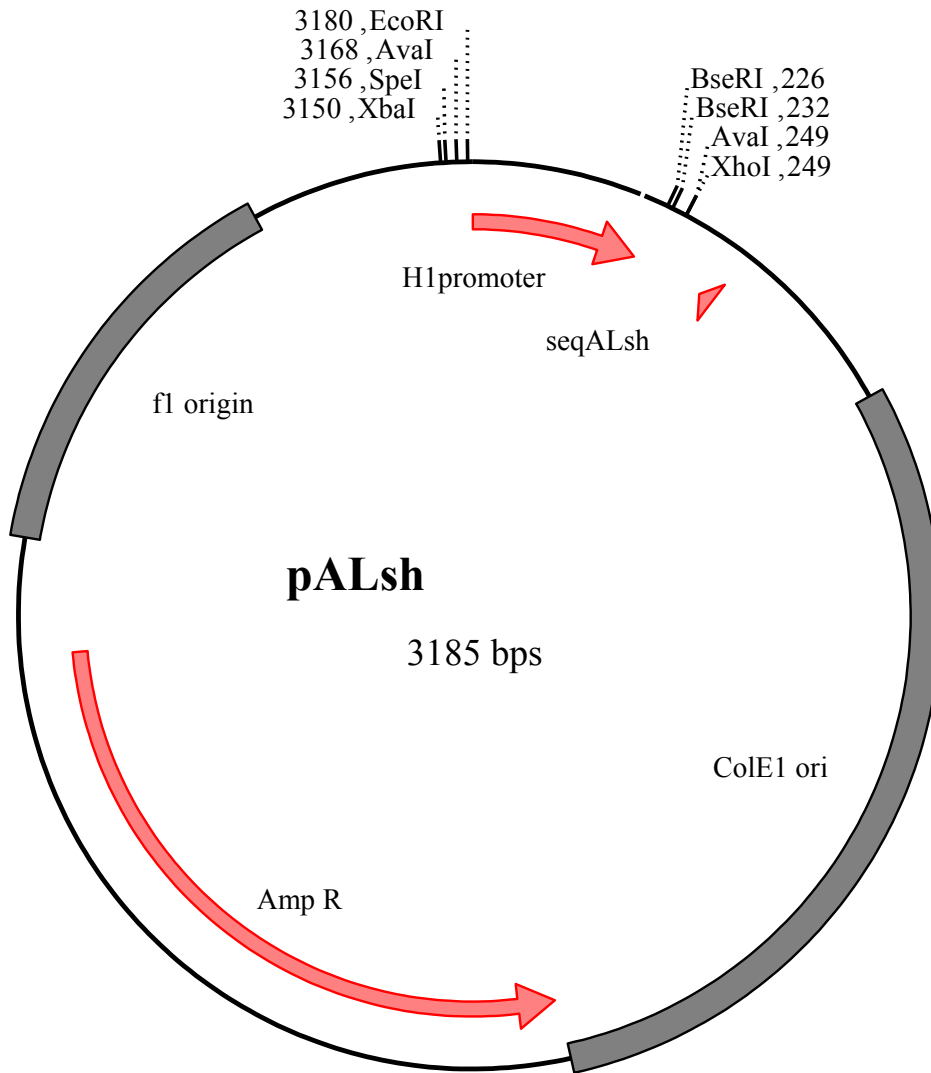
7. Appendix

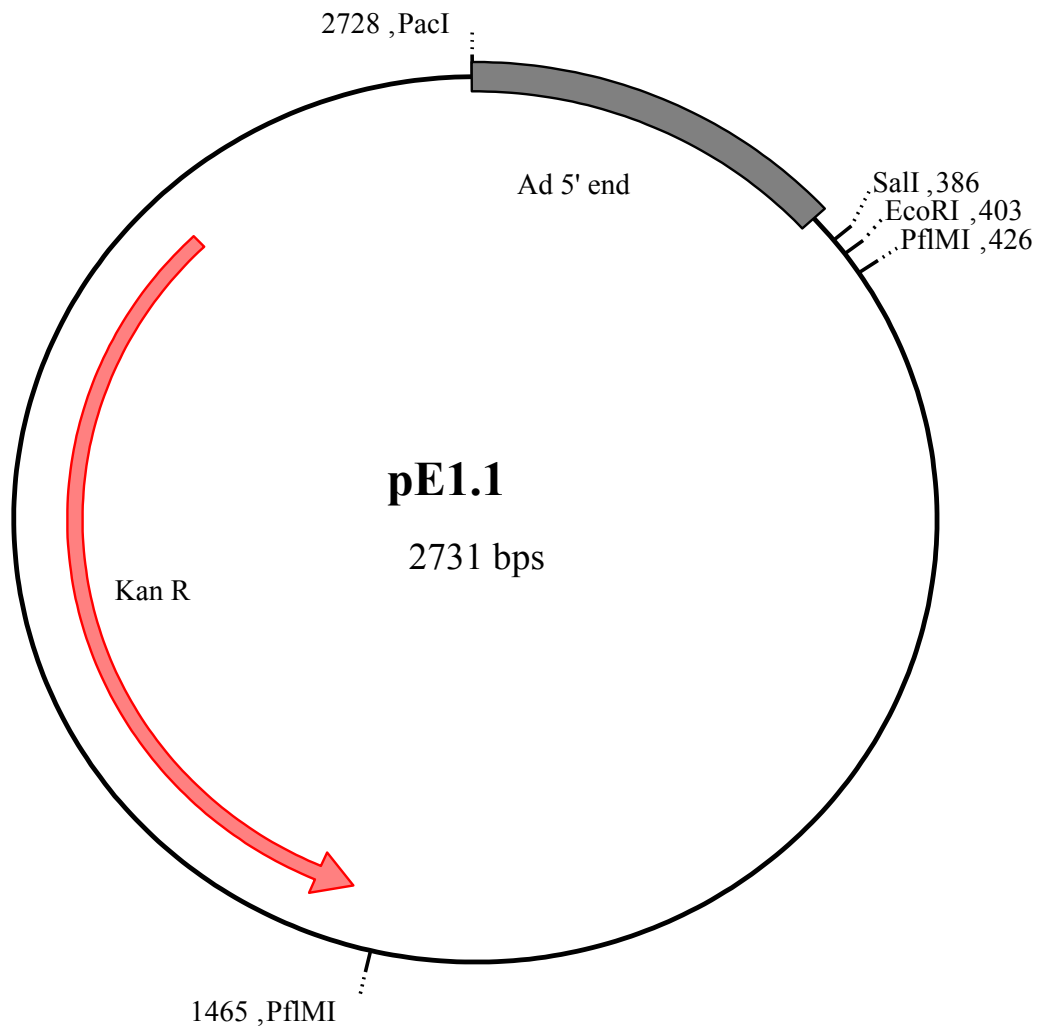
7.1. Plasmids used in the study

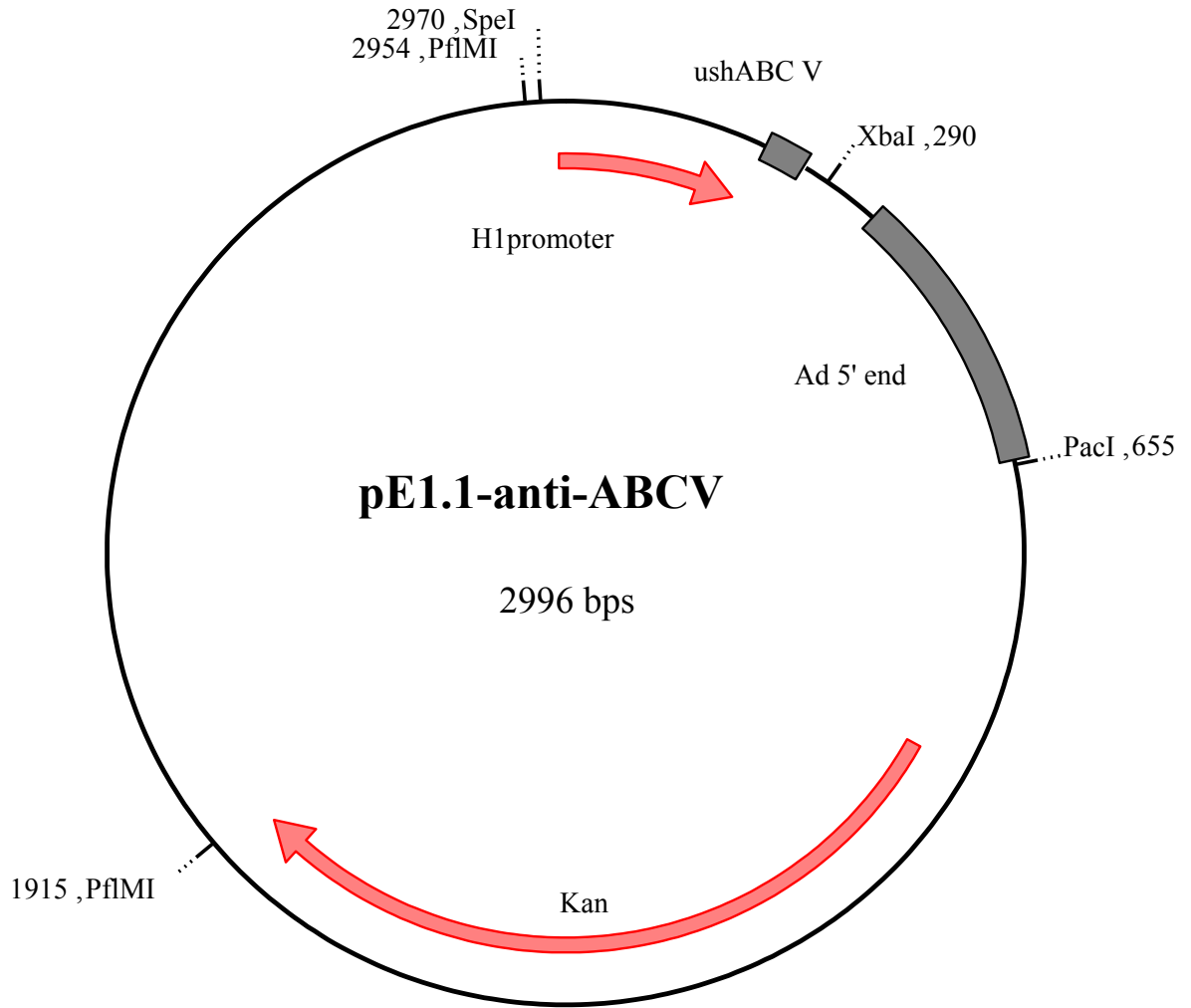
Unique endonuclease restriction positions, main elements of the plasmids and primer locations are shown below.

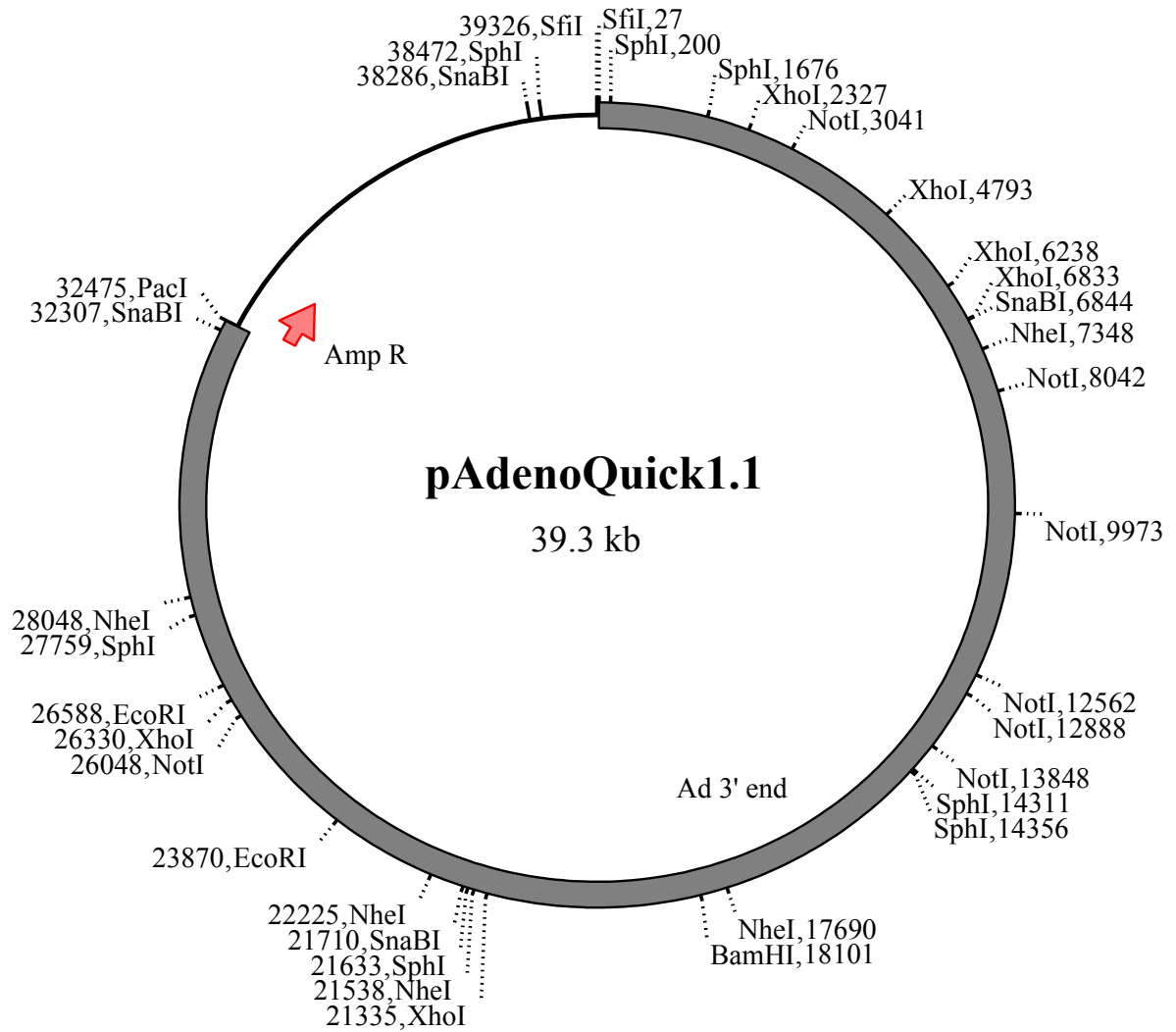


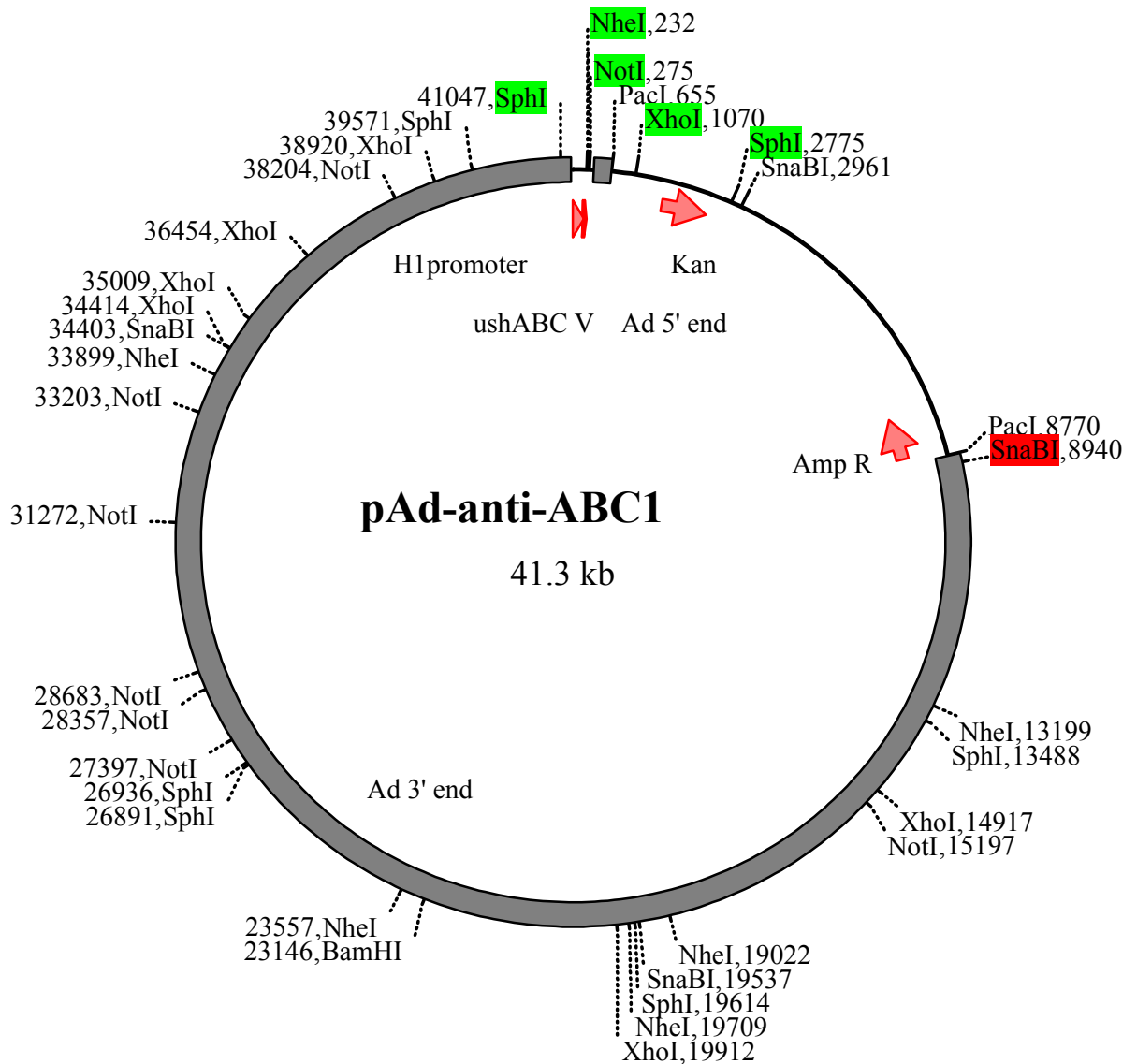












<i>NheI</i>	<i>NotI</i>	<i>SnaBI</i>		<i>SphI</i>	<i>XhoI</i>
12967	14922	14866	16576	12640	14502
10342	12200	10597*	14866	10713	13847
7589	5000	9814	9814	7277	4995
5823	3327	5979*		6126	3406
3849	2589			2948	2466
686	1931			1476	1445
	960			40	595
	326				

Some endonuclease restriction sites and molecular size of correspondent DNA fragments are shown. Sites and fragments used for the selecting of the recombinant adenoviral genome are in green. One reported *SnaBI* is not present in this plasmid (in red), which results in unexpected digestion pattern (see fig. 15)

7.2. Figures and Tables

Figure 1. Model of the topological organization of the human ABCA1	9
Figure 2. Schematic overview of possible RNA interference pathway in animals	16
Figure 3. Technical approach utilising siRNA phenomena	17
Figure 4. Schematic view of the human adenovirus particle, serotype 5	20
Figure 5. Murine ABCA1-FLAG expressing cassette in pcDNA3.1 plasmid	49
Figure 6. ABCA1 expression in human cell culture	50
Figure 7. Immunofluorescence of HEK293 cells overexpressing murine ABCA1-FLAG	51
Figure 8. Nucleotide sequence of H1 promoter region and <i>Bse</i> RI cloning sites in the plasmid pALsh	52
Figure 9. Cloning of anti-ABCA1 siRNA-expressing vector	54
Figure 10. Relative expression of endogenous human LRP and transgenic murine ABCA1 in cells transfected with various constructs expressing anti-ABCA1 siRNAs	55
Figure 11. Effects of anti-ABCA1 siRNA on murine ABCA1 overexpression <i>in vitro</i>	57
Figure 12. Ability of siRNA to suppress tgABCA1 mRNA at different time points	58
Figure 13. siRNA efficiency to inhibit transgenic ABCA1 expression from different amount of transfected cDNA	59
Figure 14. Cloning of anti-ABCA1 siRNA-expressing adenoviral vector	60
Figure 15. Cloning conformation for Ad-anti-ABCA1 adenoviral vector	61
Figure 16. Adenoviral plaque formation	62
Figure 17. Adenoviral effects on the ABCA1 expression	63
Figure 18. Detection of <i>in vivo</i> EGFP-transduction of mice liver cells with different adenoviral dose by flow cytometry	65
Figure 19. Biodistribution of adenoviral particles in mice organs	66
Figure 20. <i>In vivo</i> experimental set up	67
Figure 21. Relative body and organs weight	67
Figure 22. Comparison of mRNA levels in the liver	69
Figure 23. Expression of liver proteins	70

Figure 24. Quantification of the liver plasma membrane proteins	71
Figure 25. Cholesterol content of plasma lipoproteins fractionated by FPLC	72
Figure 26. Plasma cholesterol concentration in different lipoprotein fractions	73
Figure 27. Cholesterol related to the plasma HDL particles	74
Figure 28. Phospholipids content of plasma lipoproteins fractionated by FPLC	75
Figure 29. Plasma phospholipids levels in different lipoprotein fraction	76
Figure 30. Plasma HDL-phospholipids levels	77
Figure 31. Plasma triglyceride levels in different lipoprotein fraction	78
Figure 32. Plasma apolipoproteins 7 days post-infection	79
Figure 33. Sequence conformation of cloning anti-ABCA1(II) siRNA-expressing oligonucleotide into the plasmid pALsh	88
Figure 34. Concentration of adenoviral particles in CsCl density gradient	88
Figure 35. Adenoviral titration	89
Figure 36. Reference EGFP fluorescens spectrum	89
Figure 37. Plasma apolipoprotein CIII	89
Figure 38. Triglycerides of plasma lipoproteins fractionated by FPLC	90
Figure 39. Plasma HDL-triglyceride levels	91
Table 1. Lipoprotein particles	2
Table 2. Apolipoproteins	2
Table 3. List of some human ABC genes, chromosomal location, and function	8
Table 4. Adenoviral titres	62

7.3. Abbreviations

ABCA1	ATP binding cassette transporter A1
Ad	adenovirus
Amp	ampicilin
Apo	apolipoprotein
APS	ammonium persulphate
ATP	adenosin-5'-triphosphat
BGH	bovine growth hormone
(k)bp	base pair
BSA	bovine serum albumin
CE	cholesterol ester
CETP	cholesteryl ester transfer protein
CH	total cholesterol
CIP	alkaline phosphatase, calf intestinal
CM	chylomicrons
CMV	cytomegalovirus
CR	CM remnants
Ct	threshold cycle
Cyp7a	cholesterol-7 α -hydroxylase
(k)Da	Dalton
DAB	3,3'-diaminobenzidine
DAPI	4',6-diamidino-2-phenylindole
DMEM	Dulbecco's modified Eagle medium
DMSO	dimethylsulphoxide
(c)DNA	(coding) desoxiribonucleic acid
DNase	desoxiribonuclease
dNTP	deoxyribonucleoside 5'-triphosphate
DTT	dithiotrietol
ECL	enhanced chemoluminescence
EDTA	ethylenedinitrilotetraacetic acid
EGFP	enhanced expressed green fluorescent protein
ER	endoplasmatic rethiculum
f1	filamentous bacteriophage f1
FBS	foetal bovine serum
FC	free cholesterol
FFA	free fatty acids
fig.	figure
FPLC	fast performance liquid chromatography
HDL	high density lipoprotein
HEK293	human embryonic kidney cells
HRP	horseradish peroxidase
HSPG	heparan sulphat proteoglycans
HuH7	human hepatoma cells
IDL	intermediate density lipoprotein
ifu	infectious units
Ig	immunoglobulin
IMF	indirect immunofluorescence
Kan	kanamycin
LB	Luria broth
LCAT	lecithin:cholesterol acylt transferase
LDL	low density lipoprotein
LDLR	LDL receptor
LPL	endotelial lipoprotein lipase
LRP	LDLR-related protein
M-MLV RT	moloney murine leukemia virus reverse transcriptase
MOI	multiplicity of infection

MTP	microsomal triglyceride transfer protein
OD	optic density
p(X)	plasmid
PAGE	polyacrylamide gel electrophoresis
PBS	phosphate buffered saline
PERPP	post-ER presecretory proteolysis
PFA	paraformaldehyde
pfu	plaque forming unit
PIC	protease inhibitor cocktail
PL	phospholipids
PLTP	phospholipid transfer protein
PPD	<i>N</i> -(1-methylheptyl)- <i>N'</i> -phenyl- <i>p</i> -phenylenediamine
RCT	reverse cholesterol transport
(m)(mi)(si)(sh)RNA	(messenger) (micro) (small interfering) (small hairpin) ribonucleic acid
RNase	ribonuclease
rpm	rotation per minute
RPMI-1640	Roswell Park Memorial Institute cell culture medium
RT	room temperature
(q)RT-PCR	(quantitative) reverse transcription polymerase chain reaction
SDS	sodium dodecil sulphate
SR-BI	scavenger receptor BI
SV40	simian virus 40
T4	bacteriophage T4 virus
tab.	table
TAE	TRIS-Acetate-EDTA buffer
TBE	TRIS-Borate-EDTA buffer
TD	Tanger disease
TE	TRIS-EDTA buffer
TEMED	<i>N,N,N',N'</i> -tetramethylethylenediamine
tg	transgenic
TG	triglyceride
TRIS	Tris(hydroxymethyl)-aminomethan
TRL	triglyceride rich lipoproteins
VLDL	very low density lipoprotein
VLDLr	VLDL receptor
wt	wild type

7.4. Literature

- Aaij C, Borst P (1972). The gel electrophoresis of DNA. *Biochim Biophys Acta* **269**: 192-200.
- Acton SL, Rigotti A, Landschulz KT, Xu S, Hobbs HH, Krieger M (1996). Identification of scavenger receptor SR-BI as a high density lipoprotein receptor. *Science* **271**: 518–520.
- Amarzguioui M, Holen T, Babaie E, Prydz H (2003). Tolerance for mutations and chemical modifications in a siRNA. *Nucleic Acids Res* **31**: 589-95.
- Arakawa R, Abe-Dohmae S, Asai M, Ito JI, Yokoyama S (2000). Involvement of caveolin-1 in cholesterol enrichment of high density lipoprotein during its assembly by apolipoprotein and THP-1 cells. *J Lipid Res* **41**: 1952-62.
- Arakawa R, Yokoyama S (2002). Helical apolipoproteins stabilize ATP-binding cassette transporter A1 by protecting it from thiol protease-mediated degradation. *J Biol Chem* **277**: 22426-9.
- Assmann G, Schmitz G, Brewer Jr HB. Familial high density lipoprotein deficiency: Tangier disease. In: Scriver CR, Beaudet AL, Sly WS, Valle D, editors. The metabolic and molecular bases of inherited disease. New York: McGraw-Hill; 1985. pp. 1267-82.
- Asztalos BF, Roheim PS (1995). Presence and Formation of 'Free Apolipoprotein A-I-Like' Particles in Human Plasma. *Arteriosc Thromb Vasc Biol* **15**: 1419-23.
- Ausubel FM, Brent R, Kingston RE, Moore DD, Seidmann JG, Smith JH, Struhl K (1994). Current protocols in molecular biology. Greene Publishing Associates and Wiley-Interscience, New York.
- Awasthi V, Meinken G, Springer K, Srivastava SC, Freimuth P (2004). Biodistribution of radioiodinated adenovirus fiber protein knob domain after intravenous injection in mice. *J Virol* **78**: 6431-8.
- Baer M, Nilsen TW, Costigan C, Altman S (1990). Structure and transcription of a human gene for H1 RNA, the RNA component of human RNase P. *Nucleic Acids Res* **18**: 97-103.
- Banerjee D, Rodriguez M, Rajasekaran AK (1997). Rapid movement of newly synthesized chicken apolipoprotein AI to trans-Golgi network and its secretion in Madin-Darby canine kidney cells. *Exp Cell Res* **235**: 334-44

- Basso F, Freeman L, Knapper CL, Remaley A, Stonik J, Neufeld EB, Tansey T, Amar MJ, Fruchart-Najib J, Duverger N, Santamarina-Fojo S, Brewer HB Jr (2003). Role of the hepatic ABCA1 transporter in modulating intrahepatic cholesterol and plasma HDL cholesterol concentrations. *J Lipid Res* **44**: 296-302.
- Beisiegel U, Heeren J (1997). Lipoprotein lipase (EC 3.1.1.34) targeting of lipoproteins to receptors. *Proc Nutr Soc* **56**: 731-7.
- Beisiegel U, Krapp A, Weber W, and Olivecrona G (1994). The role of alpha 2M receptor/LRP in chylomicron remnant metabolism. *Ann NY Acad Sci* **737**: 53-69.
- Beisiegel U, Weber W, Bengtsson-Olivecrona G (1991). Lipoprotein lipase enhances the binding of chylomicrons to low density lipoprotein receptor-related protein. *Proc Natl Acad Sci U S A* **88**: 8342-46.
- Beisiegel U, Weber W, Ihrke G, Herz J, and Stanley KK. (1989). The LDLreceptor-related protein, LRP, is an apolipoprotein E-binding protein. *Nature* **341**: 162-164.
- Bergelson JM, Cunningham JA, Droguett G, Kurt-Jones EA, Krithivas A, Hong JS, Horwitz MS, Crowell RL, Finberg RW (1997). Isolation of a common receptor for Coxsackie B viruses and adenoviruses 2 and 5. *Science* **275**: 1320-3.
- Berk AJ, Sharp PA (1977). Sizing & mapping of early adenovirus mRNAs by gel electrophoresis of S1 nuclease digested hybrids. *Cell* **12**: 721-732.
- Bernstein E, Caudy AA, Hammond SM, Hannon GJ (2001). Role for a bidentate ribonuclease in the initiation step of RNA interference. *Nature* **409**: 363-6.
- Birnboim HC, Doly J (1979). A rapid alkaline procedure for screening recombinant plasmid DNA. *Nucleic Acids Res* **7**: 1513-1523.
- Bodzioch M, Orso E, Klucken J, Langmann T, Bottcher A, Diederich W, et al. (1999). The gene encoding ATP-binding cassette transporter 1 is mutated in Tangier disease. *Nat Genet* **22**: 347-51.
- Bojanovski D, Gregg RE, Zech LA, et al. (1987). In vivo metabolism of proapolipoprotein A-I in Tangier disease. *J Clin Invest* **80**: 1742-7.
- Bradford MM (1976). A rapid and sensitive method for the quantitation of microgram quantities of protein utilizing the principle of protein-dye binding. *Anal Biochem* **72**: 248-254.

- Brooks-Wilson A, Marcil M, Clee SM, Zhang LH, Roomp K, van Dam M, et al. (1999). Mutations in ABC1 in Tangier disease and familial high-density lipoprotein deficiency. *Nat Genet* **22**: 336-45.
- Brummelkamp TR, Bernards R, Agami R (2002). A system for stable expression of short interfering RNAs in mammalian cells. *Science* **296**: 550-3.
- Carr TP, Andresen CJ, Rudel LL (1993). Enzymatic determination of triglyceride, free cholesterol, and total cholesterol in tissue lipid extracts. *Clin Biochem* **26**: 39-42.
- Chalfie M, et al. (1994). Green fluorescent protein as a marker for gene expression. *Science* **263**: 802-5.
- Chambenoit O, Hamon Y, Marguet D, Rigneault H, Rosseneu M, Chimini G (2001). Specific docking of apolipoprotein A-I at the cell surface requires a functional ABCA1 transporter. *J Biol Chem* **276**:9955-60.
- Chen W, Silver DL, Smith JD, Tall AR (2000). Scavenger receptor-BI inhibits ATP-binding cassette transporter 1-mediated cholesterol efflux in macrophages. *J Biol Chem* **275**: 30794–800.
- Chiu YL, Rana TM (2002). Basis structure and functional features of siRNA. *Mol Cell* **10**: 549-61.
- Christiansen-Weber TA, Voland JR, Wu Y, et al. (2000). Functional loss of ABCA1 in mice causes severe placental malformation, aberrant lipid distribution, and kidney glomerulonephritis as well as high-density lipoprotein cholesterol deficiency. *Am J Pathol* **157**: 1017-29.
- Chroboczek J, Bieber F, Jacrot B (1992). The sequence of the genome of adenovirus type 5 and its comparison with the genome of adenovirus type 2. *Virology* **186**: 280-5.
- Chroni A, Liu T, Gorshkova I, Kan HY, Uehara Y, Von Eckardstein A, Zannis V (2003). The central helices of ApoA-I can promote ATP-binding cassette transporter A1 (ABCA1)-mediated lipid efflux. Amino acid residues 220-231 of the wild-type ApoA-I are required for lipid efflux in vitro and high density lipoprotein formation in vivo *J Biol Chem* **278**: 6719-30.
- Cormack B, et al. (1996). FACS-optimized mutants of the green fluorescent protein (GFP). *Gene* **173**: 33-38.

- Costet P, Luo Y, Wang N, Tall AR (2000). Sterol-dependent transactivation of the ABC1 promoter by the liver X receptor/retinoid X receptor. *J Biol Chem* **275**: 28240–5.
- Covey SN, Al-Kaff NS, Langara A, Turner DS (1997). Plants combat infection by gene silencing. *Nature* **385**: 781-2.
- Crowther PJ, Cartwright AL, Hocking A, Jefferson S, Ford MD, Woodcock DM (1989). The effect of *E. coli* host strain on the consensus sequence of regions of the human L1 transposon. *Nucleic Acids Res* **17**: 3469–78.
- Danthinne X (2001). Simultaneous insertion of two expression cassettes into adenovirus vectors. *BioTechniques* **30**: 612-6, 618-9.
- Dean M, Allikmets R (1995). Evolution of ATP-binding cassette transporter genes. *Curr Opin Genet Dev* **5**: 779–85.
- Dean M, Hamon Y, Chimini G (2001). The human ATP-binding cassette (ABC) transporter superfamily. *J Lipid Res* **42**: 1007–17.
- Denis M, Haidar B, Marcil M, Bouvier M, Krimbou L, Genest J Jr (2004). Molecular and cellular physiology of apolipoprotein A-I lipidation by the ATP-binding cassette transporter A1 (ABCA1). *J Biol Chem* **279**: 7384-94.
- Doench JG, Petersen CP, Sharp PA (2003). siRNAs can function as miRNAs. *Genes Dev* **17**: 438-42.
- Drobnik W, Borsukova H, Bottcher A, Pfeiffer A, Liebisch G, Schutz GJ, Schindler H, Schmitz G (2002). Apo AI/ABCA1-dependent and HDL3-mediated lipid efflux from compositionally distinct cholesterol-based microdomains. *Traffic* **3**: 268-78.
- Dykxhoorn DM, Novina CD, Sharp PA (2003). Killing the Messenger: Short RNAs that Silence Gene Expression. *Nature Revs Mol Cell Biol* **4**: 457-67.
- Elbashir SM, Harborth J, Lendeckel W, Yalcin A, Weber K, Tuschl T (2001a). Duplexes of 21-nucleotide RNAs mediate RNA interference in cultured mammalian cells. *Nature* **411**: 494-8.
- Elbashir SM, Lendeckel W, Tuschl T (2001b). RNA interference is mediated by 21- and 22-nucleotide RNAs. *Genes Dev* **15**: 188-200.

- Elbashir SM, Martinez J, Patkaniowska A, Lendeckel W, Tuschl T. (2001c). Functional anatomy of siRNAs for mediating efficient RNAi in *Drosophila melanogaster* embryo lysate. *EMBO J* **20**: 6877-88.
- Everett RS, Hodges BL, Ding EY, Xu F, Serra D, Amalfitano A (2003). Liver toxicities typically induced by first-generation adenoviral vectors can be reduced by use of E1, E2b-deleted adenoviral vectors. *Hum Gene Ther* **14**: 1715-26.
- Felts JM, Itakura H, Crane RT (1975). The mechanism of assimilation of constituents of chylomicrons, very low density lipoproteins and remnants – a new theory. *Biochem Biophys Res Commun* **66**: 1467–75.
- Fielding CJ, Fielding PE (1995). Molecular physiology of reverse cholesterol transport. *J Lipid Res* **36**: 211-28.
- Fielding PE, Fielding CJ (1991). Dynamics of lipoprotein transport in the circulatory system. In Biochemistry of Lipids, Lipoproteins and Membranes. DE Vance, and J Vance, editors. Elsevier Press, Amsterdam. 427-59.
- Fire A, Xu S, Montgomery MK, Kostas SA, Driver SE, Mello CC (1998). Potent and specific genetic interference by double-stranded RNA in *Caenorhabditis elegans*. *Nature* **391**: 806-811.
- Fisher EA, et al. 2001. The triple threat to nascent apolipoprotein B. Evidence for multiple, distinct degradative pathways. *J Bio. Chem* **276**: 27855-63.
- Fisher EA, Ginsberg HN (2002). Complexity in the secretory pathway: the assembly and secretion of apolipoprotein B-containing lipoproteins. *J Biol Chem* **277**: 17377–80.
- Foley KP, Leonard MW, and Engel JD (1993). Quantitation of RNA using the polymerase chain reaction. *Trends in Genetics* **9**: 380-5.
- Francis GA, Knopp RH, Oram JF (1995). Defective removal of cellular cholesterol and phospholipids by apolipoprotein A-I in Tangier Disease. *J Clin Invest* **96**: 78-87.
- Gibbons GF, Wiggins D, Brown AM, Hebbachi AM (2004). Synthesis and function of hepatic very-low-density lipoprotein. *Biochem Soc Trans* **32**: 59-64.
- Givan AL (2001). Flow Cytometry: first principles. New York, John Wiley & Sons, Inc.
- Glomset JA (1968). The plasma lecithin:cholesterol acyl-transferase reaction. *J Lipid Res* **9**: 155-67.

- Goldberg IJ, Kandel JJ, Blum CB, and Ginsberg HN (1986). Association of plasma lipoproteins with postheparin lipase activities. *J Clin Invest* **78**: 1523-8.
- Goldstein, JL, Brown MS, Anderson RG, Russell DW, Schneider WJ (1985). Receptor-mediated endocytosis: Concepts emerging from the LDL receptor system. *Ann Rev Cell Biol* **1**: 1-39.
- Gordon DA, Jamil H. Progress towards understanding the role of microsomal triglyceride transfer protein in apolipoprotein-B lipoprotein assembly. *Biochim Biophys Acta* **1486**: 72-83.
- Grable M, Hearing P (1990). Adenovirus type 5 packaging domain is composed of a repeated element that is functionally redundant. *J Virol* **64**: 2047-56.
- Grable M, Hearing P (1992). cis and trans requirements for the selective packaging of adenovirus type 5 DNA. *J Virol* **66**: 723-31.
- Graham FL, Smiley J, Russell WC, Nairn R (1977). Characteristics of a human cell line trans-formed by DNA from human adenovirus type 5. *J Gen Virol* **36**: 59-74.
- Greber UF, Willetts M, Webster P and Helenius A (1993). Stepwise dismantling of adenovirus 2 during entry into cells. *Cell* **75**, 477-86.
- Greber UF, Webster P, Weber J and Helenius A (1996). The role of the adenovirus protease in virus entry into cells. *EMBO J* **15**, 1766-77.
- Grosshans H, Slack FJ (2002). Micro-RNAs: small is plentiful. *J Cell Biol* **156**: 17-21.
- Haghighpassand M, Bourassa PA, Francone OL, Aiello RJ (2001). Monocyte/macrophage expression of ABCA1 has minimal contribution to plasma HDL levels. *J Clin Invest* **108**: 1315-20.
- Haidar B, Denis M, Marcil M, Krimbou L, Genest J Jr (2004). Apolipoprotein A-I activates cellular cAMP signaling through the ABCA1 transporter. *J Biol Chem* **279**: 9963-9.
- Haley B, Zamore PD (2004). Kinetic analysis of the RNAi enzyme complex. *Nat Struct Mol Biol* **11**: 599-606.
- Hammond SM, Bernstein E, Beach D, Hannon GJ (2000). An RNA-directed nuclease mediates post-transcriptional gene silencing in *Drosophila* cells. *Nature* **404**: 293-6.

- Hearing P, Samulski RJ, Wishart WL, Shenk T (1987). Identification of a repeated sequence element required for efficient encapsidation of the adenovirus type 5 chromosome. *J Virol* **61**: 2555-8.
- Heeren J, Grewal T, Laatsch A, Rottke D, Rinninger F, Enrich C, Beisiegel U (2003). Recycling of apoprotein E is associated with cholesterol efflux and high density lipoprotein internalization. *J Biol Chem* **278**: 14370-8.
- Heeren J, Weber W, Beisiegel U (1999). Intracellular processing of endocytosed triglyceride-rich lipoproteins comprises both recycling and degradation. *J Cell Sci* **112**: 349-59.
- Hillemann MR, Werner JR (1954). Recovery of a new agent from patients with acute respiratory illness. *Proceedings of the Society for Experimental Biology and Medicine* **85**: 183-8.
- Hirsch-Reinshagen V, Zhou S, Burgess BL, Bernier L, McIsaac SA, Chan JY, Tansley GH, Cohn JS, Hayden MR, Wellington CL (2004). Deficiency of ABCA1 impairs apolipoprotein E metabolism in brain. *J Biol Chem* **279**: 41197-207.
- Hussain MM, Mahley RW, Boyles JK, Fainaru M, Brecht WJ, and Lindquist PA (1989). Chylomicron-chylomicron remnant clearance by liver and bone marrow in rabbits. Factors that modify tissue-specific uptake. *J Biol Chem* **264**: 9571-82.
- Hutvagner G, Zamore PD (2002). A microRNA in a multiple-turnover RNAi enzyme complex. *Science* **297**: 2056-60.
- Hyde SC, Emsley P, Hartshorn MJ, Mimmack MM, Gileadi U, Pearce SR, Gallagher MP, Gill DR, Hubbard RE, Higgins CF (1990). Structural model of ATP-binding proteins associated with cystic fibrosis, multidrug resistance and bacterial transport. *Nature* **346**: 362-5.
- Illingworth DR (1993). Lipoprotein metabolism. *Am J Kidney Dis* **22**: 90-7.
- Ish-Horowicz D, Burke JF (1981). Rapid and efficient cosmid cloning. *Nucleic Acids Res* **9**: 2989-98.
- Jaffe HA, Danel C, Longenecker G, *et al.* (1992). Adenovirus-mediated *in vivo* gene transfer and expression in normal rat liver. *Nat Genet* **1**: 372-8.
- Jones MD (1993). Reverse transcription of mRNA by *Thermus aquaticus* DNA polymerase followed by polymerase chain reaction amplification. *Methods Enzymol* **218**: 413-19.

- Joyce CW, Amar MJ, Lambert G, Vaisman BL, Paigen B, Najib-Fruchart J, Hoyt RF Jr, Neufeld ED, Remaley AT, Fredrickson DS, Brewer HB Jr, Santamarina-Fojo S (2002). The ATP binding cassette transporter A1 (ABCA1) modulates the development of aortic atherosclerosis in C57BL/6 and apoE-knockout mice. *Proc Natl Acad Sci U S A* **99**: 407-12.
- Kennerdell JR, Carthew RW (1998). Use of dsRNA-mediated genetic interference to demonstrate that frizzled and frizzled 2 act in the wingless pathway. *Cell* **95**: 1017-26.
- Klucken J, Buchler C, Orso E, Kaminski WE, Porsch-Ozcurumez M, Liebisch G, Kapinsky M, Diederich W, Drobnik W, Dean M, Allikmets R, Schmitz G (2000). ABCG1 (ABC8), the human homolog of the *Drosophila* white gene, is a regulator of macrophage cholesterol and phospholipid transport. *Proc Natl Acad Sci U S A* **97**: 817-22.
- Krauss RM (2004). Hold the antioxidants and improve plasma lipids? *J Clin Invest* **113**: 1253-5.
- Krieger M (2001). Scavenger receptor class B type I is a multiligand HDL receptor that influences diverse physiologic systems. *J Clin Invest* **108**: 793-7.
- Laatsch A, Ragozin S, Grewal T, Beisiegel U, Heeren J (2004). Differential RNA interference: replacement of endogenous with recombinant low density lipoprotein receptor-related protein (LRP). *Eur J Cell Biol* **83**: 113-20.
- Langmann T, Klucken J, Reil M, et al. (1999). Molecular cloning of the human ATPbinding cassette transporter 1 (hABC1): evidence for sterol-dependent regulation in macrophages. *Biochem Biophys Res Commun* **257**: 29-33.
- Lewin B (1998). The mystique of epigenetics. *Cell* **93**: 301-3.
- Liang HQ, Rye KA and Barter PJ (1994). Dissociation of lipid-free apolipoprotein A-I from high density lipoproteins *J Lipid Res* **35**: 1187-99.
- Liao H, Langmann T, Schmitz G, Zhu Y (2002). Native LDL upregulation of ATP-binding cassette transporter-1 in human vascular endothelial cells. *Arterioscler Thromb Vasc Biol* **22**: 127-32.
- Lindbo JA, Silva-Rosales L, Proebsting WM, Dougherty WG (1993). Induction of a highly specific antiviral state in trans-genic plants: Implications for regulation of gene expression and virus resistance. *Plant Cell* **5**: 1749-59.

- Liss B (2002). Improved quantitative real time RT-PCR for expression profiling of individual cells. *Nucleic Acids Res* **30**,e89: 1-9.
- Liu CM, Liu DP, Dong WJ, Liang CC (2004). Retrovirus vector-mediated stable gene silencing in human cell. *Biochem Biophys Res Commun* **313**: 716-20.
- Lowry OH, Rosebrough NJ, Farr AL, Randall RJ (1951). Protein measurement with the Folin phenol reagent. *J Biol Chem* **193**: 265-75.
- Mahley R, Innterarity TL, Rall SC Jr, Weisgraber KH (1984). Plasma lipoproteins: apolipoprotein structure and function. *J Lipid Res* **25**: 1277-94
- Marcel YL, Kiss RS (2003). Structure-function relationships of apolipoprotein A-I: a flexible protein with dynamic lipid associations. *Curr Opin Lipidol* **14**: 151-7.
- Merkel M, Heeren J, Dudeck W, Rinninger F, Radner H, Breslow JL, Goldberg IJ, Zechner R, Greten H (2002). Inactive lipoprotein lipase (LPL) alone increases selective cholesterol ester uptake in vivo, whereas in the presence of active LPL it also increases triglyceride hydrolysis and whole particle lipoprotein uptake. *J Biol Chem* **277**: 7405-11.
- Modrow S, Falke F (1997). Adenoviren in Molekulare Virologie. Heidelberg, Spektrum, Akad. Verl.: 391-411.
- Mourrain P, Beclin C, Elmayer T, Feuerbach F, Godon C, Morel J, Jouette D, Lacombe A, Nikic S, Picault N, Remoue K, Sanial M, Vo T, Vaucheret H (2000). *Arabidopsis* SGS2 and SGS3 genes are required for post-transcriptional gene silencing and natural virus resistance. *Cell* **101**: 533-42.
- Munehira Y, Ohnishi T, Kawamoto S, Furuya A, Shitara K, Imamura M, Yokota T, Takeda S, Amachi T, Matsuo M, Kioka N, Ueda K (2004). Alpha1-syntrophin modulates turnover of ABCA1. *J Biol Chem* **279**: 15091-5.
- Nakabayashi H, Taketa K, Miyano K, Yamane T, Sato J (1982). Growth of human hepatoma cells lines with differentiated functions in chemically defined medium. *Cancer Res* **42**: 3858-63.
- Napoli C, Lemieux C, Jorgensen R (1990). Introduction of a chimeric chalcone synthase gene into petunia results in reversible co-suppression of homologous gene in *trans*. *Plant Cell* **2**: 279-89.
- Neufeld EB, Demosky SJ Jr, Stonik JA, Combs C, Remaley AT, Duverger N, Santamarina-Fojo S, Brewer HB Jr (2002). The ABCA1 transporter functions on

- the basolateral surface of hepatocytes. *Biochem Biophys Res Commun* **297**: 974-9
- Neufeld EB, Remaley AT, Demosky SJ, Stonik JA, Cooney AM, Comly M, Dwyer NK, Zhang M, Blanchette-Mackie J, Santamarina-Fojo S, Brewer HB Jr (2001). Cellular localization and trafficking of the human ABCA1 transporter. *J Biol Chem* **276**: 27584-90.
- Neufeld EB, Stonik JA, Demosky SJ Jr, Knapper CL, Combs CA, Cooney A, Comly M, Dwyer N, Blanchette-Mackie J, Remaley AT, Santamarina-Fojo S, Brewer HB Jr. (2004). The ABCA1 transporter modulates late endocytic trafficking: insights from the correction of the genetic defect in Tangier disease. *J Biol Chem* **279**: 15571-8.
- Neville DM Jr (1971). Molecular weight determination of protein-dodecyl sulfate complexes by gel electrophoresis in a discontinuous buffer system. *J Biol Chem* **246**: 6328-34.
- Niemeier A, Gafvels M, Heeren J, Meyer N, Angelin B, Beisiegel U (1996). VLDL receptor mediates the uptake of human chylomicron remnants in vitro. *J Lipid Res* **37**: 1733-42.
- Nykanen A, Haley B, Zamore PD (2001). ATP requirements and small interfering RNA structure in the RNA interference pathway. *Cell* **107**: 309-21.
- Olofsson SO, Stillemark-Billton P, Asp L (2000) Intracellular assembly of VLDL: two major steps in separate cell compartments. *Trends Cardiovasc Med* **10**: 338-45.
- Oram JF (2002). ATP-binding cassette transporter A1 and cholesterol trafficking. *Curr Opin Lipidol* **13**: 373-81.
- Orso E, Broccardo C, Kaminski WE, Bottcher A, Liebisch G, Drobnik W, Gotz A, Chambenoit O, Diederich W, Langmann T, Spruss T, Luciani MF, Rothe G, Lackner KJ, Chimini G, Schmitz G (2000). Transport of lipids from golgi to plasma membrane is defective in tangier disease patients and Abc1-deficient mice. *Nat Genet* **24**: 192-6.
- Ou J, Tu H, Shan B, et al. (2001). Unsaturated fatty acids inhibit transcription of the sterol regulatory element-binding protein-1c (SREBP-1c) gene by antagonizing ligand-dependent activation of the LXR. *Proc Natl Acad Sci U S A* **98**: 6027-32.

- Pan M, Cederbaum AI, Zhang Y-L, Ginsberg HN, Williams KJ, Edward A, Fisher EA (2004). Lipid peroxidation and oxidant stress regulate hepatic apolipoprotein B degradation and VLDL production. *J Clin Invest* **113**: 1277–87.
- Prevec L, Schnieder M, Rosenthal KL et al. (1989). Use of human adenovirus-based vectors for antigen expression in animals. *J Gen Virol* **70**: 429-34.
- Rhains D, Brissette L (2004). The role of scavenger receptor class B type I (SR-BI) in lipid trafficking. defining the rules for lipid traders. *Int J Biochem Cell Biol* **36**: 39-77.
- Romano G, Micheli P, Pacilio C, et al. (2000). Latest developments in gene transfer technology: achievements, perspectives and controversies over therapeutic applications. *Stem Cells* **18**: 19-39.
- Romano N, Macino G (1992). Quelling: transient inactivation of gene expression in *Neurospora crassa* by transformation with homologous sequences. *Mol Microbiol* **6**: 3343-53.
- Roth JA, Cristiano RJ (1997). Gene therapy for cancer: what have we done and where are we going? *J Natl Cancer Inst* **89**: 21-39.
- Rowe WP, Huebner RJ, Gilmore LK, Parrott RH, Ward TG (1953). Isolation of a cytopathic agent from human adenoids undergoing spontaneous degradation in tissue culture. *Proceedings of the Society for Experimental Biology and Medicine* **84**: 570-3.
- Rubinstein A, Gibson JC, Paterniti JR Jr, Kakis G, Little A, Ginsberg HN Brown WV (1985). Effect of heparin-induced lipolysis on the distribution of apolipoprotein E among lipoprotein subclasses. Studies with patients deficient in hepatic triglyceride lipase and lipoprotein lipase. *J Clin Invest* **75**: 710-21.
- Rudel LL, Marzetta CA, Johnson FL (1986). Separation and analysis of lipoproteins by gel filtration. *Methods Enzymol* **129**: 45-57.
- Rust S, Rosier M, Funke H, Real J, Amoura Z, Piette JC, et al. (1999). Tangier disease is caused by mutations in the gene encoding ATP-binding cassette transporter 1. *Nat Genet* **22**: 352-5.
- Rust S, Walter M, Funke H, von Eckardstein A, Cullen P, Kroes HY, et al. (1998). Assignment of Tangier disease to chromosome 9q31 by a graphical linkage exclusion strategy. *Nat Genet* **20**: 96-8.

- Rychlik W, Spencer WJ, Rhoads RE (1990). Optimization of the annealing temperature for DNA amplification *in vitro*. *Nucleic Acids Res* **18**: 6409-12
- Sahoo D, Trischuk TC, Chan T, Drover VA, Ho S, Chimini G, Agellon LB, Agnihotri R, Francis GA, Lehner R (2004). ABCA1-dependent lipid efflux to apolipoprotein A-I mediates HDL particle formation and decreases VLDL secretion from murine hepatocytes. *J Lipid Res* **45**: 1122-31.
- Sakurabayashi I, Saito Y, Kita T, Matsuzawa Y, Goto Y (2001) Reference intervals for serum apolipoproteins A-I, A-II, B, C-II, C-III, and E in healthy Japanese determined with a commercial immunoturbidimetric assay and effects of sex, age, smoking, drinking, and Lp(a) level. *Clin Chim Acta* **312**: 87-95.
- Sambrook J, Fritsch EF, Maniatis T (1989). Molecular cloning: a laboratory manual. Cold Spring Harbor Laboratory, Cold Spring Harbor.
- Santamarina-Fojo S, Peterson K, Knapper C, *et al.* (2000). Complete genomic sequence of the human ABCA1 gene: analysis of the human and mouse ATPbinding cassette A promoter. *Proc Natl Acad Sci U S A* **97**: 7987-92.
- Schlenck A, Herbeth B, Siest G, Visvikis S (1999). Characterization and quantification of serum lipoprotein subfractions by capillary isotachopheresis: relationships with lipid, apolipoprotein, and lipoprotein levels. *J Lipid Res* **40**: 2125-33.
- Schmitz G, Langmann T (2001). Structure, function and regulation of the ABC1 gene product. *Curr Opin Lipidol* **12**: 129-40.
- Schmitz G, Robenek H, Lohmann U, Assmann G (1985). Interaction of high density lipoproteins with cholesteryl ester-laden macrophages: biochemical and morphological characterization of cell surface receptor binding, endocytosis and resecretion of high density lipoproteins by macrophages. *EMBO J* **4**: 613-22.
- Senior JR (1964). Intestinal absorption of fats. *J Lipid Res* **53**: 495-521.
- Sharp PA, Sugden B, Sambrook J (1973). Detection of two restriction endonuclease activities in *Haemophilus parainfluenzae* using analytical agarose-ethidium bromide electrophoresis. *Biochemistry* **12**: 3055-63.
- Shen C, Buck AK, Liu X, Winkler M, Reske SN (2003). Gene silencing by adenovirus-delivered siRNA. *FEBS lett* **539**: 111-14

- Shenk T (1996). Adenoviridae: The viruses and their replication in *Fields Virology*. B. N. Fields, D. M. Knipe, P. M. Howley et al. Philadelphia, Lippincott – Raven Publishers: 2111-48.
- Sherrill BC, Innerarity TL and Mahley RW (1980). Rapid hepatic clearance of the canine lipoproteins containing only the E apoprotein by a high affinity receptor. *J Biol Chem* **255**: 1804-07.
- Silver DL, Wang N, Xiao X, Tall AR (2001). High density lipoprotein (HDL) particle uptake mediated by scavenger receptor class B type 1 results in selective sorting of HDL cholesterol from protein and polarized cholesterol secretion. *J Biol Chem* **276**: 25287-93.
- Smith JD, Waelde C, Horwitz A, Zheng P (2002). Evaluation of the role of phosphatidylserine translocase activity in ABCA1-mediated lipid efflux. *J Biol Chem* **277**: 17797-803.
- Stark GR, Kerr IM, Williams BR, Silverman RH, Schreiber RD (1998). How cells respond to interferons. *Annu Rev Biochem* **67**: 227-64.
- Stewart SA, Dykxhoorn DM, Palliser D, Mizuno H, Yu EY, An DS, Sabatini DM, Chen IS, Hahn WC, Sharp PA, Weinberg RA, Novina CD (2003). Lentivirus-delivered stable gene silencing by RNAi in primary cells. *RNA* **9**: 493-501.
- Tabara H, Sarkissian M, Kelly WG, Fleenor J, Grishok A, Timmons L, Fire A, Mello CC (1999) The *rde-1* gene, RNA interference, and transposon silencing in *C. elegans*. *Cell* **99**: 123-32.
- Takahashi Y, Smith JD (1999). Cholesterol efflux to apolipoprotein AI involves endocytosis and resecretion in a calcium-dependent pathway. *Proc Natl Acad Sci USA* **96**: 11358-63.
- Tall AR (1993). Plasma cholesteryl ester transfer protein. *J Lipid Res* **34**: 1255-74.
- Tall AR, Costet P, Wang N (2002). Regulation and mechanism of macrophage cholesterol efflux. *J Clin Invest* **110**: 899–904.
- Tang C, Vaughan AM, Oram JF (2004). Janus kinase 2 modulates the apolipoprotein interactions with ABCA1 required for removing cellular cholesterol. *J Biol Chem* **279**: 7622-8.
- Timmons L, Fire A (1998) Specific interference by ingested dsRNA. *Nature* **395**: 854.

- Tollefson AE, Scaria A, Hermiston TW, Ryerse JS, Wold LJ, Wold WS (1996). The adenovirus death protein (E3-11.6K) is required at very late stages of infection for efficient cell lysis and release of adenovirus from infected cells. *J Virol* **70**: 2296-306.
- Tollefson JH, Ravnik S, Albers JJ (1988). Isolation and characterization of a phospholipid transfer protein (LTP-11) from human plasma. *J Lipid Res* **29**: 1593-602.
- Tuschl T, Zamore PD, Lehmann R, Bartel DP, Sharp PA (1999). Targeted mRNA degradation by double-stranded RNA *in vitro*. *Genes Dev* **13**: 3191-7.
- Vaisman BL, Lambert G, Amar M, Joyce C, Ito T, Shamburek RD, Cain WJ, Fruchart-Najib J, Neufeld ED, Remaley AT, Brewer HB Jr, Santamarina-Fojo S (2001). ABCA1 overexpression leads to hyperalphalipoproteinemia and increased biliary cholesterol excretion in transgenic mice. *J Clin Invest* **108**: 303-9.
- van Blokland R, Van der Geest N, Mol JNM, Kooter JM (1994). Transgene-mediated suppression of chalcone synthase expression in *Petunia hybrida* results from an increase in RNA turnover. *Plant J* **6**: 861-77.
- van Eldik GJ, Litiere K, Jacobs JJ, Van Montagu M, Cornelissen M (1998). Silencing of beta-1,3-glucanase genes in tobacco correlates with an increased abundance of RNA degradation intermediates. *Nucl. Acids Res* **26**: 5176-81.
- van Eldik GJ, Litiere K, Jacobs JJ, Van Montagu M, Cornelissen M (1998). Silencing of beta-1,3-glucanase genes in tobacco correlates with an increased abundance of RNA degradation intermediates. *Nucl. Acids Res* **26**: 5176-81.
- Wahrle SE, Jiang H, Parsadanian M, Legleiter J, Han X, Fryer JD, Kowalewski T, Holtzman DM (2004). ABCA1 is required for normal central nervous system ApoE levels and for lipidation of astrocyte-secreted apoE. *J Biol Chem* **279**: 40987-93.
- Wang N, Lan D, Chen W, Matsuura F, Tall AR (2004). ATP-binding cassette transporters G1 and G4 mediate cellular cholesterol efflux to high-density lipoproteins. *Proc Natl Acad Sci U S A* **101**: 9774-9.
- Wang N, Silver DL, Costet P, Tall AR (2000). Specific binding of ApoA-I, enhanced cholesterol efflux, and altered plasma membrane morphology in cells expressing ABC1. *J Biol Chem* **275**: 33053-8.

- Wang N, Silver DL, Thiele C, Tall AR (2001). ATP-binding cassette transporter A1 (ABCA1) functions as a cholesterol efflux regulatory protein. *J Biol Chem* **276**: 23742-7.
- Wang Y, Oram JF (2002). Unsaturated fatty acids inhibit cholesterol efflux from macrophages by increasing degradation of ATP-binding cassette transporter A1. *J Biol Chem* **277**: 5692-7.
- Waterhouse PM, Graham MW, Wang M-B (1998). Virus resistance and gene silencing in plants can be induced by simultaneous expression of sense and antisense RNA. *Proc Natl Acad Sci U S A* **95**: 13959-64.
- Wellington CL, Brunham LR, Zhou S, Singaraja RR, Visscher H, Gelfer A, Ross C, James E, Liu G, Huber MT, Yang YZ, Parks RJ, Groen A, Fruchart-Najib J, Hayden MR (2003). Alterations of plasma lipids in mice via adenoviral-mediated hepatic overexpression of human ABCA1. *J Lipid Res* **44**: 1470-80.
- Wickham TJ, Mathias P, Cheresch DA, Nemerow GR (1993). Integrins $\alpha_v\beta_3$ and $\alpha_v\beta_5$ promote adenovirus internalization but not virus attachment. *Cell* **73**: 309-19.
- Willnow TE, Sheng Z, Ishibashi S, and Herz J (1994). Inhibition of hepatic chylomicron remnant uptake by gene transfer of a receptor antagonist. *Science* **264**: 1471-4.
- Witting SR, Maiorano JN, Davidson WS (2003). Ceramide enhances cholesterol efflux to apolipoprotein A-I by increasing the cell surface presence of ATP-binding cassette transporter A1. *J Biol Chem* **278**: 40121-7.
- Woollett LA, Spady DK, Dietschy JM (1992). Saturated and unsaturated fatty acids independently regulate low density lipoprotein receptor activity and production rate. *J Lipid Res* **33**: 77-88.
- Xia H, Mao Q, Paulson HL, Davidson BL (2002). siRNA-mediated gene silencing *in vitro* and *in vivo*. *Nat Biotech* **20**: 1006-10.
- Yamada M, Lewis JA, Grodzicker T (1985). Overproduction of the protein product of a non-selected foreign gene carried by an adenovirus vector. *Proc Natl Acad Sci U S A* **82**: 3567-71.
- Yamauchi Y, Hayashi M, Abe-Dohmae S, Yokoyama S (2003). Apolipoprotein A-I activates protein kinase C alpha signaling to phosphorylate and stabilize ATP binding cassette transporter A1 for the high density lipoprotein assembly. *J Biol Chem* **278**: 47890-7.

Zabner J, Couture LA, Gregory RJ, *et al.* (1993). Adenovirus-mediated gene transfer transiently corrects the chlorine transport defect in nasal epithelia of patients with CF. *Cell* **75**: 207-16.

Zinn KR, Douglas JT, Smyth CA, Liu HG, Wu Q, Krasnykh VN, Mountz JD, Curiel DT, Mountz JM (1998). Imaging and tissue biodistribution of ^{99m}Tc-labeled adenovirus knob (serotype 5). *Gene Ther* **5**: 798-808.

7.5. Acknowledgments

Here I would like to express my gratitude for all kinds of help I have been provided during preparation of my doctoral work and during all my academic studies in general.

To my “doctor mother”, Prof. U. Beisiegel, I wish to show my appreciations very much! I am grateful for welcoming me in her laboratory, for providing me with everything I needed for my thesis, for supervising me, for showing better ways, for correction and discussing my work.

My very special words of gratitude are devoted to Dr. Joerg Heeren. I am happy to meet such person on my scientific way. Thank you for giving me so much of philosophy of experiment and scientific writing, for your lessons in lipid metabolism, for your intuition and for correction of my work.

Here is the very big appreciation to all my teachers from my school, from Moscow State University, from UKE Hamburg and from all over the world. You all are in my heart and in my mind. I would never forget anything you gave me.

I am grateful to all laboratory of Prof. U. Beisiegel, especially to Sandra, Anneta and Dagmara for their kind support in FPLC, western, IMF, histology and animal handling.

Thank you LX&r for fruitful discussions, for helping hand in the lab, for our colossal scientific fantasies, for being an example of “perfect German scientist of old school”, for becoming my friend.

I am thankful to Dr. Merkel for experimental help and for optimism, to Dr. Niemeier for discussions, to Dr. Schnieders for introducing me to adenoviral field, for teaching me and for the friendly carrying of me.

I appreciate the contribution of Prof. Muehlbach as a reviewer of my thesis.

I am thankful to all persons who came to my disputation to be my scientific opponents, for asking me difficult questions and for debating and judging my thesis, and by doing so making my PhD title well deserved.

Thank you, Emma & Dominic, for proofreading of my thesis.

My parents, my mother and my father as well as all my relatives, thank you very much for loving me, for giving me everything you have, for making me that I am, for believing, teaching, supporting and for you praying.

My sister, Katja, who loves me and believes in me so much that I am deep in debt to her and hope to pay it once.

Alexander, Dagmara, Dima F. “Lawyer”, Dima O. “Moscow”, Igor, Martin, Sergey P., Tobias, and all other friends, thank you all for loving me, supporting me, for your criticism, for making me laugh, for being friends.

Thank you, Polina, for giving time a chance to go.

Thank you, Martina, *the Divine Mother of Joy*, for spiritual advises, for introducing to Amma and for the idea of my True Inner Gift and for so much love.
Om Shanti!

Thank you, “Delphis Dialog”, for friendly atmosphere, for place to write and to think, for coffee and fun. You are forever in my heart.

Thank you, Pavel, for always being with me, for being that you are, for giving me a chance to be that I am.

Thank you, Carsten, for loving and understanding me, for your support and for encouraging me.

Sergey Ragozin

Hamburg, at the end of 2004